Optimal system safety targets

Incorporating hydrodynamic interactions in an economic cost-benefit analysis for flood defence systems

Dupuits, Guy

DOI
10.4233/uuid:55ab05c5-4075-4546-81e7-944366c27be9

Publication date
2019

Document Version
Final published version

Citation (APA)
Dupuits, G. (2019). *Optimal system safety targets: Incorporating hydrodynamic interactions in an economic cost-benefit analysis for flood defence systems* . [Dissertation (TU Delft), Delft University of Technology]. https://doi.org/10.4233/uuid:55ab05c5-4075-4546-81e7-944366c27be9

Optimal System Safety Targets

Incorporating Hydrodynamic Interactions in an Economic Cost-Benefit Analysis for Flood Defence Systems

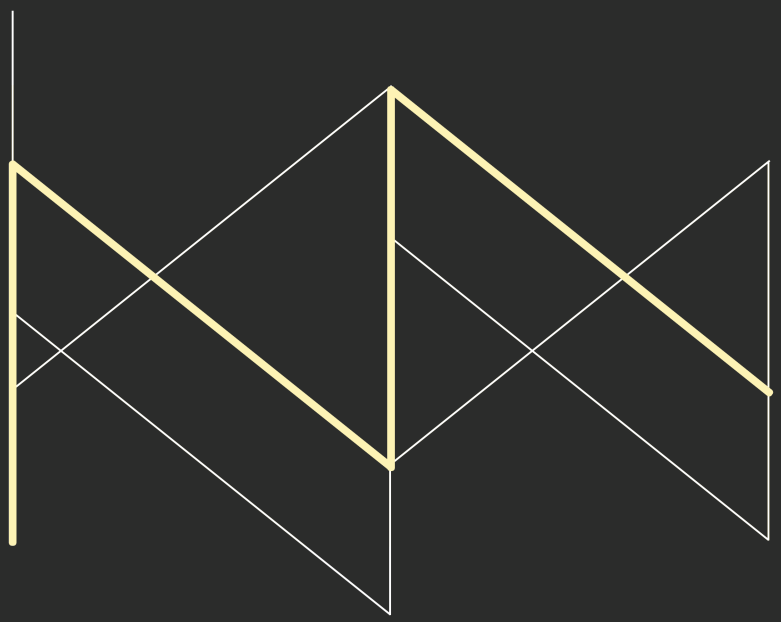

Optimal System Safety Targets

Incorporating Hydrodynamic Interactions in an Economic Cost-Benefit Analysis for Flood Defence Systems

Proefschrift

ter verkrijging van de graad van doctor
aan de Technische Universiteit Delft,
op gezag van de Rector Magnificus prof. dr. ir. T.H.J.J. van der Hagen,
voorzitter van het College voor Promoties,
in het openbaar te verdedigen op vrijdag 20 december 2019 om 10:00 uur

door

Egidius Johanna Cassianus Dupuits

Civiel Ingenieur, Technische Universiteit Delft, Nederland,
geboren te Geleen, Nederland.

Dit proefschrift is goedgekeurd door de

promotor: prof. dr. ir. M. Kok
copromotor: dr. ir. T. Schweckendiek

Samenstelling promotiecommissie:

Rector Magnificus,	voorzitter
Prof. dr. ir. M. Kok,	Technische Universiteit Delft
Dr. ir. T. Schweckendiek,	Technische Universiteit Delft
Onafhankelijke leden:	
Prof. dr. J. C. J. H. Aerts,	Vrije Universiteit Amsterdam
Prof. dr. ir. D. den Hertog,	Universiteit Tilburg
Prof. dr. ir. S. N. Jonkman,	Technische Universiteit Delft
Dr. S. Vorogushyn,	GFZ German Research Centre for Geosciences
Dr. ir. B. G. van Vuren,	Rijkswaterstaat
Prof. dr. ir. P. H. A. J. M. van Gelder,	Technische Universiteit Delft, reservelid

Keywords: Economic optimisation, cost-benefit analysis, system reliability, flood risk, flood defences

Printed by: proefschriften.nl

ISBN 978-94-6332-593-6

An electronic version of this dissertation is available at
http://repository.tudelft.nl/.

It's just the danger
When you're riding at your own risk
She said you are the perfect stranger
She said baby let's keep it like this

Dire Straits - Tunnel of Love

CONTENTS

SUMMARY

Historically, people in flood-prone areas world-wide have (to a certain degree) accepted the risk of being flooded because of the benefits that flood-prone areas can provide; examples of such benefits are rich agricultural lands or trade advantages. Acceptance and benefits notwithstanding, people living in flood-prone areas have tried, and will continue to try, to reduce and manage their vulnerability and degree of exposure to floods. A typical risk reduction measure is building flood defences.

As more and more of such flood defences were built close to each-other and (for example) alongside a river, these flood defences together form flood defence systems. Such a system is often formed or modified in such a way that the system as a whole provides additional protection beyond what the individual flood defences provide independently. However, if one of these flood defences were to fail, other flood defences in that same system might be affected by the flooding. In this thesis, these phenomena are called hydrodynamic interactions.

The hydrodynamic interactions considered are related to the failure (e.g. breaching) of a flood defence. Specifically, the impact of such a failure on the hydrodynamic loads and related risks associated with other flood defences in the same system. Generally speaking, the impact of hydrodynamic interactions can be classified based on the net result (in terms of reliability and/or risk) on the other defences in the system and the position (upstream or downstream). For example, a failure of an upstream river levee typically leads to an increase of load on downstream defences.

In this thesis, two common cases are discussed extensively with respect to their case-specific risk profile: coastal and riverine systems. Coastal systems can have multiple lines of defence. A simple form of a coastal system would be a front defence (i.e. storm surge barrier), separated by a large body of water from rear defences (i.e. levees) which protect the hinterland. For coastal systems, loads increase for the rear defences if the front defence fails. On the other hand, riverine systems are considered in this thesis as a collection of flood defences (or flood defence sections, typically levees) which are adjacent to one or more river streams. For riverine systems, typically load decreases can be expected (i.e. discharge reduction downstream due to storage behind a breached flood defence), though load increases can occur in complex systems.

An economic cost-benefit analysis can be used to determine the acceptable risk for a flood prone area. The basic principle behind the economic optimisation of flood defences is finding the minimum of the total costs. From a risk-neutral perspective, the total costs are the sum of the discounted annual risk costs and discounted investment costs over a given time period. Hydrodynamic interactions in a flood defence system

influence the flood risk of the associated flood defences. And, hence, the annual risk costs as part of the economic optimisation are directly affected. From this description, the relevance to include hydrodynamic interactions in an economic cost-benefit analysis of flood defence systems becomes evident. The aim of this thesis is to investigate the influence of hydrodynamic interactions between flood defences on the associated economically optimal safety targets, and the associated investment and risk costs.

However, in terms of computational load, obtaining risk cost estimates with hydrodynamic interactions is much harder than without interactions. Furthermore, because a number of flood defences are interdependent, the economic optimisation has to be done on the system as a whole. While assuming independence, the optimisation can be done for each flood defence section independently. For interdependent defences, the number of possible system configurations (i.e. unique combinations of resistance levels for all the relevant defences) rises exponentially.

In order to still be able to efficiently estimate what the economically optimal safety targets are for the flood defences in an interdependent system, three subjects are investigated in this thesis. The first subject relates to the behaviour of the economic optimisation for a flood defence system. To that end, analytical derivations are discussed and solved in Chapters 3 & 5 which give a first impression on what to expect of an economic optimisation. The second subject revolves around reducing the number of risk estimates required by the economic optimisation, which resulted in a reduction of about a factor of two. The third subject focuses on using simplified hydrodynamic models (both for a coastal system and a riverine system) and surrogate models in an effort to reduce the computational cost of obtaining risk estimates. Though the computational cost of obtaining sufficient risk estimates for an economic optimisation with interdependence remains high, these three areas of improvement did make such an optimisation computationally tractable.

The analytical derivations revolve around the idea that hydrodynamic interactions due to an upstream breach result either in a load increase or in a load decrease on the downstream flood defence(s). To that end, (simplified) relations and flood defence systems are contemplated within an economic optimisation. For a load reduction, these derivations show that the economically optimal flood probabilities are expected to be approximately the same with and without hydrodynamic interactions. For a load increase a larger effect is expected than due to a load decrease, but overall the expected impact on the economically optimal flood probabilities is insignificant. Notable exceptions to these general findings are flood defence systems with large differences in potential flood damages of individual flood defences, or flood defence systems with large differences between the scenarios with and without hydrodynamic interactions occurring (for example due to a failing storm surge barrier).

In order to analyse complex flood defence systems and obtain economically optimal investment patterns in time, numerical methods are needed. Hydrodynamic models of complex flood defence systems with interactions are computationally expensive for pro-

ducing risk estimates. This computational cost rises exponentially if all possible system configurations need to be calculated in order to find the economically optimal configuration. By only executing the hydrodynamic simulation until it is actually needed by the economic optimisation, the number of required hydrodynamic simulations is reduced by approximately a factor of two. Furthermore, simplifying the hydrodynamic simulations, whilst keeping the fundamental hydrodynamic interactions, is a computationally efficient method as well (i.e. moving from a 2D to a 1D hydrodynamic model). With these improvements, a case study based on a real case in the Netherlands was investigated with acceptable calculation times (i.e. hours).

The results of a numerical economic optimisation were, in this thesis, measured with the economically optimal flooding probabilities and the economically optimal investment scheme (i.e. the sequence of optimal system configurations over time). The behaviour of the economic optimisation in case studies for flood defence systems showed that, aside from some special cases, the economically optimal flooding probabilities were (similar to the analytical derivations) hardly affected by including hydrodynamic interactions. This does not contradict existing studies which found significantly different flooding probabilities with hydrodynamic interactions. These studies found a significant difference because the existing (non-optimal) flood defence system configuration was used in an assessment, while in an economic optimisation, the configuration is optimised.

Significant differences were found in the (economically optimal) configuration of a flood defence system with and without hydrodynamic interactions. When comparing an economically optimal flood defence system configuration with and without hydrodynamic interactions, significant differences were found both in the size of investments (e.g. higher or lower flood defences) and regarding the timing of investments (e.g. advancing or postponing investments). Furthermore, in the riverine case study a reduction of 40% was found in (the present value of) the investment costs for the economically optimal system configuration with hydrodynamic interactions (versus without incorporating hydrodynamic interactions), meaning that by including hydrodynamic interactions a more efficient allocation of investments was found whilst keeping similar economically optimal flooding probabilities. These results strongly supports that hydrodynamic interactions must always be considered for a more cost-effective flood protection and investment strategies.

SAMENVATTING

Historisch gezien hebben mensen in overstromingsgevoelige gebieden (tot op zekere hoogte) het risico op een overstroming geaccepteerd vanwege de voordelen die overstromingsgevoelige gebieden kunnen bieden. Voorbeelden van zulke voordelen zijn vruchtbare landbouwgronden of een gunstige ligging om handel te drijven. Desalniettemin proberen mensen die in overstromingsgevoelige gebieden wonen hun kwetsbaarheid voor overstromingen te beperken. Een typische maatregel die wordt genomen is het bouwen van waterkeringen.

Zodra meerdere waterkeringen dicht bij elkaar worden gebouwd langs (bijvoorbeeld) een rivier, dan vormen deze keringen samen een waterkeringsysteem. Een dergelijk systeem wordt dikwijls op een dusdanige wijze gevormd of aangepast dat het systeem meer bescherming biedt dan de som van de onafhankelijke delen. Dit betekent ook dat als een onderdeel van het systeem faalt, andere onderdelen van hetzelfde systeem ook beïnvloed kunnen worden door het falende onderdeel. In deze thesis worden dit soort verschijnselen hydrodynamische interacties genoemd.

Deze hydrodynamische interacties relateren aan het falen (bressen) van een waterkering. Specifiek wordt hiermee bedoeld de impact van het falen op de hydrodynamische belastingen en gerelateerde risico's voor andere waterkeringen in hetzelfde waterkeringsysteem. Algemeen kan gesteld worden dat de impact van hydrodynamische interacties geclassificeerd kan worden op basis van het nettoresultaat (in termen van betrouwbaarheid en/of risico) op andere keringen in het waterkeringsysteem, en de relatieve positie ten opzichte van deze andere keringen (bovenstrooms of benedenstrooms). Een bovenstroomse bres in een rivierdijk zal typisch leiden tot een verlaagde benedenstroomse rivierwaterstanden en daarmee tot een verlaagd overstromingsrisico van benedenstroomse keringen.

In deze thesis worden twee typische toepassingen uitgebreid besproken met betrekking tot hun toepassingsspecifiek risicoprofiel: kust- en riviersystemen. Kustsystemen kunnen bestaan uit meerdere keringslinies. Een eenvoudig voorbeeld van een dergelijk kustsysteem is een systeem bestaande uit twee linies gescheiden door een groot waterlichaam. Deze twee linies bestaan typisch uit een voorliggende kering (bijvoorbeeld een stormvloedkering) en een achterliggende kering (bijvoorbeeld dijken). Voor dit soort kustsystemen betekent dit dat de hydrodynamische belastingen toenemen op de achterliggende keringen indien de voorliggende kering faalt. Hier kunnen riviersystemen tegenover gezet worden. Riviersystemen zijn in deze thesis gedefinieerd als een collectie van waterkeringen (of strekkingen van dijken) die naast elkaar liggen naast een of meerdere rivieren of riviertakken. In het geval van een riviersysteem kan dan just een

verlaging van de hydrodynamische belastingen worden verwacht, aangezien een bovenstroomse bres zal leiden tot minder water en dus lagere waterstanden benedenstrooms. Riviersystemen zijn echter vaak complexer dan kustsystemen, waardoor zowel belastingverlagingen als ook belastingverhogingen kunnen optreden.

Een economische kosten-batenanalyse is een methode die gebruikt kan worden om het aanvaardbare overstromingsrisico te bepalen voor een overstromingsgevoelig gebied. Het primaire principe achter een economische optimalisatie is het bepalen van de minimale totale kosten. De totale kosten zijn gedefinieerd als de som van de verdisconteerde jaarlijkse risicokosten en de verdisconteerde investeringskosten over een bepaalde periode. Hydrodynamische interacties in een waterkeringsysteem beïnvloeden het overstromingsrisico, en beïnvloeden daarmee ook direct de jaarlijkse risicokosten in de economische kosten-batenanalyse. Deze beschrijving laat de relevantie zien van het meenemen van hydrodynamische interacties in een economische kosten-batenanalyse van waterkeringsystemen. Het doel van deze thesis is dan ook om de invloed van hydrodynamische interacties tussen waterkeringen te onderzoeken, specifiek wat betreft de economisch optimale beschermingsniveaus van de waterkeringen en de bijbehorende economisch optimale investeringskosten en risicokosten.

Desalniettemin, het berekenen van risicoschattingen met hydrodynamische interacties kost normaal gesproken significant meer rekenkracht dan risicoschattingen zonder interacties. Daarnaast moet, met hydrodynamische interacties, de economische optimalisatie van het waterkeringsysteem ook op systeemniveau gedaan worden in plaats van per strekking waterkering. Voor waterkeringen die van elkaar afhankelijk zijn op systeemniveau stijgt het aantal mogelijke systeemconfiguraties (unieke combinaties van de afzonderlijke beschermingsniveaus per waterkering) exponentieel.

Om alsnog de economisch optimale beschermingsniveaus per waterkering in een waterkeringsysteem te kunnen bepalen op een efficiënte manier, zijn drie aspecten onderzocht in deze thesis. Het eerste aspect relateert aan het gedrag van een economische optimalisatie van een waterkeringsysteem. Om dit gedrag beter te begrijpen, zijn analytische afleidingen beschreven in in Hoofdstuk 3 & 5. Deze hoofdstukken geven een eerste indruk van wat verwacht kan worden van het gedrag van een economische optimalisatie. Het tweede aspect draaide om het reduceren van het aantal te berekenen risicoschattingen in een economische optimalisatie, wat resulteerde in ongeveer een halvering van het aantal benodigde risicoschattingen. Het derde aspect focuste op het gebruiken van versimpelde hydrodynamische modellen (zowel voor kust- als voor riviersystemen) en surrogaatmodellen in een poging om de benodigde rekenkracht voor risicoschattingen te reduceren. Hoewel de benodigde rekenkracht voor het bepalen van risicoschattingen met systeemwerking hoog blijft, hebben deze drie aspecten een economische optimalisatie met systeemwerking behapbaar gemaakt.

In de analytische afleidingen staat het idee centraal dat hydrodynamische interacties door een bres in een bovenstroomse waterkering of een hogere, of een lagere hydrodynamische belasting veroorzaken bij benedenstroomse waterkering(en). Dit idee is ver-

werkt in een aantal (vereenvoudigde) vergelijkingen en simpele waterkeringsystemen. Deze vergelijkingen laten zien dat een lagere hydrodynamische belasting door een bovenstroomse bres resulteert in ongeveer dezelfde economisch optimale overstromingskansen met en zonder hydrodynamische interacties. Een hogere hydrodynamische belasting by benedenstroomse waterkeringen resulteert sneller in significante verschillen tussen de economisch optimale overstromingskansen met en zonder hydrodynamische interacties, maar in het algemeen is de verwachte impact op de economisch optimale overstromingskansen niet significant. Uitzonderingen op deze verwachting zijn systemen met grote verschillen in de verwachte overstromingsschade tussen individuele waterkeringen, of waterkeringsystemen met grote verschillen tussen de scenario's met en zonder hydrodynamische interacties (bijvoorbeeld door een falende stormvloedkering).

Voor het analyseren van complexere waterkeringsystemen, met als doel het vinden van economisch optimale investeringspatronen in de tijd, zijn numerieke methoden nodig. Daarnaast vereisen hydrodynamische modellen van complexe waterkeringsystemen met hydrodynamische interacties veel rekenkracht. De benodigde rekenkracht stijgt exponentieel als niet één, maar alle mogelijke systeemconfiguraties moeten worden doorgerekend om de economisch optimale configuratie te vinden. Door het uitvoeren van de berekening uit te stellen totdat deze daadwerkelijk nodig is voor de economische optimalisatie, is maar ongeveer de helft van het aantal mogelijke hydrodynamische berekeningen daadwerkelijk nodig. Daarnaast is het ook mogelijk om de benodigde rekenkracht te verlichten door de hydrodynamische simulaties te versimpelen; deze versimpelde hydrodynamische simulaties bevatten dan nog wel de fundamentele hydrodynamische interacties. Met deze verbeteringen is een casus (die gebaseerd is op een echte casus in Nederland) geanalyseerd met acceptabele rekentijden.

De resultaten van een numerieke economische optimalisatie zijn, in deze thesis, gekwantificeerd met behulp van de economisch optimale overstromingskansen en het economisch optimale investeringsschema (de volgorde van de optimale systeemconfiguraties in de tijd). De (netto contante waarde van de) totale kosten van een geoptimaliseerd waterkeringsysteem is alleen vergeleken voor een aantal casussen. Het gedrag van de economische optimalisatie voor een waterkeringsysteem liet zien dat in het algemeen de economisch optimale overstromingskansen vergelijkbaar zijn met en zonder hydrodynamische interacties. Dit komt overeen met de bevindingen van de analytische economische optimalisaties. Dit spreekt eerdere studies die significante verschillen vonden tussen overstromingskansen bepaald met en zonder hydrodynamische interacties *niet* tegen. Deze studies vonden de significante verschillen omdat de bestaande configuratie van het waterkeringsysteem was gebruikt. In een economische optimalisatie is juist de configuratie een integraal onderdeel van de optimalisatie.

Significante verschillen zijn gevonden in de (economisch optimale) systeemconfiguratie van een waterkeringsysteem met en zonder hydrodynamische interacties. Deze verschillen uitten zich vooral in investeringssom (waterkeringen met een hoger of lager beschermingsniveau) en in het tijdstip van investeren (wanneer waterkeringen versterkt

worden). Daarnaast is in de riviersysteem casus een reductie van 40% gevonden in de (verdisconteerde) waarde van de investeringskosten voor de economisch optimale systeemconfiguratie bepaald met hydrodynamische interacties (versus zonder hydrodynamische interacties). Dit is een krachtig signaal dat het effect van hydrodynamische interacties altijd overwogen moeten worden voor het vinden van een kosten-effectievere overstromingsbescherming en investeringsstrategieën.

1

INTRODUCTION

1

1.1. FLOOD RISK

Flood risk is a concept that will be used a lot in this thesis, mostly in relation with quantitative descriptions. A general description of this term, and the context in which it is used, would be saying that flood risk is the possibility of having negative consequences due to an excess amount of water (in the form of a flood) occurring where humans do not want it to occur. This is a description that works for flood-prone areas, such as land that can be flooded due to (for example) high river discharge or storm surges at sea.[1] However, in hydraulic engineering, flood risk has been defined as a function of probabilities and consequences [1]. Another way of describing flood risk can be found in [2]:

> *"...Flood risk is a concept that concerns both the possible impact of flooding and the probability that it will occur. It indicates the consequences, and also the probability of these consequences."*

Historically, people in flood-prone areas world-wide have (to a certain degree) accepted the risk of being flooded because of the benefits that flood-prone areas can provide; examples of such benefits are rich agricultural lands or trade advantages. Acceptance and benefits notwithstanding, people living in flood-prone areas have tried, and will probably continue to try, to mitigate and manage their vulnerability and degree of exposure to floods. Pulling back to the generic term 'negative consequences', these consequences can be for example loss of life, loss of economic and/or ecological value [1].

Over time, and certainly since the industrial revolution, the degree of exposure to floods and water-related hazards has increased world-wide; this increased exposure is typically attributed to population growth and increased economic value [3, 4]. Another factor is climate change, though the why and how much of climate change are still debated: for example, anthropogenic climate change has (so far) not been found to have a significant impact on disaster losses [3]. In efforts to reduce the vulnerability to floods, flood defences have been built in coastal and riverine areas. Particularly in river deltas this can lead to an complex system of coastal flood defences and riverine flood defences along multiple river branches. A schematic example of such a system resembling the Dutch main water system can be seen in Figure 1.1. Determining the flood risk of such a complex system is important to not only determine how well such a system is protected against flooding, but also as an important input in the context of (political) decisions on where, when and how much to invest in flood risk mitigation.

[1] Though not discussed in this dissertation, this description does not work for other water-related hazards such as droughts or pollution.

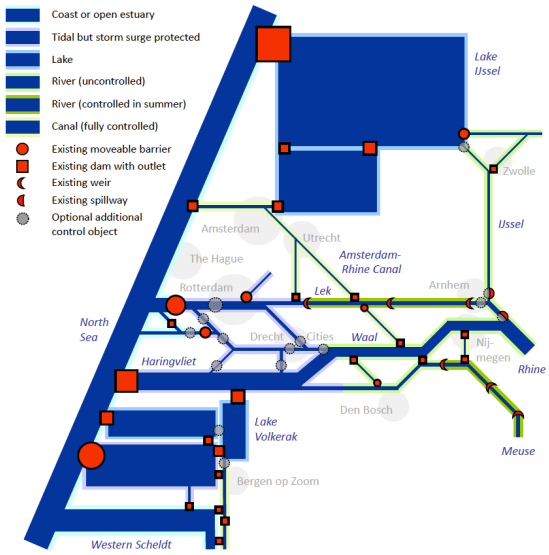

Figure 1.1: Schematic overview of the Dutch system of flood defences, picture taken from [5].

1.2. ACCEPTABLE FLOOD RISK

Flood risk management is managing the vulnerability to floods, the degree of exposure to floods, the nature and the probability of floods. This can be done by either reducing the probability of a flood to reach a flood-prone area (e.g. stronger flood defences), or by reducing the potential damage in case of a flood. Typically, choices in the context of flood risk management need to be made in the face of budget constraints. In order to evaluate which measures are necessary and/or which measures are the most efficient, metrics are needed to compare such possible measures.

For the Netherlands, flood risk management has a strong place in history. Shortly after the catastrophic flood of 1953, the Delta Committee was formed and asked to advise on how to prevent such a terrible flood to re-occur. One of the proposals of the Delta Committee [6] was that protection standards for flood defences can be derived from cost-benefit analyses. This economic approach has since become an important instrument in finding standards for flood defences [2]. A typical economic cost-benefit analysis contains the sum of the discounted flood risk cost (often defined as the probability of flooding multiplied by the flood damage[2]) and the discounted investment costs associated with building or reinforcing flood defences. Additionally, maintenance and operation costs can also be included in these kind of cost-benefit analyses. If the sum of all costs is minimised, the economically optimal configuration of flood defence levels can be determined.

[2]This simple multiplication does not always hold for more complex flood risk calculations. A more generic description, as found in [1], is that flood risk is a *function* of probabilities and consequences.

However, (at least in the Netherlands) an economic cost-benefit analysis is just one method to assist in determining what the acceptable risk should be. Besides the economic flood risk, two other criteria for determining the acceptable flood risk are defined in the Dutch 'Fundamentals of flood protection' (Dutch: 'Grondslagen voor hoogwaterbescherming') [2]: the individual risk and societal risk (see also Figure 1.2). The individual risk is defined in [2] as the (annual) probability that an individual dies due to a flood, taking into consideration the possibility and effectiveness of evacuation,[3] while the societal risk is a measure for the likelihood of having a large number of casualties due to a flood. Societal risk and individual flood risk can also be described as life safety, see for example see [7] & [8]. These three criteria for acceptable flood risk can be (and, in the Netherlands, are) used as input for political decisions on flood risk standards.

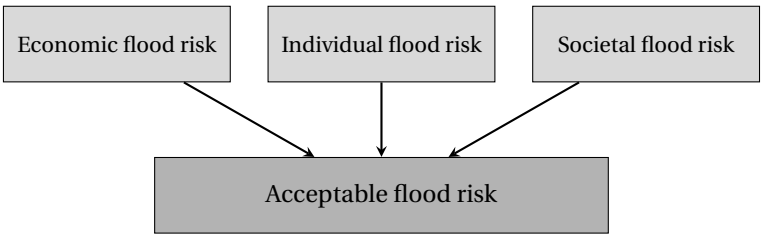

Figure 1.2: Criteria for determining the acceptable flood risk in the Netherlands: individual risk, societal risk and economic risk. All three criteria need to be at an acceptable level in order to have an acceptable flood risk.

1.3. FLOOD RISK IN THE NETHERLANDS

Where, when and how much to invest in flood safety has been (and probably will be) an important topic in the Netherlands. Since the first inhabitants of the Netherlands moved to flood prone areas, they were concerned with floods. In those early days, they used either natural or man-made mounds to reduce the possibility of flooding.

As the population of the Netherlands grew, more flood-prone areas were settled, which also meant that more people and land needed to be protected against flooding. The growing size of flood prone areas which needed to be protected resulted in a growing collaborative flood protection effort: first on a regional level (water boards) and later on a national level (Rijkswaterstaat). Flood defences were usually built to withstand the highest then-known flood level. Despite this collaborative effort many floods still occurred over the centuries, the latest major one in the year 1953 which caused a terrible loss of life and huge economic damage.

In the previous section, flood risk was described as as a concept that indicates the consequences and the possibility of these consequences. The consequences of flooding

[3] The definition of individual risk in this introduction has been purposefully simplified for legibility from the actually used 'local individual risk'. The *local* individual risk is the probability that a person *residing at a fixed location* dies due to a flood, taking into account the possibility of evacuation.

can be severe for the Netherlands, as, at the time of writing, about 60% of the country is flood-prone (Figure 1.3). The probability of a flood prone area to actually flood depends on the (hydraulic) loads (e.g. storm surge levels, wave height) and the strength of relevant flood defences.

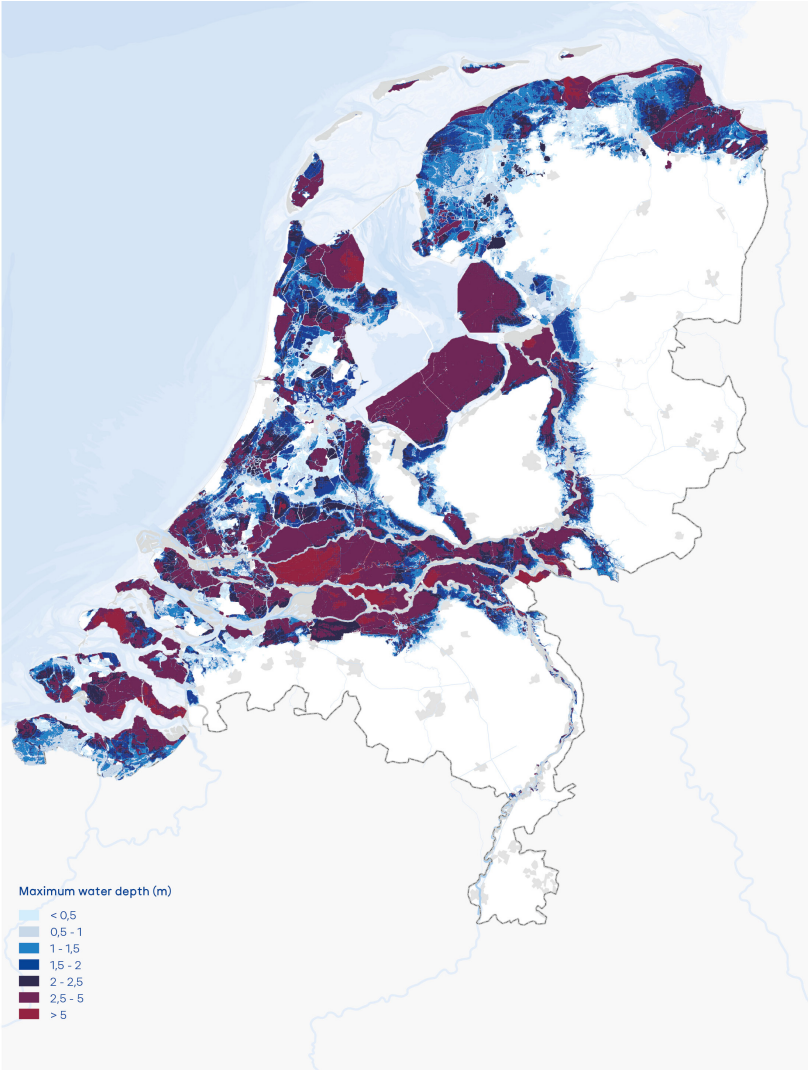

Figure 1.3: Sixty percent of the Netherlands can experience a flood from the sea, lakes and major rivers. The maximum water depths (in meters) are indicated in the figure and can exceed five meters. Picture reproduced from [2].

The first Delta committee based their definition of acceptable risk on an economic cost-benefit analysis, which was largely based on the work of Van Dantzig (e.g. see [9]).

1

In this economic cost-benefit analysis, both the flooding probabilities and consequences were simplified. Typically, a flooding probability is closely linked to the failure probability of one or more flood defences. This failure probability is typically illustrated with the help of a reliability equation, where failure occurs when the load (e.g. water level) is greater than the resistance (e.g. flood defence).

In the work by the first Delta committee, the flooding probabilities were reduced to exceedance probabilities of critical water levels that should be resisted by a flood defence [6]. Furthermore, in the economic optimisation the consequences of a flood were considered to be independent of the loads caused by the flood (i.e. a 'constant damage'). Using the exceedance of a critical water level as a proxy for the probability of flooding meant that the uncertainty of the strength of a flood defence was not explicitly considered. Furthermore, the assumption of a constant flood damage simplified the severity of a flood to a single damage-state and neglected possible varying flooding patterns.[4] However, it has to be noted that in the period when Van Dantzig presented his research (1956), flooding probabilities where difficult to quantify [10], which led to Van Dantzig (and the Delta Committee in [6]) using the aforementioned approximations. An illustration of the resulting probabilities and flooding consequences is shown in Figure 1.4.

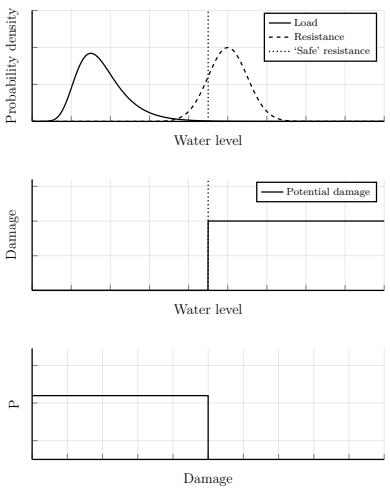

Figure 1.4: Conceptual illustrations of the flooding probabilities (top) and flood consequences (bottom) as used by Van Dantzig. The top picture shows the load as a stochastic probability density function (PDF), whereas the strength is represented as a straight vertical line ('safe' resistance) which is at a representative, critical water level. The middle picture shows a conceptual relation between damage and water level where, at the critical water level, a constant expected damage occurs. The resulting bottom picture depicts the exceedance probability of the expected damage in a flood-damage curve.

[4] Depending on the level and shape of the protected land, this may or may not be a good approximation. For example, if all the economic value is concentrated in a low lying, flat area which fills up fast (not unlike a bathtub), the approximation of constant damage works well.

As research and computational power progressed, nowadays flooding probabilities can be better estimated, for example as has been done in the project VNK2 in the Netherlands as described in [10]; VNK2 is an acronym for 'Veiligheid Nederland in Kaart 2', which translates to 'Flood Risk in The Netherlands 2'. The VNK2 approach makes it possible to explicitly incorporate the uncertainty of the strength of flood defences, as well as to incorporate multiple possible flooding patterns. All this leads to a more explicit and therefore better approximation of the flooding probabilities (and the associated Expected Annual Damage or EAD)[5]. A simplified illustration of this is shown in Figure 1.5.The resistance is now a distribution of critical water levels, which, for example, can be also linked to a distribution of critical flood defence heights.

Recently, research in literature paid attention to how multiple flood defences interact with each-other hydrodynamically as a system during an extreme event, and how it affects the flood risk. Examples of recent literature regarding systems of riverine flood defences can be found in [12–16]. Specifically, the impact of breaches on the flood risk was investigated. In other words, the impact of one or more breaches in flood defences on the (increased or decreased) hydraulic load of the other flood defences in the same system. These studies found significant differences in flood risk estimates in case a system as a whole was studied instead of as separate, independent elements. This is illustrated in Figure 1.6. Flooding patterns might change as well due to system interdependency, though this is considered outside of the scope of this thesis.

[5]The expected annual (flood) damage is an aggregation of all flood consequences weighted by their probability of occurring in any year [1]. The bottom plot in (for example) Figure 1.5 can also be used to determine the EAD by calculating the area under the graph (summation of flood consequences weighted by their annual exceedance probabilities, [11]).

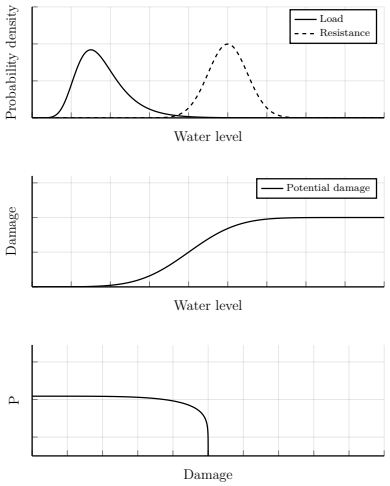

Figure 1.5: Conceptual illustration of the modelled flooding probabilities (top) and consequences (middle) as used by VNK2 (e.g. see [10]). Contrary to Figure 1.4, the top picture now has distributions for both the load and strength, showing that the strength is no longer a line of 'safe' resistance, but a stochastic distribution. Furthermore, the middle picture shows that flood damage can now depend on the severity of a flood. The resulting bottom picture depicts the exceedance probability of the potential damage in a flood-damage curve.

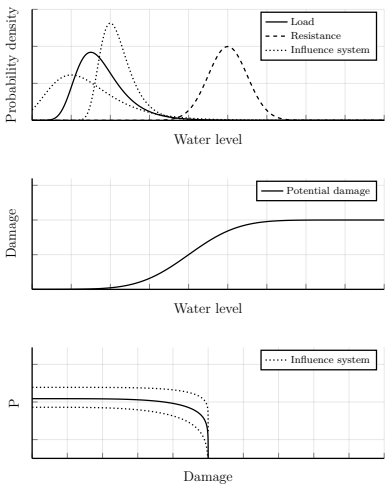

Figure 1.6: The top picture has distributions for both the load and strength, while the middle picture shows that flood damage depends on the severity of a flood. Compared to Figure 1.5, the load in the top pictures can change depending on the reliability of other flood defences in the same system (i.e. 'influence system'). The flood-damage curve in the bottom picture changes accordingly, because the load is affected by the system interdependency.

1.4. OBJECTIVE

Determining flood risk is a key element in order to determine whether or not the safety against flooding is acceptable, whether it concerns the individual risk, societal risk and/or the economic flood risk. This thesis focuses specifically on the economic flood risk.

Large sums of flood risk costs and investment costs are typically involved in cost-benefit analyses regarding flood safety. Large investments have been made in the Netherlands and will continue to be made in an effort to protect flood prone areas. Because of the large investments, even a small relative improvement of these cost-benefit analyses can lead to a different optimal solution: when, where and how much to invest. However, the complexity of regional or national cost-benefit analysis (due to the scale and number of flood defences involved) has led to the use of relatively simple relations to express flooding probabilities, even in recent publications (i.e. an exponential function describing exceedance probabilities, for example see [17]).

A significant part of the simplicity in the relations of an economic optimisation is that reliability and consequences are determined independent of breaches elsewhere, both in terms of probabilities as well as hydrological effects. As discussed in Section 1.3, this independence assumption can be (and often is) an oversimplification. Including hydrodynamic interactions in flood risk estimates for the cost-benefit analysis can therefore lead to improved economically optimal safety standards and more efficient investments.

However, research towards hydrodynamic interactions between flood defences has shown that including this interdependency leads to a significantly greater computational strain. Therefore, one of the key challenges in including interdependency between multiple lines of flood defences in an economic optimisation is maintaining computational efficiency. Assuming independence alleviates the computational strain, but it remains to be seen whether or not assuming independence is a justifiable simplification.

The aim of this thesis is to investigate the influence of hydrodynamic interactions between flood defences on the associated economically optimal safety targets. This is done by investigating three subjects. First, a framework is developed in order to incorporate the effect of interdependence in flood defence systems with multiple flood defences in a cost-benefit analysis. Secondly, insight is developed into when hydrodynamic interactions between flood defences lead to a significant difference on the associated economically optimal safety targets. Thirdly, the practical impact and computational performance (i.e. by reducing the computational burden) of hydrodynamic interactions is tested in case studies. This aim can also be posed as an overall research question, with three sub-questions:

> *What is the influence of hydrodynamic interactions on the economically optimal safety targets, and the associated investment and risk costs of a system of flood defences?*
>
> i. How can hydrodynamic interactions be incorporated within an economic cost-benefit analysis in a computationally efficient manner?

ii. What are the expected changes due to incorporating hydrodynamic interactions on an economic optimisation of a system of flood defences?

iii. How are coastal and riverine flood defence systems affected by hydrodynamic interactions, and what are the differences between the two types in the context of an economic optimisation?

1.5. OUTLINE

Figure 1.7 provides a visual overview of the chapters and their relations to each-other. To start, Chapter 2 aims to give insight in the relation between hydrodynamic interactions risk and an economic cost-benefit analysis. This is done by giving a brief description of both concepts, as well as some aspects of selected analytical cost-benefit analyses. These descriptions are used to introduce a general framework of how hydrodynamic interactions can be explicitly included in an economic cost-benefit analysis.

Chapter 3 explores the behaviour of a cost-benefit analysis with and without interdependence for a coastal flood defence system. The influence of interdependence between the lines of defence is made clear by means of an analytical derivation, which shows how the flood risk with interdependence can change the economically optimal safety targets. In order to avoid simplifications in the analytical derivations, a numerical solution of the economically optimal solution with and without interdependence is investigated as well.

In order to numerically find the economically optimal solution for flood defence systems with an arbitrary number of defence lines, a graph-based method is proposed in Chapter 4. The primary reason for introducing a new method is to reduce the number of required (computational costly) risk estimates, thereby reducing the computational cost of an economic optimisation. The proposed method usually needs only roughly half of all the potential risk calculations, which leads to a significant lower computational strain.

With both analytical insight and a numerical method ready to evaluate a flood defence system with hydrodynamic interactions, a larger case study is considered in Chapter 5. This case study concerns a riverine flood defence system at the Bovenrijn/IJssel area in the Netherlands, and deals with the practical implementation issues of using an existing flood risk model which accounts for interdependency in conjunction with the proposed framework of Chapter 4. Finally, conclusions and recommendations are presented in the final chapter (Chapter 6).

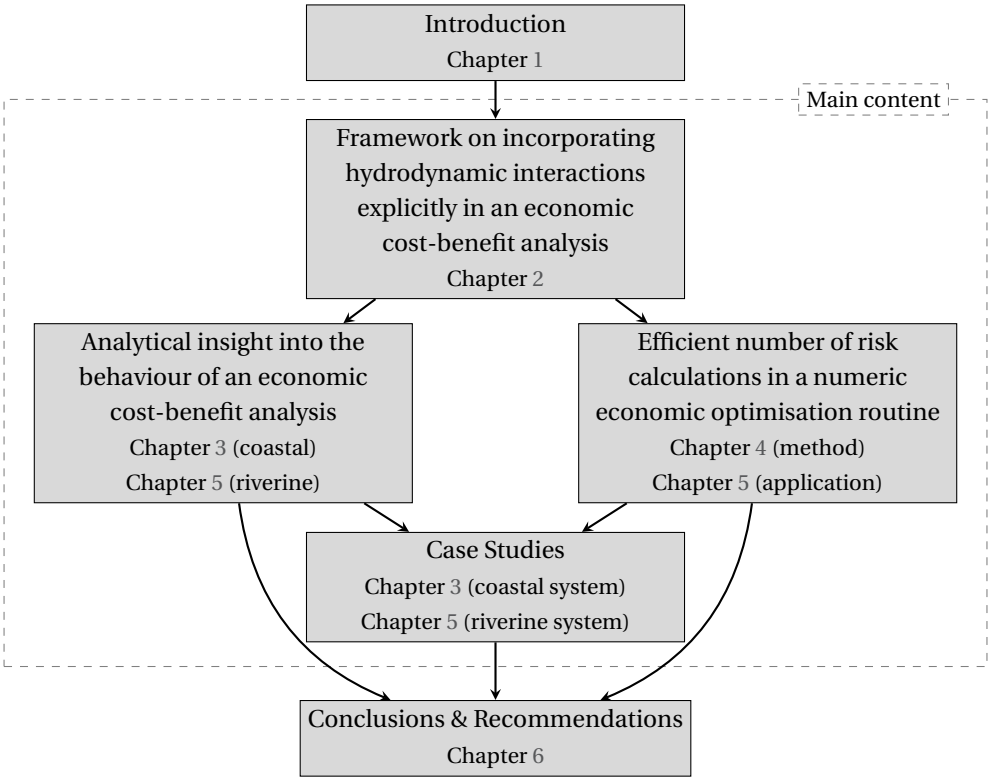

Figure 1.7: Visual thesis outline.

2

HYDRODYNAMIC INTERACTIONS AND ECONOMIC COST-BENEFIT ANALYSES

In the introduction, it was mentioned that hydrodynamic interactions can result in interdependencies in a system of flood defences and thereby change the flood risk estimates within such a system. Because flood risk is an integral part of an economic cost-benefit analysis, it logically follows that these interdependencies influence the optimisation of such an economic cost-benefit analysis in some way. Before the type(s) of influence and the extent of this influence can be explored, the outlines of hydrodynamic interactions and economic cost-benefit analyses are discussed separately. This serves as a step-up for the following chapters where the type of influence and the extent of the influence is examined by explicitly incorporating these interdependencies in economic cost-benefit analyses.

2.1. HYDRODYNAMIC INTERACTIONS

Hydrodynamic interactions are often related to a sequence of events that follow upon a breach in a flood defence system. These interactions can be characterised by different qualifications. One of these qualifications is the character (i.e. severity increasing or decreasing) of the following sequence of events on other flood defences in the same flood defence system [12, 16]. A severity decreasing interaction occurs when the load on the remaining flood defences is less than before the breach. Consequently, a severity increasing interaction occurs when the load on the remaining flood defences is higher than before the breach.

Another way of looking at hydrodynamic interactions is by looking at the type of hazard and the type of flood defence system. From that perspective, classifications such as a coastal flood defence system (hazard stemming from ocean or sea) or a riverine flood defence system (hazard stemming from on or more rivers) are possible. A coastal flood defence system can consist of one or multiple layers of defence (Figure 2.1), whereas a riverine flood defence system is a sequence of flood defences alongside one or more rivers which each can be seen as a line of defence (Figure 2.2).

Figure 2.1: A hypothetical cross section of a coastal flood defence system with a front defence (B) and rear defence (A). In case the front defence breaches, the loads on the rear defence will increase.

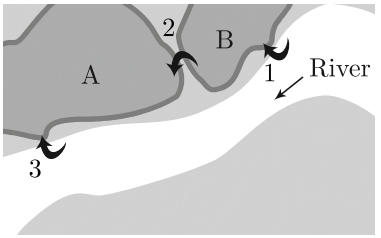

Figure 2.2: Top down-view of a hypothetical riverine system with multiple flood defences. Breaches (indicated by the curved arrows) at area B can impact the flood risk of area A.

A related system concept which has been the subject of previous (optimisation) research is that of multi-layer safety, for example in [18] or in [19] where it is called a 'hierarchical flood protection systems'. This type of system looks to not only include protection, but also to include damage limitation by for example land use planning and evacuation management. Therefore, it can be argued that a coastal and riverine flood defence system are special cases of the multi-layer safety concept However, in this research the choice was made to consider them as different types of systems. In this thesis, the perceived key difference between a multi-layer safety system and a coastal or riverine flood defence system is that not every layer in a multi-layer safety concept interacts with the system hydrodynamics, while this *is* assumed to be the case for the aforementioned coastal and riverine flood defence systems.

2.2. ECONOMIC COST-BENEFIT ANALYSIS

As mentioned in the introduction of Section 1, the fundamental principle behind an economic optimisation, as it is used mostly in The Netherlands, is minimising the total cost. The present value of the total costs is the sum of investment cost and Expected Annual Damages (EAD), where the present value is found by discounting future cash flows by a discount rate. An example of the yearly investment costs and EAD for an (optimised) investment scheme are shown in Figure 2.3 and Figure 2.4, respectively. These figures show some commonly expected behaviour: optimal investments are done infrequently, but periodically (see also Section 2.2.1). Furthermore, barring investments the non-discounted EAD typically have a tendency to increase over time because of for example economic growth and/or an increased load (e.g. more extreme river discharges or annual sea level rise).

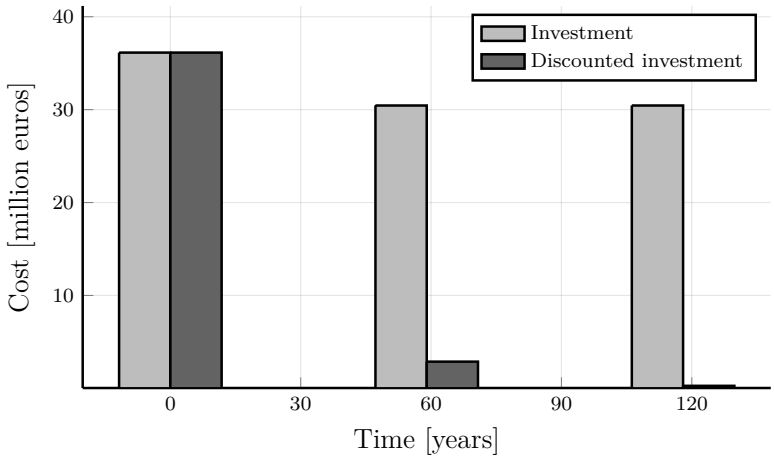

Figure 2.3: Example of the annual investment costs belonging to an optimised investment scheme for a flood defence.

Generally speaking, there are two ways to explore the behaviour and results of a cost-benefit analysis: analytically and numerically. An analytical analysis has the benefit that it provides insight in the fundamental behaviour of an economic cost-benefit analysis through the investigation of its analytical solutions. The downside is that an (understandable) analytical solution is usually only achieved by using simplified relations in the cost-benefit analysis. If for whatever reason these simplifications make the optimisation unattractive from a practical point of view, a numerical cost-benefit analysis might be a better choice. Recent publications/research tend to move to numerical methods. The increased flexibility and freedom in defining investment costs and risk costs make a numerical economic optimisation a logical choice for incorporating hydrodynamic interactions, because these interactions will most likely require the additional flexibility and freedom given by a numerical method. Numerical cost-benefit methods will be dis-

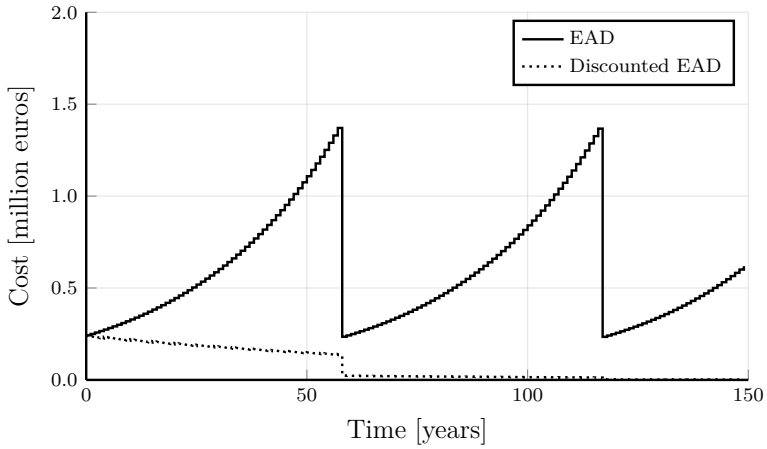

Figure 2.4: Example of the Expected Annual Damages (EAD) belonging to an optimised investment scheme for a flood defence.

cussed further in Chapter 4.

Both analytical and numerical cost-benefit analyses have their uses, and are therefore discussed in this research. Because including hydrodynamic interactions is expected to complicate an analytical cost-benefit analysis, first some existing analytical cost-benefit derivations are discussed and compared (Section 2.2.1). These analytical analyses also serve as a more in-depth, technical introduction into the optimisation of an economic cost-benefit analysis.

2.2.1. ANALYTICAL COST-BENEFIT ANALYSES

The following is an overview and discussion of three studies that researched the analytical economical optimisation of flood defences. These three studies are not meant to give a complete overview of existing literature, however they are considered as important milestones in the development of analytical cost-benefit analyses.

PIONEERING WORK BY VAN DANTZIG

In 1953, a storm which coincided with spring tide caused huge damages in The Netherlands. The damages were huge both in terms of economic losses and loss of life. Shortly thereafter, the first Delta committee was formed. A significant part of the research done by this Delta committee was on how the safety level of Dutch flood defences should be determined. One of these approaches was posed by Van Dantzig, who posed the determination of the optimal safety level of a flood defence as an economic decision problem [9]. Specifically, the sum of discounted investment costs (I) and discounted expected future losses (R) is defined in [9] as the total costs (TC), where the optimal solution follows from minimising the total costs:

$$TC = I + R \tag{2.1}$$

Van Dantzig presented two sets of assumptions in [9] which aid in further defining Eq. 2.1. The first set assumes a linear investment function based on the height increase of a flood defence, with only a single investment at $t = 0$. Furthermore, a constant potential flood damage and an exponentially distributed probability of exceeding a critical water level in an arbitrary year are assumed (Eq. 2.2). These assumptions are used to determine the total costs for a height increase X for the entire future:

$$P_f(X) = c_0 e^{-\alpha H_0} e^{-\alpha X} = P_0 e^{-\alpha X} \tag{2.2}$$

$$TC(X) = C_f + C_v X + \sum_{i=0}^{\infty} P_f(X) \frac{V_0}{(1+r)^i} = C_f + C_v X + P_f(X) \frac{V_0}{r} \tag{2.3}$$

where C_f is the fixed investment cost, C_v is the variable investment cost, P_0 is the initial exceedance probability of the flood defence at its initial height H_0, r is the discount rate, and V_0 is the potential flood damage. In this equation, the multiplication of the exceedance probability and the potential flood damage is the expected losses in an arbitrary year (or Expected annual Damage, EAD).[1] The EAD, investment cost and total cost are also shown graphically in Figure 2.5.

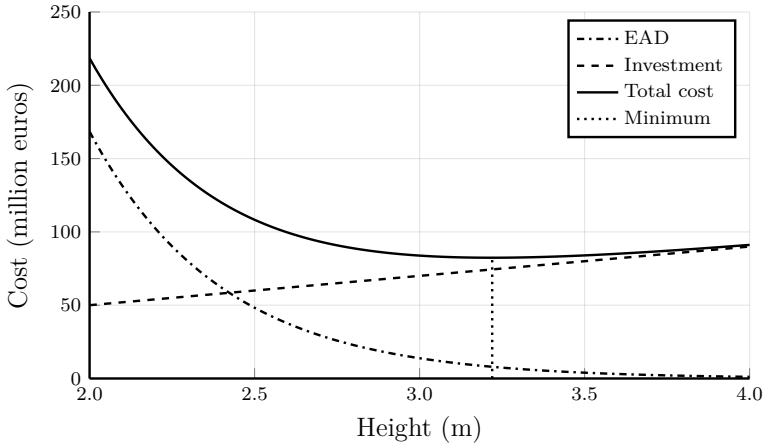

Figure 2.5: Example of an economic cost-benefit analysis for a flood defence. The total costs are the sum of the EAD and investment, and the optimal point can be found at the minimum of the total cost.

The optimal value of X can be found at the minimum of Eq. 2.3, and can be found by taking the derivative of this function to X and equating this derivative to zero. From this, the optimal height increase $\hat{X}_1$ can be expressed as follows:

$$\hat{X}_1 = \frac{1}{\alpha} \ln\left(\frac{P_0 V_0 \alpha}{r C_v}\right) \tag{2.4}$$

[1] This is a simplification of the definition in for example [1], where the multiplication is defined as "really a combination across all floods". If the flood damage is constant across floods, the combination reduces to the multiplication as shown in Eq.2.2. See also Section 1.3 regarding the assumption of a constant flood damage. In this thesis, a variable flood damage is used in Chapter 5.

Eq. 2.4 is equal to equation 6 in [9], though Eq. 2.4 uses different symbols to be consistent with other, similar equations further on in this chapter. Furthermore, Eq 2.4 can be called a 'static' optimisation because the system that is optimised (i.e. the extreme water levels, the flood defence, and the land protected by the flood defence) are modelled to not change over time. In reality, changes within the system are to be expected, notably changes such as economic growth (increasing the potential flood damage), sinkage of the land (decreasing the height of a flood defence), and, in case of a coastal defence, rising sea levels.

Van Dantzig recognised this, and noted that the decrease of safety should be repaired with periodic investments. Specifically, if the sea level rise is η meter per year, after a period of T years a flood defence should be increased by ηT meters (this is labelled as wrong by Eijgenraam, see also Section 2.2.1). Therefore, in the second set of assumptions, the economic growth was assumed to function as a reduction on the discount rate, and the sea level rise/sinkage of land is represented as a yearly occurring reduction on the height of the flood defence. Furthermore, in order to more easily accommodate these assumptions mathematically, the discounting was changed from yearly to continuous compounding. This resulted in the following optimal height increase $\hat{X}_2$:

$$\hat{X}_2 = \frac{1}{\alpha} \ln\left(\frac{P_0 V_0 \alpha}{\left(r - \gamma - \alpha\eta\right) C_v} \cdot \frac{1 - e^{-(r-\gamma-\alpha\eta)T}}{1 - e^{-(r-\gamma)T}} \right) \tag{2.5}$$

where γ is the yearly economic growth, and η is the yearly flood defence height reduction due to for example sea level rise. The period between investments (T) was pre-set to $1/\eta$ years in [9]. Eq. 2.5 is equation 14 in [9], though Eq. 2.5 uses different symbols to be consistent with other, similar equations further on in this thesis. In more recent publications, Eq. 2.5 is revised and expanded both by Vrijling and van Beurden in [21] and Eijgenraam in [20, 22]. These two methods will be described in the following sections.

SEA LEVEL RISE AND OPTIMAL INVESTMENT TIMING BY VRIJLING AND VAN BEURDEN

In [21], Vrijling and van Beurden investigated the impact of an uncertain sea level rise (η) on the optimal height. In their model, the period between investment (T) is determined as part of the optimisation (whereas Van Dantzig pre-set the period), resulting in an optimal period between periodic investments. Vrijling and van Beurden left out economic growth in their analysis, which means that after a period of T years a flood defence should be increased by ηT meters; because economic growth was left out, sea level rise is the only factor that needs to be 'repaired' after some time.

It is assumed that for Van Dantzig, the question when to make the first investment was probably not a question at all. After all, the consequences of the 1953 disaster were still felt, and action had to be taken as quickly as possible. However, in 1990 (when [21] was published), there was no longer an implicit need to improve flood defences as soon as possible. Therefore, Vrijling and van Beurden introduced a 'waiting time' (T_w) for the initial investment. In case this waiting time is zero, the initial investment should still be

made as soon as possible. This waiting time expanded the investment and risk equations in [21] to Eqs. 2.6[2] & 2.7[3]:

$$I = \left(C_f + C_v \cdot \left(X + \eta T_w\right) + \left(C_f + C_v \eta T\right) \cdot \frac{1}{e^{rT} - 1}\right) \cdot e^{-rT_w} \tag{2.6}$$

$$R = \frac{V_0}{r - \alpha\eta} \cdot P_0 \cdot \left(1 - e^{-(r-\alpha\eta)T_w}\right) + \frac{V_0}{r - \alpha\eta} \cdot P_f(X) \cdot \frac{1 - e^{-(r-\alpha\eta)T}}{1 - e^{-rT}} \cdot e^{-rT_w} \tag{2.7}$$

By finding the partial derivative $\frac{\partial TC}{\partial X}$ and equating it to zero, Vrijling and van Beurden found the following expression for the optimal probability of failure (Equation 12 in [21]):

$$\hat{P}_f = \frac{\left(r - \alpha\eta\right) C_v}{V_0 \alpha} \cdot \frac{1 - e^{-rT}}{1 - e^{-(r-\alpha\eta)T}} \tag{2.8}$$

Eq. 2.8 can be rewritten in terms of the initial investment X by equating it to Eq. 2.2:

$$\hat{X}_3 = \frac{1}{\alpha} \ln\left(\frac{P_0 V_0 \alpha}{\left(r - \alpha\eta\right) C_v} \cdot \frac{1 - e^{-(r-\alpha\eta)T}}{1 - e^{-rT}}\right) \tag{2.9}$$

Eq. 2.9 is dependent only on the period T and can be substituted in Eqs. 2.6 & 2.7. The sum of Eqs. 2.6 & 2.7 is the total cost which is now only dependent on the period T and waiting time T_w. In [21], Vrijling and van Beurden mention that the period T is the same regardless of the waiting time T_w, which means the period T can first be found by setting the waiting time T_w to zero (and finding the minimum of the total costs, which now only depend on the period T). After the period T has been found, the waiting time T_w can be found by (again) minimising the total costs which, with the period T now known, only depends on the waiting time T_w.

GLOBAL OPTIMAL SOLUTION BY EIJGENRAAM *et al.*

In 2006 [20] and 2016 [22], Eijgenraam *et al.* again expanded the total cost equation. This expansion encompassed a non-linear investment function and damage costs that depend on the height of a flood defence. Furthermore, Eijgenraam *et al.* proved in [22] that their expanded solution is the global, optimal solution. The non-linear investment cost relation that is used in [22] is shown in Eq. 2.10, while the damage function of [22] is shown in Eq. 2.11.

$$I(h^-, u) = \begin{cases} 0 & \text{if } u = 0 \\ \left(C_f + C_v u\right) e^{\lambda(h^- + u)} & \text{if } u > 0 \end{cases} \tag{2.10}$$

$$S(t) = P_0 e^{\alpha\eta t} e^{-\alpha(H_t - H_0)} \cdot V_0 e^{\gamma t} e^{\zeta(H_t - H_0)} \tag{2.11}$$

[2] Vrijling and van Beurden used a different form of the exponential exceedance probability. Their form has been rewritten into the form of Van Dantzig as shown in Eq. 2.2 for consistency; see also Appendix A.1.

[3] Equation 14 in [21], which should be equal to Eq. 2.7, is incomplete; the complete equation can be found in [23].

In Eq. 2.10, u is the increase in flood defence height, h^- is the height of the flood defence just before heightening, and λ is a non-linear investment constant. In [22] mention is made of an investment relation with two constants as well, but in the remainder of their paper Eijgenraam *et al.* use Eq. 2.10. In Eq. 2.11, $S(t)$ is the expected loss at time t, H_t the height of the flood defence at time t, and ζ a constant representing the increase in damage due to the height increase of a flood defence. The total costs that are minimised in [22] are:[4]

$$I = \sum_{i=1}^{\infty} \left(C_f + C_v u_i\right) e^{\lambda\left(\sum_{l=1}^{i-1} u_l + u_i\right)} e^{-r t_i} \tag{2.12}$$

$$R = \frac{P_0 V_0}{\alpha\eta + \gamma - r} \sum_{i=0}^{\infty} e^{-(\alpha-\zeta)\sum_{l=1}^{i} u_l} \left(e^{\alpha\eta+\gamma-r} t_{i+1} - e^{\alpha\eta+\gamma-r} t_i\right) \tag{2.13}$$

where the optimisation parameters are u_1, u_2, ... and t_1, t_2, ..., which are the increases in height at their corresponding time steps [22].

In [22], a proof is given that shows that the optimal solution is periodic after one or two periods. The solution is periodic after one period in case the first investment does not have to be done immediately (i.e. a waiting time). The solution is periodic after two periods in case there is a 'backlog' in safety (i.e. immediate investment needed, no waiting time). Besides proving that the optimal solution is periodic after one or two periods, another important result from the analysis of [22] is that the optimal periodic increase ($\hat{u}$) should no longer just repair the sea level rise/sinkage of the land, but also account for the economic growth. The optimal periodic time between investments ($\hat{T}$) was found in [22] to be:[5]

$$\hat{T} = \frac{\alpha - \zeta + \lambda}{\alpha\eta + \gamma} \hat{u} \tag{2.14}$$

In case there is a backlog in safety, and immediate investment is required, equations are given in [22] that can be solved for the required initial investment. In principle, these could be used to compare to the results found in Eqs. 2.4, 2.5 & 2.9. However, due to the expanded equations (because of the non-linear investment and non-constant damage relations) this is not straightforward. Fortunately, in earlier work ([20], specifically equation 30) a linear investment relation and constant damage is used to express the optimal initial investment in case of a backlog in safety:

$$\hat{X}_4 = \frac{1}{\alpha} \ln\left(\frac{P_0 V_0 \alpha}{\left(r - \gamma - \alpha\eta\right) C_v} \cdot \frac{1 - e^{-\left(r-\gamma-\alpha\eta\right)T}}{1 - e^{-rT}}\right) \tag{2.15}$$

Comparing Eq. 2.15 and Eq. 2.5, the difference is in the second denominator within the natural logarithm. This difference can be attributed to Van Dantzig incorporating the economic growth by subtracting the economic growth from the discount rate. Therefore,

[4] In [22], two separate discount rates are mentioned: one for the investment costs and one for the expected loss. However, in the applications of [22] a single, common discount rate is used.

[5] The relation between the optimal periodic increase and optimal periodic time can be found in Appendix A.2.

economic growth is applied to both the investment costs and the expected loss costs, where Eijgenraam only adds economic growth to the expected loss costs. The resulting solution of the method in [22] is shown graphically in Figure 2.6. In this figure, it can be seen that the optimal exceedance probability decreases over time, to compensate for economic growth, which was one of the key findings of Eijgenraam *et al.*.

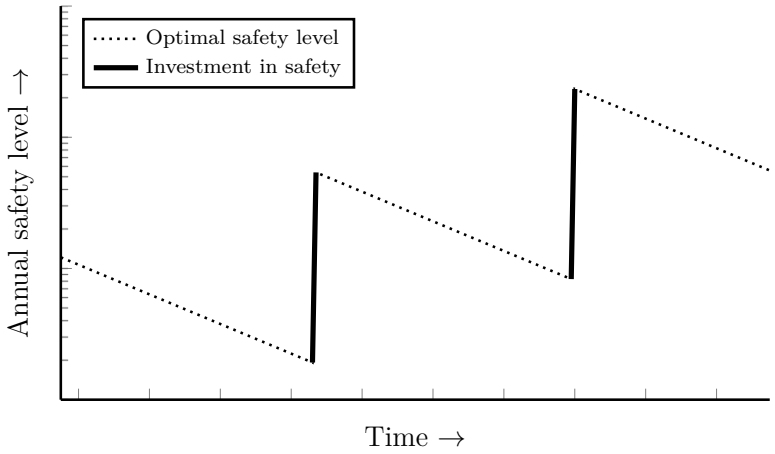

Figure 2.6: Example of an optimal investment scheme using the solution of [22]. In this figure, the periodic investments (i.e. the 'jumps' in safety level) and gradual increase in the optimal safety level can be seen (i.e. each investment leads to a higher safety level than the previous investment).

COMPARISON OF THE REQUIRED INITIAL INVESTMENT

The previous descriptions implicate that the method by Eijgenraam *et al.* is the preferred method. Indeed, it is the most complete description for the relations which are imposed: exponential exceedance probabilities, investment relations which can be linear or exponential and flood damages that depend on the associated flood defence height. For the Dutch situation, as described in [22], these imposed relations seem to work well. Nevertheless, two situations can be thought of where the method by Eijgenraam *et al.* is either too complex or too restrictive. These two situations do not in any way diminish the relevancy of the approach by Eijgenraam *et al.*. Nevertheless, these two situations are worth discussing:

1. When insight is needed in the behaviour of an economic optimisation. This often requires (heavily) simplified relations. See for example [24].

2. When a complex flood defence system is investigated, where the reliability of different components in the system are interdependent; see for example [16]. In this case, flood defences will likely not adhere to the used exponentially distributed probability of exceedance.

The second situation implies more complex flooding probabilities, which can depend on each-other. Incorporating these in an economic optimisation will be done in this research with the help of two types of cases; this incorporation is further described in Section 2.3. On the other hand, the first situation requires simplified solutions which, with broad strokes, describe the behaviour of an economic optimisation. Such a simplified solution could be similar to Eq. 2.4.

However, Eq. 2.4 was shown to be incomplete under the assumption of for example economic growth and/or sea level rise. This raises the question what the magnitude of the error is when compared to the solution given in Eq. 2.15. The missing part of Eq. 2.4 when compared to Eq. 2.15 is named here as $X_{missing1}$), and is chosen in such a way that if $X_{missing1} = 1$, the following equation reduces to Eq. 2.4:

$$\hat{X}_4 = \frac{1}{\alpha}\ln\left(\frac{P_0 V_0 \alpha}{r C_v} X_{missing1}\right) = \frac{1}{\alpha}\ln\left(\frac{P_0 V_0 \alpha}{r C_v}\right) + \frac{1}{\alpha}\ln\left(X_{missing1}\right) \tag{2.16}$$

$$X_{missing1} = \frac{r}{r-\gamma-\alpha\eta} \cdot \frac{1-e^{-(r-\gamma-\alpha\eta)T}}{1-e^{-rT}} \tag{2.17}$$

Eq. 2.17 follows from equating Eq. 2.15 to Eq. 2.16. Assuming that all separate variables in Eq. 2.17 are greater than zero with $r \neq \gamma + \alpha\eta$, two situations can occur for $X_{missing1}$: either $r > \gamma + \alpha\eta$, or $r < \gamma + \alpha\eta$. In case $r > \gamma + \alpha\eta$, the first term and second term of Eq. 2.16 will be positive and larger than one, while in the second situation both terms will be negative with each an absolute value larger than one. This means that $X_{missing1}$ will always be larger than one, under the assumption that all separate variables in Eq. 2.17 are greater than zero with $r \neq \gamma + \alpha\eta$. If the missing part is larger than one, the second term in Eq. 2.16 will always be positive, therefore meaning that the initial investment $\hat{X}_1$ of Eq. 2.4 *underestimates* the initial investment $\hat{X}_4$ by $\frac{1}{\alpha}\ln\left(X_{missing1}\right)$.

If the discount rate is greater than the economic growth, this underestimation can be partly corrected by replacing the discount rate with a discount rate that is reduced with the economic growth (i.e. $r-\gamma$). Note that this is the same substitution that Van Dantzig used in [9], which means that economic growth will also be applied to the investment costs; this is not the case in the solution by Eijgenraam *et al.* ([22]). Therefore, the correction will not be a complete correction, and will not lead to the exact same results as in [22]. Furthermore, this correction places an additional restriction because the discount rate needs to be greater than the economic growth (see also [25]). However, it is interesting to see how much this correction reduces the size of $X_{missing1}$.

$$\hat{X}_4 = \frac{1}{\alpha}\ln\left(\frac{P_0 V_0 \alpha}{(r-\gamma) C_v} X_{missing2}\right) \tag{2.18}$$

$$X_{missing2} = \frac{r-\gamma}{r-\gamma-\alpha\eta} \cdot \frac{1-e^{-(r-\gamma-\alpha\eta)T}}{1-e^{-rT}} = \frac{r-\gamma}{r} \cdot X_{missing1} \tag{2.19}$$

Eq. 2.18 is the formulation of Eq. 2.15 with the reduced discount rate and a new missing part called $X_{missing2}$. This $X_{missing2}$ is defined in Eq. 2.19, and, compared to

$X_{missing1}$, is $\frac{r-\gamma}{r}$ smaller. In case r is equal to 0.04, and γ is equal to 0.02, $X_{missing2}$ will be half the size of $X_{missing1}$. However, due to the logarithm that is applied in order to get to the actual initial height increase, the reduced discount rate results in the *initial height* to be increased by a constant of $\ln(0.5)/\alpha$.

In more practical terms, the previous methods have been compared to the solution of Eijgenraam *et al.* for dike rings in need of immediate heightening, based on Tables 1 and 2 in [22]. Additionally, the case study of Van Dantzig as described in [20, Table 4.1] is added as well and called '1956'. In order to compare all methods, only the initial increase in height is compared (as the static optimisation of Van Dantzig does not prescribe a periodic solution). The baseline reference is the solution of [22], with a linear investment cost relationship and constant damage (i.e. λ and ζ set to zero). All methods use a discount rate (r) of 0.04 and an economic growth (γ) of 0.02. The results are shown in Figure 2.7.

Figure 2.7 shows that indeed the 'static' solution of Van Dantzig consistently underestimates the correct solution of Eijgenraam *et al.*. The adjusted version (i.e. Eq. 2.18 with $X_{missing2}$ set to one), can be applied because the discount rate (0.04) is greater than the economic growth (0.02) and performs better. Furthermore, Figure 2.7 shows the other optimal initial investment sizes of the methods discussed in previous sections. 'Dantzig dynamic' is Eq. 2.5, while 'Vrijling dynamic' is Eq. 2.9. Because Eq. 2.9 does not contain any economic growth, it consistently underestimates the solution of Eijgenraam *et al.*. On the other hand, Eq. 2.5 seems to have a bias for underestimation as well, which is probably due to applying economic growth to the investment costs, which makes investments more expensive than the solution of Eijgenraam *et al.*.

Interestingly, the 'Dantzig static adjusted' seems to perform similarly to the 'Dantzig dynamic' solution of Eq. 2.5 in Figure 2.7. This can be attributed to the specific combination of values used in Figure 2.7. The values for climate change (η) are relatively low when compared to the impact of economic growth (γ) and discount rate (r) on Eq. 2.5; the impact of the climate change parameter η will become more profound for larger values of η and will therefore probably lead to larger deviations between 'Dantzig static adjusted' and 'Dantzig dynamic'.

The previous shows that while the error of a static optimisation such as shown in Eq. 2.4 is significant, the result is still usable for gaining insight into the behaviour of an economic optimisation. Furthermore, with a relative straightforward change (i.e. Eq. 2.18), the numeric answer can be improved under certain conditions. Whether or not to apply this change depends on the case characteristics (i.e. $r > \gamma$) and whether or not the improvement in the numerical answer is really needed, especially in the context of gaining insight into the behaviour of an economic optimisation.

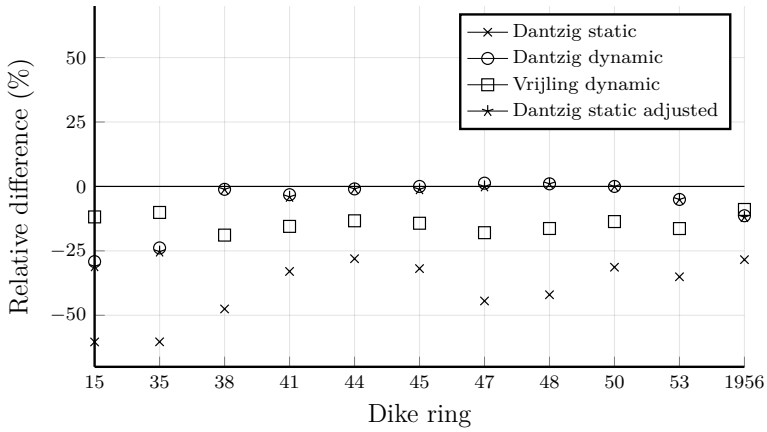

Figure 2.7: Relative differences for the approaches by Van Dantzig [9] and Vrijling and van Beurden [21] compared to the solutions as presented by Eijgenraam *et al.* [22] for the initial height increase. In this figure, the solutions as presented in [22] were re-calculated with a constant damage and a linear investment function. Furthermore, 'Dantzig static adjusted' refers to Eq. 2.18 with $X_{missing2}$ set to one. The relative difference of a solution to the one presented by Eijgenraam *et al.* were found by dividing the difference of the two solutions by the solution of Eijgenraam *et al.*.

2.3. IMPACT OF INCLUDING HYDRODYNAMIC INTERACTIONS IN AN ECONOMIC COST-BENEFIT ANALYSIS

In Section 1.3, a short overview was given of how hydrodynamic interactions can impact the flood risk and therefore the EAD (Expected Annual Damage) of an area protected by a flood defence system. Two types of flood defence systems (coastal and riverine) were introduced in Section 2.1 together with a short overview of the type of impact that hydrodynamic interactions can have on coastal and riverine flood defence systems. Section 2.2 gave an overview of some selected analytical optimisations of an economic cost-benefit analysis for flood defences. From these sections, it can be concluded that hydrodynamic interactions will directly impact the EAD estimates in an economic cost-benefit analysis, and therefore the optimisation of an economic cost-benefit analysis (i.e. economic optimisation). Therefore, hydrodynamic interactions impact an economic optimisation at its core (see also the generic framework in Figure 2.8).

As an economic optimisation can be done both analytically and numerically, the choice between these two approaches will depend on what kind of answer is needed. In case insight is needed into the behaviour of the solution, an analytical optimisation seems to be an obvious choice. On the other hand, in case a more complex system is investigated, a numerical optimisation will be a better choice as it will be a more practical choice and/or be able to more accurately model the aforementioned complexities. An example where an analytical optimisation won't be (directly) applicable is when an existing numerical 2D flooding model needs to be used directly in an economic optimi-

sation.

A more complex system will most likely involve more and more complex risk calculations as well, which will increase the computational cost of these risk calculations. If this computational cost becomes too high, attention will need to be paid to doing these risk calculations as efficiently as possible. This is summarised in Figure 2.9.

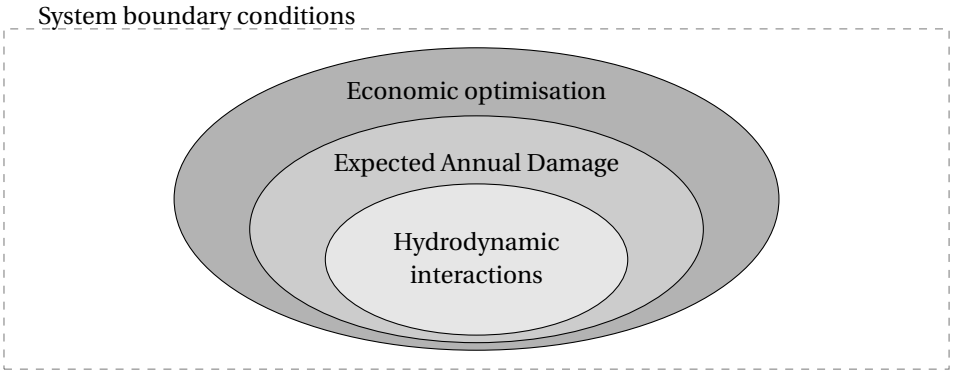

Figure 2.8: Generic framework for an economic optimisation with hydrodynamic interactions. The hydrodynamic interactions will affect the risk estimates, which in turn will affect the Expected Annual Damage (EAD) estimates and thus the economic optimisation. However, all these rings will in some way be affected by the system boundary conditions.

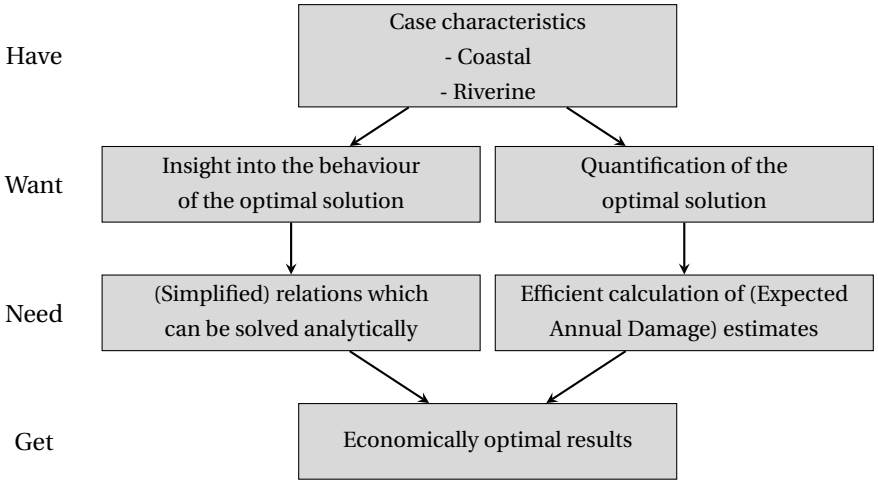

Figure 2.9: Economic optimisation: starting from a type of case, an analytical and/or numerical economic optimisation can be made depending on what the desired type of answer needs to be.

3

ANALYTICAL AND NUMERICAL ECONOMIC OPTIMISATION OF A COASTAL FLOOD DEFENCE SYSTEM

Using the analytical insight of the analysed cost-benefit analyses in Chapter 2, this chapter looks to extend an analytical economic optimisation towards a relatively simple flood defence system with interdependence. This flood defence system is a coastal system with a front defence (e.g. a storm surge barrier) and a rear defence (e.g. an earthen levee).

Furthermore, a numerical approach is developed in order to get rid of limitations imposed by the analytical derivation. This approach uses an existing numerical economic optimisation method developed by by Zwaneveld and Verweij [27] for a study regarding the lake IJssel case study. Where the analytical derivation focuses on the impact of interdependence on how much should be invested, the numerical approach factors in time as well by looking at both how much and when investments should be made.

The contents of this chapter have been published in [26].

3.1. INTRODUCTION

Coastal areas are often densely populated [28]. In order to protect the low-lying coastal areas against flooding, flood defences can be constructed [29]. These flood defences can be part of a flood defence system with multiple lines of defence. A typical example of a coastal flood defence system with multiple lines is that of a storm surge barrier closing off a large water body and levees surrounding the large water body. Such a system is shown in Figure 3.1, where the barrier is the front defence and the levees are the rear defences. Examples of such coastal flood defence systems can be found in Lake IJssel and the Eastern Scheldt in the Netherlands, and in Neva Bay, close to Saint Petersburg in Russia.

Figure 3.1: Simplified cross section of a front defence (B) and rear defence (A).

The front defence in Figure 3.1 affects the hydrodynamic conditions at the rear defence, for example by reducing surge levels. Reduced surge levels result in a reduced load at the rear defence, which means the flood risk is reduced as well. A different flood risk implies that an economic optimisation will be affected as well, because in an economic optimisation the sum of investment and risk costs is minimized in order to obtain economically optimal safety targets for the flood defences (see also Sections 3.3 & 3.4). As the load reduction influences the risk cost, including this in an economic optimisation can possibly lead to a different set of economically optimal safety values for both the front and rear defences. On the other hand, not including the interaction between the two defences simplifies the economic optimisation, because the front and rear defence can then be evaluated independently from each other. For (a) analyzing the flood risk and (b) establishing economically optimal safety targets it is, hence, important to model the system appropriately, accounting for the load reduction when necessary.

The economic optimisation of a single line (coastal) flood defence system has been discussed by a number of authors over the years; an example of a recent application can be found in [30]. Already in 1956, Van Dantzig described the economic optimisation of a homogeneous dike ring [9]. This case and the work by Van Dantzig has been revisited and extended by a number of authors, for example in [20] with the addition of economic growth, or in [31] where the impact of uncertainty is discussed. Some analytical cost-benefit analyses were discussed in Chapter 2 as well.

The fundamental method behind these economic optimisations of single line flood defence systems has also been extended to flood defence systems with multiple lines or elements of defence. For example, [32] described optimising elements in a dike ring, while a polder terminal case was described in [33]. Multiple lines of defence are some-

times also referred to as 'multi-layer safety' (e.g. [18, 24, 34, 35]) or as 'hierarchical flood protection systems' [19]. In these descriptions of multiple lines of defence, the lines of defence can also include measures such as evacuation or improved spatial planning; for example, see [36] regarding optimal flood plain planning or [37] regarding optimal levee setback and height. A coastal flood defence system was analyzed in a case study by [27], but focused on the results for the Lake IJssel case in The Netherlands.

A generic description of the economically optimal safety targets of a coastal flood defence system can, for example, provide the conditions in which a front defence is needed, or how much the economically optimal safety target of a rear defence is affected by the load reduction of a front defence. At the time of writing, such a generic description has not been presented yet. Therefore, the aim of this chapter is to develop a framework in order to assess whether including the influence of such a load reduction influences the economically optimal safety targets of a coastal flood defence system.

In order to quantify the effect of a load reduction in a coastal flood defence system (Section 3.2), two economic optimisation approaches are proposed. The first is a simplified economic optimisation method which is derived in Section 3.3 and is partly based on earlier work in [38], and is used to describe the characteristics of the economically optimal safety targets of a coastal flood defence system. The second approach is a flexible numerical approach which removes a number of the limitations of the simplified method, making it more suitable for real world applications. This numerical approach, described in Section 3.4, combines the existing economic optimisation method as used in [27], and couples it with a risk framework which is inspired by system flood risk frameworks such as described in [14]. Emphasis is placed on the applicability and tractability from an engineering perspective.

Finally, the Galveston Bay near Houston is considered as a hypothetical case study in Section 3.5. The Galveston Bay area has millions of inhabitants and represents a large economic value. It does not yet have an integral flood defence system, but the feasibility of such a system is being investigated because it is situated in a hurricane prone area (e.g. see [39]). Even though this study describes an economic optimisation of a coastal flood defence system with a front and rear defence, the numerical approach is flexible enough to be generically applied to flood defence systems with two lines of defence. With modifications to the used risk method and optimisation algorithm, the numerical approach can also be used for more than two lines of defence.

3.2. FLOOD RISK OF COASTAL SYSTEMS

In coastal systems, as shown in Figure 3.1 a front defence will reduce the load on a rear defence; thereby improving the reliability of the rear defence. In the following, this reliability improvement is first described from a physical point of view (Section 3.2.1). This explanation is then used to incorporate the reliability improvement in a set of risk equations (Section 3.2.2). Furthermore, in the remainder of this paper the term 'coastal systems' is used for coastal flood protection systems with a front and rear defence.

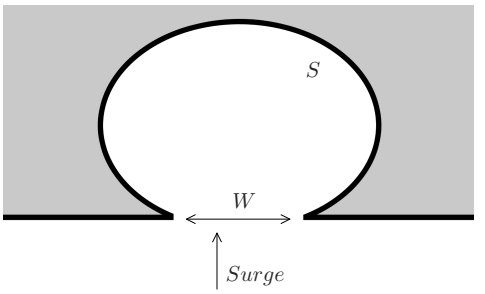

Figure 3.2: Top view of a typical basin, with inlet width W and surface area S.

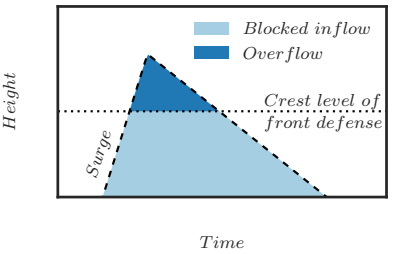

Figure 3.3: A front defence can block surge from flowing into a basin; however, any overflow will still enter the basin.

3.2.1. LOAD REDUCTION BY A FRONT DEFENCE

A functioning front defence blocks partly, or even completely, the inflow into the large body of water behind the front defence. Examples of such front defences are dams or storm surge barriers (see also Section 3.1). In this chapter, the inflow blockage is seen as the primary source of load reduction. However, the effects of this load reduction depend on the properties of the basin containing the large body of water. In the following, this reduction is described from a physical stance for a subset of coastal flood defence systems that fit the description of a short basin where the 'pumping mode' assumption is valid (length of the basin $\ll$ tidal wave length).

A front defence is typically built near the inlet of a basin, denoted by width W in Figure 3.2. The extra inflow entering the basin during a storm event depends on the amount of blockage by the front defence. Typically, less inflow will be able to enter the basin as the front defence height increases. This is illustrated in Figure 3.3.

The inflow due to the storm event will result in increased basin water levels inside the basin, where the amount of basin water level increase depends on the basin surface area (S in Figure 3.2). However, as strong winds usually occur during storm events, wind setup will at least partially negate the reduction of basin water levels, as wind setup is inversely related to basin water level (e.g. see [40]); this is particularly noticeable in shallow basins. At some point, any further increase of the front defence height will no longer result in a (significant) decrease of the basin water level. Either the front defence already completely blocks the surge inflow, or the inflow reduction is negated by an increased wind setup. In other words, at some point the load reduction by the front defence will be constant, which in the remainder of this paper will be referred to as the 'maximum load reduction'.

3.2.2. ANNUAL SYSTEM RISK

Based on [41], system failure is defined as the situation where at least one of the flood defences has failed. Furthermore, risk is defined as the probability of failure times the

damage due to failure. The annual system risk (C_R, \$/year) of a coastal flood defence system can then be described as a summation of the annual risk per flood defence:

$$C_R = P_A D_A + P_B D_B \tag{3.1}$$

$$P_A = P_B P_{A|B} + P_{\overline{B}} P_{A|\overline{B}} \tag{3.2}$$

where P_B is the failure probability of the front defence, and $P_{\overline{B}}$ is the complement of P_B. The failure probability of the rear defence, P_A, is found using the chain rule for probability and the law of total probability. Furthermore, the conditional failure probabilities of the rear defence, dependent on the failure (P_B) or functioning of the front defence ($P_{\overline{B}}$), are $P_{A|B}$ and $P_{A|\overline{B}}$, respectively. Finally, D_A and D_B (both in \$) are the damages that belong to the failure of the rear and front defence, respectively, and are assumed to be otherwise independent of the performance of the defences (i.e. the expected damage if both A and B fail is $D_A + D_B$).

3.3. SIMPLIFIED ECONOMIC OPTIMISATION

3.3.1. GENERAL

The purpose of a simplified economic optimisation is to explore the behavior of the economically optimal safety levels of a coastal flood defence system with a front and rear defence. The simplifications are made both in the system description (i.e. Figure 3.1), and in the economic optimisation assumptions (Section 3.3.1). The economic optimum is defined as the minimum of the total costs, similar to, for example, [9, 20]:

$$\min\left\{TC = \sum PV(C_R) + \sum PV(C_I)\right\} \tag{3.3}$$

where TC is the total cost, $\sum PV(C_R)$ is the summed present value of the risk costs and $\sum PV(C_I)$ is the summed present value of the investment costs; both the risk and investment costs are defined in Section 3.3.2. Using the total cost equation, further equations for the economically optimal safety targets for both the front and rear defence are found in Section 3.3.3. Finally, the effect of including the load reduction by a front defence is discussed in Section 3.3.4.

For this section, the flood damages in Eq. 3.1 are solely based on economic valuations of damages. In a complete risk evaluation, concepts such as individual risk and societal risk should be included (e.g. see [10]). An overview of risk acceptance measures can be found in, for example, [29]. Furthermore, time dependent processes such as sea level rise or economic growth are ignored in this section. Ignoring these processes means, for the economic optimisation, that only a single investment needs to be calculated. This investment is assumed to be done immediately at the start of the strengthening project; these assumptions reduce the investment term of Eq. 3.3 to C_I, because there is only a single term which does not need to be discounted. Including time dependent processes

(e.g. see [20]) necessitates repeated investments over time, and are an integral part of the numerical economic optimisation in Section 3.4.

3.3.2. RISK AND INVESTMENT COSTS

Discounting the annual risk of Eq. 3.1 with a real interest rate (r, > 0) over an infinite time horizon is a geometric sequence (e.g. [9]), which converges as follows:

$$\sum_{t=0}^{\infty} PV(C_R) = P_A \frac{D_A}{r} + P_B \frac{D_B}{r} \tag{3.4}$$

where $PV(C_R)$ is the present value of the risk cost of a system with a front and rear defence.

The investment cost relations are chosen similarly to for example [9] & [24], assuming linear functions dependent on the crest level of the defence. Because the investment is chosen to be done immediately at the start of the strengthening project, the related costs do not need to be discounted:

$$C_{I,i} = C_{f,i} + C_{v,i} h_i \tag{3.5}$$

where $C_{I,i}$ is the investment cost for flood defence i (which is either A or B). Furthermore, $C_{f,i}$ and $C_{v,i}$ (both > 0) are respectively the fixed and variable cost to strengthen flood defence i to height h_i. Linear investment functions are a simple way of depicting the investment costs; other types of investment functions are treated in Section 3.4.

3.3.3. ECONOMICALLY OPTIMAL FAILURE PROBABILITIES

The economic optimum was defined earlier as the minimum of the total costs. The optimal values, corresponding to the location of the minimum of the total costs, can be found with the partial derivatives of the total cost equation. However, the failure probabilities have not been defined yet. It is assumed that a failure probability is dependent on the height h of a flood defence, and therefore a probability distribution dependent on this flood defence height is used to get to the associated annual failure probability P. For this simplified economic optimisation, the annual failure probabilities of the flood defences are simplified from annual probability of exceedance of safety level to annual exceedance of crest level h, making the assumption that overflow/overtopping is the dominant failure mechanism (analogue to [9, 20, 24]). Furthermore, it is assumed that the annual extreme water level follows an exponential distribution with parameters $\alpha \geq 0$ and $\beta > 0$; other failure mechanisms besides overflow/overtopping and other distribution types are discussed in Section 3.4:

$$P = 1 - F(h) = \exp\left(-\frac{h-\alpha}{\beta}\right) \tag{3.6}$$

where h is the height of either the front defence (h_B) or the rear defence (h_A). The parameters α and β differ between the front and rear defence. For the rear defence, as the load on the rear defence is influenced by the front defence, the parameters for the rear defence can also differ depending on the state (failure/non-failure) and safety level of the front defence. The optimal values of the front and rear defence height can now be found by taking the partial derivatives of the total cost with respect to h_A and h_B, and equating these to zero (i.e. $\frac{\partial TC}{\partial h_B} = 0$ in Eq 3.7 and $\frac{\partial TC}{\partial h_A} = 0$ in Eq 3.8):[1]

$$\frac{\beta_B C_{v,B} r + \beta_B D_A \left(\widehat{P}_B \frac{\partial \widehat{P}_{A|B}}{\partial h_B} + \widehat{P}_{\overline{B}} \frac{\partial \widehat{P}_{A|\overline{B}}}{\partial h_B} \right)}{D_B + D_A \left(\widehat{P}_{A|B} - \widehat{P}_{A|\overline{B}} \right)} = \widehat{P}_B \tag{3.7}$$

$$\left(\widehat{P}_B \frac{\widehat{P}_{A|B}}{\beta_{A|B}} + \widehat{P}_{\overline{B}} \frac{\widehat{P}_{A|\overline{B}}}{\beta_{A|\overline{B}}} \right) = \frac{C_{v,A} r}{D_A} \tag{3.8}$$

where the circonflexe above a variable indicates the economically optimal value of that variable. In earlier work ([38]), simplified versions of these equations above were derived. The relation between Eqs. 3.7 & 3.8 and this earlier work is shown in Appendix B.2.

Furthermore, Eq. 3.7 contains the derivatives of the conditional failure probabilities of the rear defence with respect to the height of the front defence. The expected behavior of the failure probability of the rear defence as a function of the height of the front defence can be explained using the load reduction description of Section 3.2.1. This load reduction indicates that a higher front defence results in lower failure probabilities of the rear defence. Sketches of the conditional failure probabilities of the rear defence are shown in Figure 3.4 & 3.5.

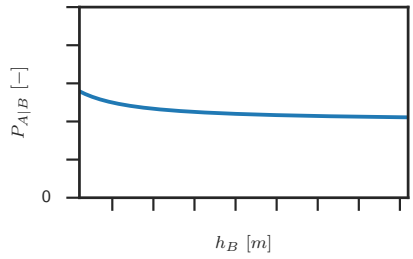

Figure 3.4: Even if the front defence has failed, a higher/stronger front defence (h_B) might still reduce the inflow, resulting in a lower $P_{A|B}$.

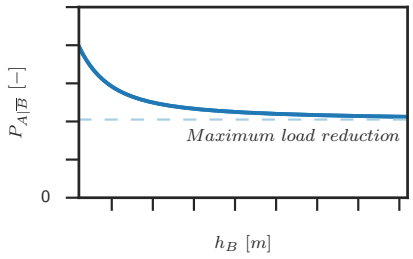

Figure 3.5: A higher, functioning front defence (h_B) should result in a smaller $P_{A|\overline{B}}$, but is limited by the maximum load reduction (Section 3.2.1).

The derivatives of the functions in Figure 3.4 & 3.5 start out negative, but both derivatives are assumed to converge to zero as the front defence becomes higher and the point

[1] A more elaborated derivation can be found in Appendix B.1.

of the maximum load reduction (see Section 3.2.1) is achieved. If these derivatives are indeed zero, Eq. 3.7 can be simplified to Eq. 3.9:

$$\frac{\beta_B C_{v,B} r}{D_B + D_A \left(\widehat{P}_{A|B} - \widehat{P}_{A|\overline{B}} \right)} = \widehat{P}_B \tag{3.9}$$

Wrongfully using the simplified Eq. 3.9 instead of Eq. 3.7 will lead to an incorrect, larger economically optimal failure probability of the front defence. This also follows from the underlying assumption of Eq. 3.9, which assumes that the maximum constant load reduction is valid for the entire range of safety values for the front defence; this assumption overestimates the load reduction effect of a low front defence on a rear defence.

3.3.4. IMPACT OF A LOAD REDUCTION ON THE OPTIMAL SAFETY TARGETS

If no load reduction by the front defence on the rear defence is assumed, the two defences can be evaluated independent of each other. In for example [24], an economically optimal solution for a single flood defence was derived. This single flood defence was characterised similarly as in Section 3.3.3, with a linear investment relation and exponential failure probabilities. The solution as found in [24] is shown in Eq. 3.10, although in a different notation:

$$\widehat{P}_{i,single} = \frac{\beta_i C_{v,i} r}{D_i} \tag{3.10}$$

where i can either be B for the front defence, or A for the rear defence. Eqs. 3.7 & 3.8 reduce to Eq. 3.10 when no load reduction is used ($\widehat{P}_{A|B} = \widehat{P}_{A|\overline{B}}$, $\frac{\partial \widehat{P}_{A|B}}{\partial h_B} = \frac{\partial \widehat{P}_{A|\overline{B}}}{\partial h_B} = 0$). The following can be said regarding the influence of a load reduction, when comparing the solutions with and without load reduction:

Optimal front defence failure probability: The optimal front defence failure probability with load reduction will be equal to, or smaller than, the optimal failure probability without load reduction, because it not only needs to cover the risk of the front defence, but also a part of the risk of the rear defence. The equation with load reduction ($\widehat{P}_B$, Eq. 3.7) has an extra risk term in the denominator when compared to the solution without load reduction ($\widehat{P}_{B,single}$, Eq. 3.10). Because all elements in this extra term are positive, and because $\widehat{P}_{A|B} \geq \widehat{P}_{A|\overline{B}}$, the optimal failure probability with load reduction is equal to, or smaller than, the optimal failure probability of a single flood defence. This can also be seen visually in a hypothetical application in Appendix B.3.

Optimal front defence height: Because the height and the failure probability of a front defence are linked via the exponential distribution of Eq. 3.6, this means the optimal height of the front defence with load reduction is higher than, or equal to, the

height of the front defence without load reduction. This can also be seen visually in a hypothetical application in Appendix B.3.

Optimal rear defence failure probability: Because of the beneficial influence of the front defence, the optimal rear defence failure probability with load reduction will be equal to, or smaller than the value without load reduction. The optimal solution for the rear defence (Eq. 3.8) is bound between $\widehat{P}_{A|B}$ and $\widehat{P}_{A|\overline{B}}$, depending on the value of the optimal front defence failure probability $\widehat{P}_B$. Assuming that $\widehat{P}_{A|B} \approx \widehat{P}_{A,single}$, this means that the optimal rear defence failure probability with load reduction ($\widehat{P}_A$) is equal to, or smaller than the value without load reduction ($\widehat{P}_{A,single}$). This can also be seen visually in a hypothetical application in Appendix B.3.

Optimal rear defence height: The optimal height of the rear defence with load reduction is difficult to predict a priori: according to the exponential distribution, a smaller optimal failure probability should lead to a higher optimal height of the rear defence with load reduction. However, two different exponential distributions have been assumed for the rear defence, conditional on whether or not the front defence has failed. As the conditional failure probability with a functioning front defence ($\widehat{P}_{A|\overline{B}}$) becomes more dominant (which occurs when the front defence failure probability decreases), the optimal height could also go down, because the exponential distribution for a rear defence conditional on a functioning front defence leads to lower heights (since $\beta_{A|B} \geq \beta_{A|\overline{B}}$). Based on the hypothetical application in Appendix B.3, it is expected that the height goes down.

In order to provide a more explicit description of the behavior of the height of the rear defence, the expression for the rear defence failure probability (Eq. 3.2) is approximated with a single exponential distribution, which consequently also leads to a simpler expression of the optimal rear defence failure probability:

$$P_A \approx e^{-\frac{h_A - a_A}{\beta_X}} \tag{3.11}$$

$$\widehat{P}_A \approx \frac{C_{v,A} r \beta_X}{D_A} \tag{3.12}$$

where β_X decreases for smaller values of the front defence failure probability (P_B), and is bound between $\beta_{A|\overline{B}}$ and $\beta_{A|B}$ (with $\beta_{A|B} \geq \beta_{A|\overline{B}}$). Combining Eqs. 3.11 & 3.12 leads to an approximate expression for $\widehat{h}_A$. If the derivative with respect to the front defence failure probability (P_B) of this approximation is greater than zero, the optimal height of the rear defence ($\widehat{h}_A$) is expected to decrease for lower (optimal) failure probabilities of the front defence (P_B):

$$\frac{\partial \widehat{h}_A}{\partial P_B} > 0 \;\rightarrow\; \beta_X < \exp\left(-1 - \ln\left(\frac{C_{v,A} r}{D_A}\right)\right) \tag{3.13}$$

Because the upper limit of β_X is $\beta_{A|B}$, it follows that the derivative will be positive, as long as the right-hand side of Eq. 3.13 is larger than $\beta_{A|B}$. In practice, the term $\frac{C_{v,A}r}{D_A}$ is expected to often be (much) smaller than one, which in turn leads to the right-hand side of Eq. 3.13 being (much) larger than one. This indicates that, in practice, a positive derivative can be expected, which means that the optimal height of the rear defences is expected to be smaller than or equal to the optimal height without load reduction.

In conclusion, this section shows a formal reasoning why in the past flood defence systems with multiple lines of defence were built. Intuitively, building a front defence reduces the load on a rear defence, which should also reduce the required (optimal) height of a rear flood defence. The benefit of the formal treatment in this section is that, from an economic perspective, some key factors in the optimal safety targets of a coastal system were identified. Even considering the limitations imposed in this section in order to get to an analytical answer, these key factors can be used to indicate when the impact of a load reduction on the optimal safety targets is significant or not. The insight gained in this section will be applied in a (hypothetical) case study in Section 3.5.

3.4. NUMERICAL ECONOMIC OPTIMISATION

In order to cope with more complex conditions than described hitherto in this chapter, a numeric approach is proposed, shown in Figure 3.6. This approach is an more specific version of the general framework of Figure 2.8 in Section 2.3, and describes the necessary steps to go from a system description of a coastal flood defence system to the numerical economic optimal safety targets of the flood defences. The description of the approach focuses on the practical applicability and tractability of the approach and its parts from an engineering perspective. Note that the approach assumes that a flood defence type and cost function does not change over time. If, for example, an earthen levee needs to be compared with a concrete wall, multiple runs of the approach are needed. The steps in a single run are:

- Starting from the system description, with a predetermined system configuration of flood defences, a system risk estimate is produced. This risk estimate is used to prescribe per flood defence the hydraulic loads, fragility functions and damage models. See also Section 3.4.1.

- The numerical economic optimisation finds the optimal system configuration from a set of discrete safety levels for the flood defences. Each combination of safety levels needs to have accompanying (investment) cost and flood risk values, see also Section 3.4.3.

- The (investment) costs are usually found using the system description and the type of flood defence, and need to be able to produce cost figures for the discrete set of safety levels. See also Section 3.4.2.

- Finally, the flood risk and (investment) cost values are used in a numerical economical optimisation, which also uses a number of system specific input parameters such as the rate of economic growth. See also Section 3.4.3.

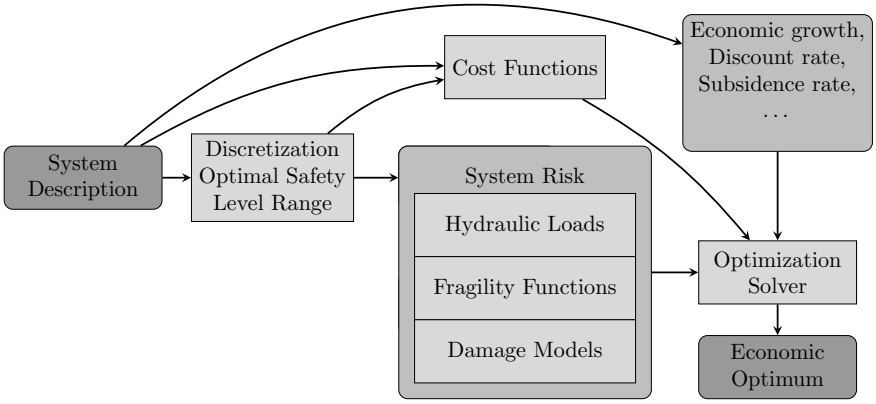

Figure 3.6: Overview of necessary steps in the numeric approach used to obtain economic optimal values for a coastal flood defence system.

3.4.1. RISK CHARACTERISATION

Risk is defined as probability of failure times the damage due to failure. Conceptually, the reliability of a flood defence is expressed by means of a reliability equation Z:

$$Z = Strength - Load \tag{3.14}$$

where failure is defined as $Z < 0$. Both the strength and (hydraulic) loads are usually considered as uncertain.

HYDRAULIC LOADS

Load distributions for the front defences can be found by analyzing historical datasets, running hydrodynamic models, or a combination of the two. However, load distributions for the rear defences can often only be found by means of hydrodynamic models, assuming the system with both a front and rear defence does not exist yet.

A common technique to acquire a distribution from an hydraulic model is Monte Carlo sampling, where a large number of model runs are made in order to approximate the load distribution. Usually a large number of samples are required, specifically for reasonable estimates of the tails. The number of required samples can be reduced by using techniques such as Importance Sampling (as applied in for example [16]).

Depending on the complexity of the hydrodynamic model and the number of required samples, approximating these load distributions can be computationally intensive. Because of this, it is recommendable to do these computations asynchronous of

the economic optimisation model. These computations could, for example, be stored in a table, which allows the economic optimisation model to quickly look up the required values during its run; this approach is similar to what is proposed in for example [14].

FRAGILITY CURVES

Fragility curves are a way to represent the strength term in Eq. 3.14 and are governed by the failure modes and type of flood defence. In the case of flood defences, fragility curves often show the probability of failure as a function of the water level. There are multiple, possibly correlated, ways a flood defence can fail (failure mechanisms), and the water level does not necessarily need to exceed the crest height to induce failure (e.g. due to piping). In an economic optimisation, typically a large number of possible flood defence designs are compared. These designs can, for example, vary the height of a flood defence. This also means that each flood defence alternative needs a fragility curve. An application of height-based fragility curves can be found in Section 3.5.1. For a more in-depth description on constructing fragility curves, see for example [42] or [43].

DAMAGE MODELS

Damage modelling entails combining flooding scenarios with the expected economic damage and fatalities per flooding scenario [10]. A flooding scenario is defined in [10] as "a unique sequence of events following the failure of a flood defence at one or more locations under specific high water conditions". Recognizing that in reality a large number of flooding scenarios are possible, and that these scenarios commonly use computationally intensive 2D models, two proposals were made in [10] for keeping the damage modelling tractable:

1. Define stretches of flood defences which approximately show the same flooding pattern, independent of where the actual breach occurs in that particular stretch.

2. Find a limited set of flooding scenarios which represent the most likely scenarios.

However, the state of a flood defence will influence the most likely scenario. As an example, the most likely flooding scenario without a flood defence compared with the failure of a five meter high flood defence will likely be significantly different. A possible way of including this effect is shown in [20], where a constant ζ was introduced which depicts the "increase of loss per cm dike heightening". A more generally applicable approach, especially for potentially widely varying safety levels, would be re-running the damage modelling for a set of representative safety levels.

3.4.2. INVESTMENT COSTS

The linear investment function of Eq. 3.5 in Section 3.3.2 is approximately valid for small increments of the height of a flood defence; this limitation was already mentioned in [9]. For earthen levees a convex function might be more suitable. This can be explained when comparing the increase of height versus the increase of the associated cross-sectional

area: the relative increase in cross-sectional area will be more than the relative height increase (see also for example page 145 in [32]). A convex function is used in for example [20] or [17]. Specifically, in [17] an exponential function is used. This function is repeated here with a slightly different notation for consistency with the earlier used symbols:

$$C_{I,i} = \left(C_{f,i} + C_{v,i}\, u_i\right) e^{\lambda(u_i+W)} \,, \tag{3.15}$$

where u_i is the height increase of the flood defence, W is the sum of all the previous height increases, and λ is a scale parameter [17]. A similar equation and estimates for $C_{f,i}$, $C_{v,i}$ and λ are shown in [25, Appendix C.4]. The data in [25] also showed that the estimates for $C_{f,i}$, $C_{v,i}$ and λ can differ significantly per case study. Preliminary estimates for a wider range range of flood defences in an international context can be found in for example [44]. If λ is equal to zero, the exponential relation in Eq. 3.15 reduces to a linear investment relation.

3.4.3. ECONOMIC OPTIMISATION

In a general sense, an economic optimisation model indicates when to (repeatedly) invest where, and how much, by minimizing of the total costs (Eq. 3.3). Examples of recent numerical economic optimisation methods can be found in [45] or [46]. The methods by [27, 45, 46] use similar techniques in order to quickly get from a large set of potential combinations of risk and investment costs to an optimal investment path with minimal total costs. A conceptual visualization of the set of potential combinations for the risk costs is shown in Figure 3.7. These techniques involve linear or nonlinear programming. A method sharing the same fundamental approach from [46] was used in [27] to find the economic optimal safety levels for the Lake IJssel case; Section 3.5 uses this method as well.

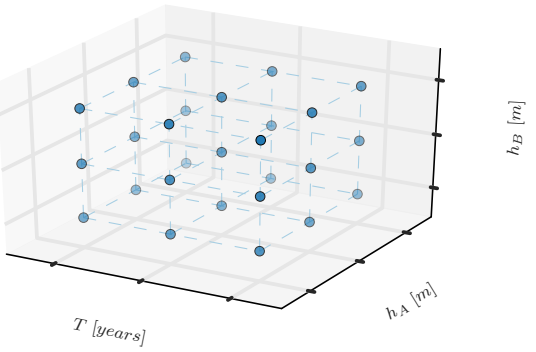

Figure 3.7: Conceptual illustration of the solution space of risk costs for a front (h_B) and rear defence (h_A). Each dot represents a unique combination of time T and heights, and each unique combination is coupled to a risk estimate. This risk estimate is calculated for the period which starts at the current time T and ends at the next point in time.

3.5. APPLICATION

This section presents an application of both the economic optimisation approaches in Section 3.3 & 3.4 in order to quantify the difference of including the load reduction effect of a front defence. The application is based on the work from a real, ongoing case study in the Galveston Bay area near Houston, Texas, which has been significantly reduced in complexity. Therefore, the results should not be considered directly for decision making for the Galveston Bay area. The Galveston Bay consists of a large bay with barrier islands (Figure 3.8), and hosts millions of people and a large economic value. It does not yet have an integral flood defence system, but the feasibility is being investigated because the area is hurricane prone (e.g. see [39]).

For this hypothetical case study, a number of defences has been set to a fixed level: defences $F1$, $F2$ and $F3$ in Figure 3.8. Moreover, only a single system configuration will be considered: the number, type and location of all the considered flood defences is predetermined and shown in Figure 3.8. Consequently, this leaves Figure 3.8 with only three defences which will be part of the economic optimisation: a single front defence in the form of a storm surge barrier ($B1$), and two rear defences ($A1$ and $A2$).

3.5.1. RISK CHARACTERISATION

Four separate flood prone areas can be identified: the island protected by $F1$, the island protected by $F2$ and $A1$, and two main land areas protected by $F3$ and $A2$. This leads to the following annual risk for the system ($C_{R,bay}$):

$$C_{R,bay} = P_{F1}D_{F1} + (P_{F2} + P_{A1})\,D_{F2} + P_{F3}D_{F3} + P_{A2}D_{A2} \tag{3.16}$$

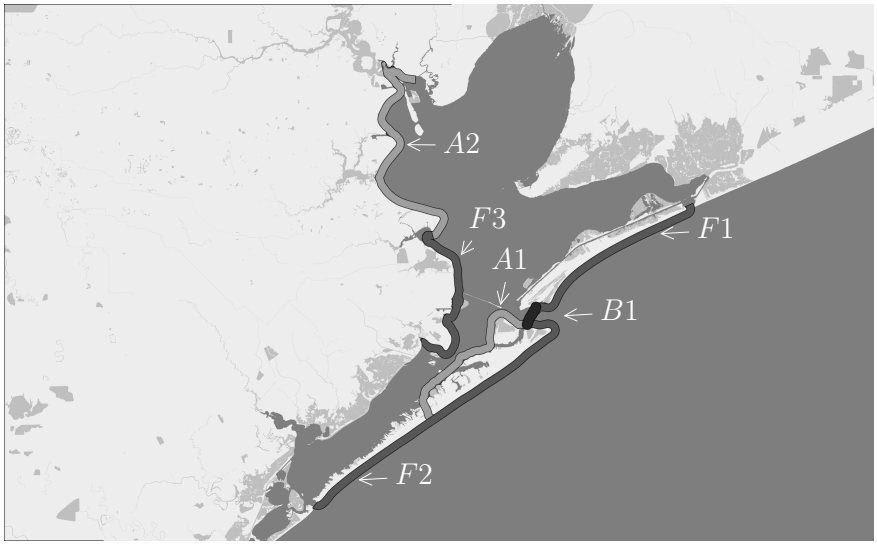

Figure 3.8: Galveston Bay area with contours indicating the defence types for the hypothetical application. Three types of defences exist: A defence with a fixed safety level ($F1$, $F2$ and $F3$), a front defence ($B1$) and a rear defence ($A1$ and $A2$). Note that the contours are indicative only and do not necessarily correspond with the position of existing flood defences. Map data is modified from OpenStreetMap (© OpenStreetMap contributors, http://www.openstreetmap.org/copyright).

where the defences $F2$ and $A1$ are assumed to protect the same area (D_{F2}), and are assumed to be independent with a negligible probability that $F2$ and $A1$ fail simultaneously. Eq. 3.16 is simplified further by assuming that the defences $B1$ and $F1$ do not protect any value of their own ($D_{B1} \approx 0$, $D_{F1} \approx 0$):

$$C_{R,bay} = (P_{F2} + P_{A1})\, D_{F2} + P_{F3} D_{F3} + P_{A2} D_{A2} \tag{3.17}$$

where the flood damage estimates D_{F2}, D_{F3} and D_{A2} will be loosely based on the residential and industrial flood damage estimates found in [47, Section 6]. Finally, the annual failure probabilities of the flood defences behind the front defence $B1$ (i.e. $A1$, $A2$ and $F3$) can be elaborated in a similar way as in Section 3.2.2 to incorporate the possible load reduction of the front defence:

$$P_{A1} = P_{B1} P_{A1|B1} + P_{\overline{B1}} P_{A1|\overline{B1}} \tag{3.18}$$

$$P_{A2} = P_{B1} P_{A2|B1} + P_{\overline{B1}} P_{A2|\overline{B1}} \tag{3.19}$$

$$P_{F3} = P_{B1} P_{F3|B1} + P_{\overline{B1}} P_{F3|\overline{B1}} \tag{3.20}$$

LOADS AND RESISTANCE

The hydraulic loads used in this illustration are based on the following assumptions:

- The load distributions for defences $A1$, $A2$ and $F3$, under influence of either a functioning or failed front defence $B1$, are modelled using a hydraulic model as proposed in [48]. This 1D hydraulic model simulates the hurricane surge and wind setup inside the bay; where a front defence can influence the surge by reducing the inflow into the bay. In case of a failed front defence, the water is assumed to flow unrestricted into the bay (i.e. as if the front defence was never built); this is a conservative assumption as in reality even a failed front defence will still restrict flow into the bay.
- All flood defences are assumed to have a ground level of two meters above Mean Sea Level (MSL). In other words, even without any flood defence this means that flooding can only occur if the water levels exceed two meters above MSL. The only exception is the front defence $B1$, which is assumed to have a ground level at MSL. Because of limitations in the hydraulic model, a front defence height below MSL is not considered.
- The maximum, constant load reduction effect by a front defence on the water levels behind the front defence is applied for every front defence height. This reduces the number of hydraulic load computations, but overestimates the impact of a front defence, especially at small heights (see also Section 3.2.1);
- The defences $F1$ and $F2$ are assumed to be high enough so that overtopping and/or overflow of these defences has no contribution to the bay inflow.
- The surge levels inside and outside the bay are transformed into annual water level exceedance probabilities by means of crude Monte Carlo simulations using $5 \cdot 10^4$ samples. These extreme water level distributions are used as the 'Load' part of the reliability equation Z in Eq. 3.14.

The 'Strength' part of the reliability equation Z (Eq. 3.14) is chosen to be a lognormal distribution, where the height of the flood defence functions as the mean, with a Coefficient of Variation (COV) estimated at twenty percent. The height of the defence is assumed to be equal to the critical water level (at which the defence breaks). The choice for the lognormal distribution is of a practical nature, because it produces strictly positive real values. Using a strength distribution based on the height of a flood defence, instead of a deterministic height, represents that additional failure mechanisms can occur besides overflow/overtopping. For example, piping can lead to failure for surge levels below the crest level (e.g. see [49]).

ESTIMATION OF FAILURE PROBABILITIES

The raw Monte Carlo results of the surge simulations in Section 3.5.1 are approximated with generalized Pareto distributions (GP, threshold parameter fixed at 0) using maximum likelihood estimation in Matlab. Using probability distributions allows a straightforward application of, for example, a First Order Reliability Method (FORM) or a nu-

merical integration routine. An overview of the used heights, flood damages, and load distributions can be found in Table 3.1.

Table 3.1: Reference level ($h_{i,ref}$, relative to MSL), height (h_i, relative to $h_{i,ref}$), potential flood damage (D_i) and annual Generalized Pareto (GP) water level distribution parameters for all the flood defences.

defence i	$h_{i,ref}$ $[m]$	h_i $[m]$	D_i $[10^9\$]$	$P_{i\|\overline{B1}}(\xi, \sigma)$	$P_{i\|B1}(\xi, \sigma)$
$B1$	0.0	0.0 - 20.0	0.0	-0.30, 2.2	-0.30, 2.2
$F2$	2.0	3.0	2.4	-0.30, 2.2	-0.30, 2.2
$F3$	2.0	3.0	4.8	-0.14, 0.56	-0.082, 0.89
$A1$	2.0	0.0 - 20.0	see $F2$	-0.14, 0.56	-0.082, 0.89
$A2$	2.0	0.0 - 20.0	38.5	-0.15, 0.77	-0.14, 1.3

Table 3.2: Investment costs for the to-be optimised flood defences.

defence i	$C_{f,i}$ [\$]	$C_{v,i}$ [\$/m]	Comments
$B1$	$3 \cdot 10^9$	$1 \cdot 10^9$	Storm surge barrier: Based on an estimated cost range of four to ten billions dollars [47].
$A1$	$300 \cdot 10^6$	$150 \cdot 10^6$	Levee: Estimated at ten million dollar per kilometer length, per meter defence heightening, which is on the high end of the range for the United States according to [44]. The length is estimated at 15 kilometers.
$A2$	$1 \cdot 10^9$	$300 \cdot 10^6$	Levee: Uses the same base estimate as defence $A1$. An additional 400 million dollars is added to the fixed costs to account for a gate solution at the north side of the bay [47]. The length is estimated at 30 kilometers.

Finally, because the loads and strength are now defined, each (conditional) failure probability of Eqs. 3.17 - 3.20 can be found. This involves solving the reliability equation Z (Eq. 3.14) where $Z < 0$, and is done using numerical integration. Assuming independence between the load S and strength R, the reliability equation where $Z < 0$ can be rewritten into a failure probability $P(Z < 0)$ as is done in, for example, [42]:

$$P(Z < 0) = \int_{-\infty}^{\infty} F_R(h)\, f_S(h)\, dh \tag{3.21}$$

where $F_R(h)$ is the cumulative distribution function of the resistance, and $f_S(h)$ is the probability density function of the load. The computed (conditional) failure probabilities will be used in Eq. 3.17 to calculate annual system risks.

3.5.2. INVESTMENT COSTS

The investment costs will be crude estimates based on [47] and [44]. In the case of [47], single value estimates are given for constructing defences, while in [44] unit costs (per kilometer) are given. Without making an actual design, it will be difficult to obtain accurate investment costs, especially in the form of Eq. 3.15 where estimates of both fixed and variable costs are required. Therefore, the investment costs (Table 3.2) are loosely based on numbers found in [44] & [47], using an exponential investment relation (Eq. 3.15). The exponential scale parameter λ for the investment relation of Eq. 3.15 is estimated at 0.02/m. An exponential relation is chosen because it allows to incorporate the assumed notion that costs increase exponentially for higher flood defences. For example, with λ set at 0.02, an increase of defence $B1$ from zero to five meters would result in 8 billion dollars and 8.8 billion dollars for a linear and an exponential relation, respectively.

3.5.3. ECONOMIC OPTIMISATION AND TIME DEPENDENT PARAMETERS

As mentioned in Section 3.4.3, the economic optimisation model uses the same model as used in [27]. For all flood defences, a potential height range between zero and twenty meters was evaluated, with steps of one meter. The evaluated time period is 300 years, with steps of one year for the first twenty years, steps of five years between 20 and 100 years, and steps of ten years between 100 and 300 years. This time discretization is based on [46]. Because the time periods have a variable length, the risk for a period is calculated by finding the integral over that period for the (discounted and adjusted for economic growth) risk. Furthermore, a minimum timespan between investments of five and ten years was imposed for consecutively the rear and front defences.

The time dependent parameters economic growth, interest rate and sea level rise are assumed to be constant in time for all flood defences. First, the economic growth is estimated at six percent, which is at the low end of the average economic growth in a recent period of twelve years according to [50]. Secondly, the real interest rate in recent years varied between zero and four percent [51], and is estimated at two percent. Lastly, the sea level rise is determined using [52], and is estimated at 6.9 millimeters per year.

3.5.4. RESULTS

Both the simplified method of Section 3.3 and the numerical approach of Section 3.4 are applied to the case study using the gathered input of the previous sections. The results are used to assess the load reduction effect of a front defence in this case study.

LOAD REDUCTION EFFECT: SIMPLIFIED METHOD

Before the simplified method of Section 3.3 can be applied, a number of simplifications need to be made: the rear defences $A1$ and $A2$ are summed into a single flood defence which uses the water level distribution of $A1$, flood defences $F1$, $F2$ and $F3$ are ignored, economic growth and sea level rise are ignored, and the reliability of each flood defence is converted into an exponential function as used in Section 3.3.3. The results of these simplifications can be found in Table 3.3 and Figure 3.9.

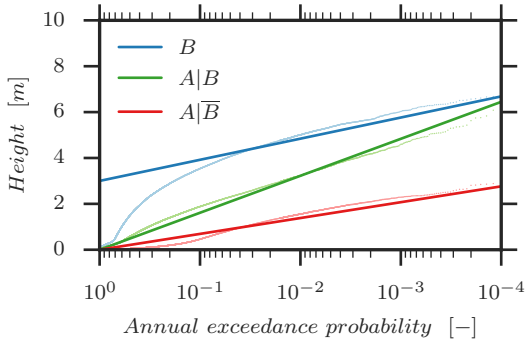

Figure 3.9: Exponential annual water level exceedance probabilities (solid lines, see also Table 3.3) which are used for the front defence B (line B) and the rear defence A (line $A|B$ if the front defence failed, otherwise line $A|\overline{B}$). The dotted lines are the Monte Carlo results.

The exponential functions in Figure 3.9 had to be manually fitted in order to get a reasonable approximation of the results found in Section 3.5.1. This figure shows that for annual exceedance probabilities larger than approximately $5{\cdot}10^{-2}$, the exponential fit significantly overestimates the associated water levels. However, the simplified method is meant to give insight into the behavior of the load reduction effect in a coastal system and not an accurate answer of the economically optimal safety targets. For the purpose of the simplified method, the exponential fits are considered acceptable.

The results of the simplified economic optimisation are shown in Figure 3.10. First of all, the graph in this figure indicates that there is no difference regarding the optimal safety targets with or without a load reduction. Secondly, not building a front defence ($\widehat{P}_B = 1$) should be economically optimal. And thirdly, although arguably less relevant given the manually fitted exponential distributions, the economically optimal failure probability of the rear defences should be in the order of $2 \cdot 10^{-4}$, which coincides with a levee height of approximately six meter.

The added value of the simplified model is that it can explain why there is no difference between including the load reduction and not including the load reduction. First of all, because the flood damage associated with a failed front defence (D_B) is set to zero, the logical consequence is that, if a load reduction is not included, not building a front defence is the economically optimal choice (see also Eq. 3.10). When the load reduction is included, Eq. 3.10 changes into Eq. 3.9, where only the denominator is different. In order for a front defence to be economically efficient and thus have a failure probability smaller than one, the denominator should be larger than the numerator:

$$D_A\left(\widehat{P}_{A|B} - \widehat{P}_{A|\overline{B}}\right) > \beta_B C_{v,B} r \tag{3.22}$$

If Eq. 3.22 is used with the input of Table 3.3, together with a height of six meters for the rear defence, the result is $7.75 \cdot 10^6 > 8.00 \cdot 10^6$. This means that the risk reduction for the rear defence by the front defence (left hand side of Eq. 3.22) is not efficient when compared to the required investment of the front defence (right hand side of Eq. 3.22). However, the difference between the two numbers is relatively small, which means that if any of the relevant parameters change, a front defence might become an economically efficient choice after all. These parameters can change for example by including economic growth, sea level rise, or better approximations of the reliability of the defences. In order to assess the effect of these potential changes, a numerical economic optimisation is needed.

Parameter	Value	Unit
$\alpha_{A\|B}$	0.0	m
$\beta_{A\|B}$	0.7	m
$\alpha_{A\|\overline{B}}$	0.0	m
$\beta_{A\|\overline{B}}$	0.3	m
α_B	3.0	m
β_B	0.4	m
$C_{v,A}$	$450 \cdot 10^6$	$\$/m$
$C_{v,B}$	$1.0 \cdot 10^9$	$\$/m$
D_A	$40.9 \cdot 10^9$	$
D_B	0.0	$
r	0.02	–

Table 3.3: Input values for the application of the simplified economic optimisation in the Galveston Bay area.

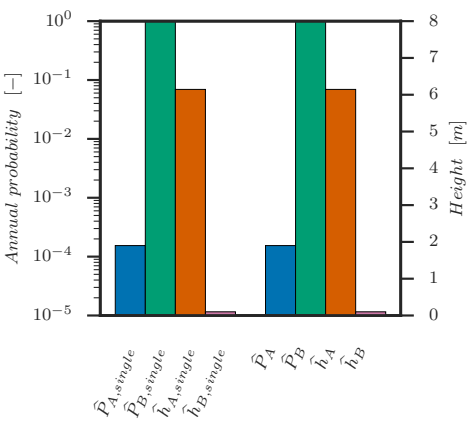

Figure 3.10: Result of the simplified economic optimisation for the Galveston Bay area, using the input values of Table 3.3.

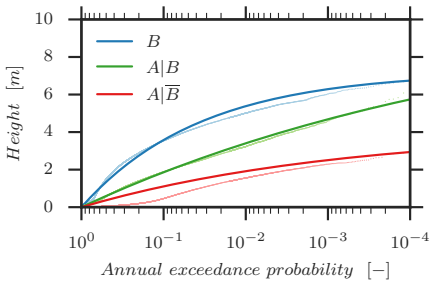

Figure 3.11: Annual water level exceedance probabilities which are used for flood defences $B1$ & $F2$ (line B), and $A1$ & $F3$ (line $A|B$ if the front defence failed, otherwise line $A|\overline{B}$). The Generalized Pareto distributions (solid lines) are fitted to the Monte Carlo results (dotted lines).

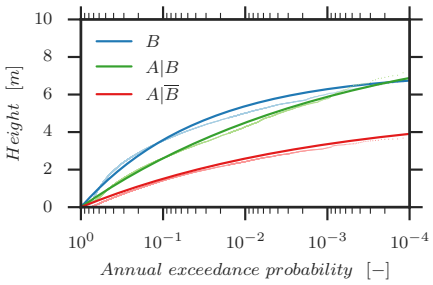

Figure 3.12: Annual water level exceedance probabilities which are used for flood defences $B1$ & $F2$ (line B), and $A2$ (line $A|B$ if the front defence failed, otherwise line $A|\overline{B}$). The Generalized Pareto distributions (solid lines) are fitted to the Monte Carlo results (dotted lines).

LOAD REDUCTION EFFECT: NUMERICAL METHOD

In contrast to the application of the simplified method, the numerical approach is not limited to exponential water level distributions and can therefore use the better fitting generalized Pareto distributions of Table 3.1. The used water level distributions are shown in Figure 3.11 & 3.12.

The numerical approach was applied to the case study with and without the load reduction effect of the $B1$ front defence. Because the flood damage associated with a front defence failure (D_B) is set to zero, this implies that when the load reduction effect is not included, a front defence will never be economically optimal. The results of applying the numerical approach described in Section 3.4, using the input of Sections 3.5.1 - 3.5.3, are shown in Table 3.4 and Figure 3.14 (with load reduction) and in Table 3.5 and Figure 3.15 (without load reduction).

The load reduction effect can be observed when comparing the results of the numerical economic optimisation in Table 3.4 and Figure 3.14. The rear defences, after their initial upgrade in year 0, do not get upgraded until year 150. However, because of the load reduction effect of the front defence, upgrading the front defence $B1$ at $T = 30$ and $T = 100$ decreases the failure probabilities of the rear defences as well. Additionally, the optimal heights of the rear defences with the load reduction effect in Table 3.4 are also lower than the optimal heights without a load reduction effect in Table 3.5. Not only does the optimal system configuration change significantly from Table 3.5 to Table 3.4, the total cost estimate changes as well. For the first 50 years, the total cost decreases from $245.5 \cdot 10^9$ for the optimal investment scheme of Table 3.5 to $\$220.3 \cdot 10^9$ for the optimal investment scheme of Table 3.4. This can also been seen in Figure 3.13, where the development of the total cost over time for the first 100 years is plotted. In this figure, the total cost over time *with* the influence of a front defence remains below the total cost over time *without* the influence of a front defence.

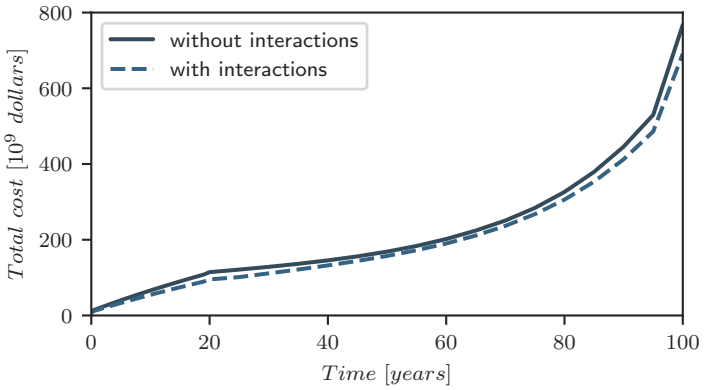

Figure 3.13: Development of the total cost over time for the first 100 years. The two lines represent the results *without* the influence of a front defence ('without interactions') and the results *with* the influence of a front defence ('with interactions'). The total cost does not converge to a single number because the economic growth is larger than the discount rate.

The insight of the simplified method can be used to further explain some of these findings provided by the numerical method. First of all, the height reduction of the rear defences when a load reduction is taken into account was already predicted in Section 3.3.4, and can be observed in Table 3.4 & 3.5. Secondly, Section 3.5.4 predicted that building no front defence was economically optimal, however the distance to the tipping point (where a front defence is economically viable) was found to be relatively small. This meant that the point where a front defence becomes economically viable could be reached in time when the time dependent parameters of Section 3.5.3 are included. The numerical approach predicts in Table 3.4 that this tipping point is reached after thirty years.

Finally, the optimal values of the simplified method for the rear defence in Figure 3.10 match the optimal values of the numerical approach for the first thirty years in Table 3.4 and Figure 3.14, despite the simplifications and exponential distributions used in the simplified method. This can possibly be explained by the fact that the exponential distributions fit reasonably well in the region of the found optimal failure probability ($\approx 10^{-4}$). Nevertheless, this does not change the fact that the simplified method of Section 3.3 still has too many simplifications for accurately quantifying economically optimal targets in practice; the simplified method should only be used to gain additional insight in parallel to a numerical economic optimisation as described in Section 3.4.

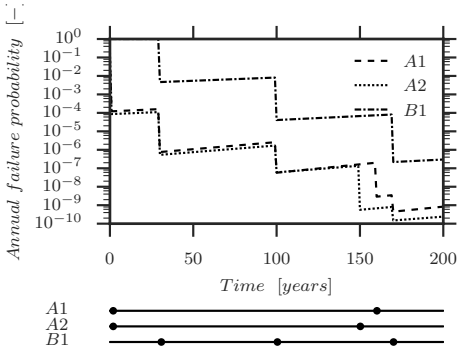

Figure 3.14: Safety values in time for flood defences $B1$, $A1$ and $A2$ of Table 3.4, *with* the influence of a front defence. The corresponding timing of the investments per defence is shown as well.

Year	defence	Height increase
0	$A1$	from 0 to 5 meter
160	$A1$	from 5 to 7 meter
0	$A2$	from 0 to 7 meter
150	$A2$	from 7 to 10 meter
30	$B1$	from 0 to 7 meter
100	$B1$	from 7 to 11 meter
170	$B1$	from 11 to 15 meter

Table 3.4: Optimal investment scheme for the Galveston Bay example using the numerical approach of Section 3.4, *with* the influence of a front defence.

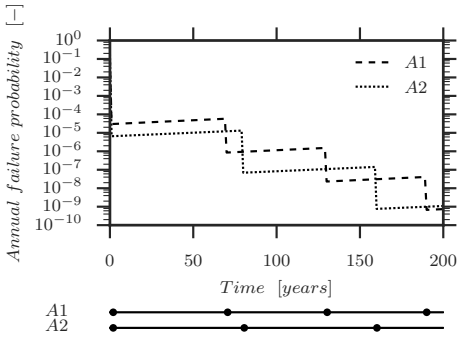

Figure 3.15: Safety values in time for flood defences $A1$ and $A2$ of Table 3.5, *without* the influence a front defence. The corresponding timing of the investments per defence is shown as well.

Year	defence	Height increase
0	$A1$	from 0 to 6 meter
70	$A1$	from 6 to 9 meter
130	$A1$	from 9 to 12 meter
190	$A1$	from 12 to 15 meter
0	$A2$	from 0 to 9 meter
80	$A2$	from 9 to 13 meter
160	$A2$	from 13 to 17 meter

Table 3.5: Optimal investment scheme for the Galveston Bay example using the numerical approach of Section 3.4, *without* the influence of a front defence.

3.6. CONCLUSIONS

The aim of this chapter was to assess whether including the influence of a load reduction by means of a front defence influences the economically optimal safety targets of a coastal flood defence system with both a front and rear defence. This was done with the development of a simplified method, a flexible numerical approach and a case study.

The simplified method has a number of assumptions which make it not suitable for an actual quantification of the economically optimal safety targets, but it does provide additional insight into the influence of a load reduction on the economically optimal safety targets of a coastal flood defence system with a front and rear defence. This additional insight is provided in the form of analytical predictions regarding the expected effects of including a load reduction by a front defence. First of all, it showed that, in practice, the optimal height of rear defences decreases when the load reduction effect is included. Secondly, the simplified method showed that the influence of a load reduction on the optimal safety target of a front defence is determined by the relative impact this front defence has on the flood risk of the rear defences.

The answer of the simplified method does not account for a changing flood risk over time due to time dependent parameters such as economic growth or sea level rise. A changing flood risk over time opens up the possibility that even though a front defence is not the optimal choice right now, it might become economically optimal in the future. In order to be capable of providing practically applicable answers which include time dependency, a numerical approach is proposed.

The proposed numerical approach is capable of incorporating these time dependent parameters and can produce optimal safety targets over time. Furthermore, the numerical approach lifts a number of the restrictions set in the simplified method, therefore making it more practically applicable. It does this by integrating practically applicable hydraulic models, probabilistic methods and economic optimisation methods.

Whether or not a load reduction has a significant effect on the economically optimal safety targets depends strongly on the particular characteristics of a flood defence system. To that end, a hypothetical case study (based on an actual case study) was contemplated in order to quantify the effects of a load reduction in this case study. This particular case study showed a significant effect by the load reduction on the economically optimal safety targets over time. Moreover, the load reduction effect significantly reduced the estimate of the total costs as well. Given the potentially large efficiency improvements regarding both the economically optimal safety targets and total cost estimate, not including the load reduction effect by a front defence on the economically optimal safety targets in coastal systems should be the exception to the rule.

4

A GRAPH-BASED ECONOMIC OPTIMISATION WITH AN EFFICIENT EVALUATION OF EAD ESTIMATES FOR INTERDEPENDENT FLOOD DEFENCES

The coastal flood defence system in Chapter 3 was a relatively simple flood defence system with only two layers of defence. For coastal flood defence systems, a limited number of lines of defence is reasonable expectation. However, for riverine flood defence systems, the number of interdependent lines of defences can be much larger. This in turn will lead to a large number of potential risk calculations in a numerical economic optimisation. The computational burden of this large number of potential risk calculations can be relieved by reducing the cost of a risk calculation, or by reducing the number of actually executed risk calculations. This chapter investigates reducing the number of risk calculations in an economic optimisation for a flood defence system with an arbitrary number of lines of defence. To that end, a numeric economic optimisation algorithm is proposed. The aims of this numerical method are to require less risk calculations (which often represent the bulk of the computational strain), and to be easily applicable to an arbitrary number of defences.

The contents of this chapter have been published in [53].

4.1. INTRODUCTION

Economic optimisation of flood defences, as applied in the Netherlands, is based on a cost-benefit analysis of the sum of the annual flood risks balanced against the sum of the investment costs for flood defences. This type of cost-benefit analysis was originally developed in the 1950's by [9] and is still used and discussed to this day [17, 20]. The basic principle behind the economic optimisation of flood defences is finding the minimum of the total costs as illustrated in Figure 4.1. The total costs (TC, Eq. 4.1) are the sum of the annual risk costs ($\sum_{t=0}^{p} R(t)$) and investment costs ($\sum_{t=0}^{p} I(t)$) over a given time period (p years). The total costs are expressed as the present value of the (future) annual risk costs and investment costs, which means these costs are discounted at a discount rate r. The annual risk cost $R(t)$ is defined in Eq. 4.2 as the annual probability of flooding at time t ($P_{flood,t}$), multiplied by the expected damages due to flooding at time t ($D_{flood,t}$).[1] An alternative term for the annual risk cost is the Expected Annual Damage, or EAD. Generally speaking, a larger investment will lead to a lower EAD; this is where the economic optimisation tries to find an optimal solution (i.e. the lowest total cost).

$$TC = \sum_{t=0}^{p} R(t)e^{-rt} + \sum_{t=0}^{p} I(t)e^{-rt} \tag{4.1}$$

$$R(t) = \mathrm{EAD}(t) = P_{flood,t} \cdot D_{flood,t} \tag{4.2}$$

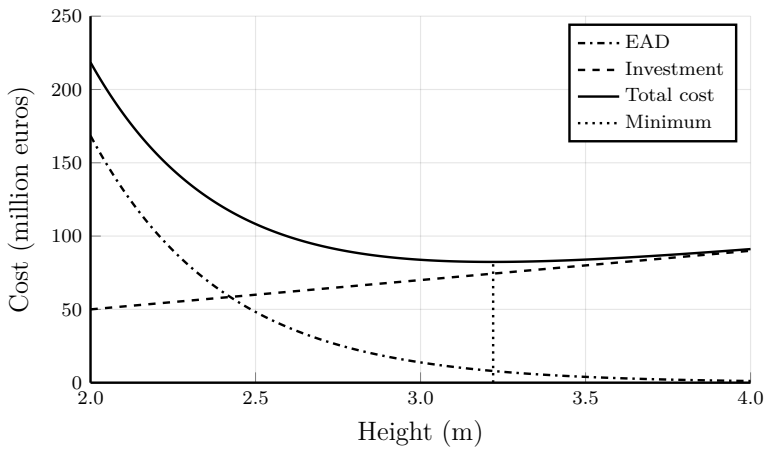

Figure 4.1: Schematic view of an economic cost-benefit analysis for a flood defence. The total costs are the sum of the risk and investment costs, and the optimum can be found at the minimum of the total costs.

[1] This is a simplification of the definition in for example [1], where the multiplication is defined as "really a combination across all floods". If the flood damage is constant across floods, the combination reduces to the multiplication as shown in Eq.2.2. See also Section 1.3 regarding the assumption of a constant flood damage. In this thesis, a variable flood damage is used in Chapter 5.

Recent publications regarding economically optimal safety targets for the Netherlands can be found in the publications by [20], [45] and [27, 46]. In [20] and [22], a set of equations were derived which describe the economically optimal safety target for a single homogeneous flood defence system (i.e. dike ring). Because they incorporated influence of time-dependent parameters such as economic growth and climate model parameters, these equations also describe the number of (repeated) investments, as well as the optimal time between these investments. Repeated investments are necessary to 'repair' the effect of, for example, economic growth (i.e. a higher expected losses in case of a flood) or subsidence (i.e. a higher flood probability). A schematic view of the result of such an economic optimisation with time-dependent parameters is shown in Figure 4.2. This figure shows that as the safety level goes down over time, recurring investments are needed to repair the effects over time of time-dependent parameters such as economic growth and climate change.

The equations described in [22] are analytically solvable and the method results in a global minimum of the total costs for a relatively simple homogeneous system. However, dike rings in the Netherlands often consist of mutually different, non-homogeneous sections in which case, the homogenous case needs to be extended to account for these non-homogeneous sections. In [45], a possible, heuristic solution is given by modelling the problem as a mixed-integer nonlinear programming (MINLP) problem. [46] improved on this method by developing a graph-based modelling approach to solve the non-homogeneous case to proven optimality.

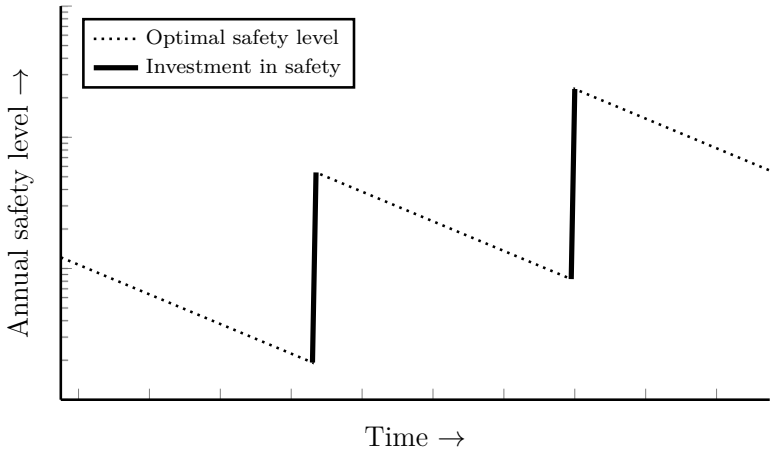

Figure 4.2: Schematic view of an economic cost-benefit analysis for a flood defence, with time-dependent parameters. Because of these time-dependent parameters (e.g. economic growth or subsidence), recurring investments in safety are needed.

[20], [45] and [46] assess independent flood prone areas in which individual flood defences within a dike ring area fail under identical circumstances. No interdependencies

exists in their modelling approaches, however, the notion of interdependent flood defences expresses that failure of one flood defence might alter the EAD of other defences. Moreover, a dike ring may fail under different circumstances. A practical example of a flood defence system with multiple interdependent flood defences is shown in Figure 4.3. In this figure, a breach occurring at upstream area B impacts the flood risk at area A. This impact can either increase or decrease the flood risk at area A. An increase would occur if a shortcut is formed between area A and an already flooded area B at arrow 2. Whereas a decrease would occur if the breach at arrow 1 reduces the probability of a breach at arrow 3 (because part of the river discharge is diverted into area B). This notion of interdependent flood defences has been, from a flood risk perspective, the main topic of a number of recent papers (e.g. [12–14, 16]). All of these papers showed that viewing the flood defence system as a whole, will result in different EAD estimates than viewing the flood defences as separate, independent defences.

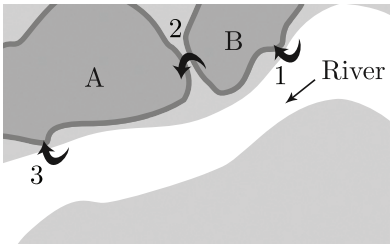

Figure 4.3: A hypothetical example of a system with interdependent flood defences. The flood risk in area A is is not only impacted by the flooding probability at its own defence (arrow 3), but also what happens at the flood defence of area B (arrow 1) and the connecting flood defences between area A and B (arrow 2).

As the EAD changes, the economic optimisation will also be affected. Thus, it makes sense to explicitly integrate the effect of multiple interdependent flood defences on the EAD in the economic optimisation routines. A method to provide a modelling approach to the economic optimisation of a flood defence system with multiple dependent and independent dikes was first presented in [27]. In their study (in Dutch), a graph-based modelling approach is used to obtain economically optimal safety norms and heights for multiple lines of flood defences. Furthermore, they mentioned that the economic optimisation problem can be formulated in the form of a minimal cost flow graph or a shortest path problem. Three approaches (to solve economic optimal safety problems for multiple flood defences) were identified by [27] & [54]: (1) a heuristic approach based on closed form formulas, (2) a dynamic programming/shortest-path approach (as also used in [22]) and (3) a branch-and-cut/ILP approach. In [27] the branch-and-cut/ILP-approach is preferred and applied. An English description of the model in [27] can be found in [55, Chapter 5].

However, a consequence of using an ILP approach in [27] is that, prior to starting the optimisation routine, all EAD estimates for each and every possible combination of flood defences in time need to be computed. Generally speaking, finding EAD estimates for a

number of these combinations is not necessary. For example, it is unlikely that is economically optimal to keep all flood defences at their lowest level for the next 300 years. Calculating these EAD estimates can be costly, especially if hydrodynamic interactions are included since acquiring a single EAD estimate can take hours [16] or even days [14]. In these cases, computational efficiency will be largely determined by the time it takes to compute EAD estimates.

Furthermore, the method of [27] is modelled in the modelling language GAMS and solved using the commercial solver CPLEX. While the method of [27] is, in principle, applicable to an arbitrary number of lines of defence, in practice the model code must be manually extended with new equations to implement any additional lines of defence. While these extensions are trivial for anyone with experience in integer programming and GAMS, automating these steps can further lower the threshold for using and applying these models.

Reducing the number of EAD estimates that will be computed can be done based on the principle of 'lazy evaluation', which delays calculations until they are actually required. However, 'lazy evaluation' requires a tight coupling between the EAD estimation and the economic optimisation routine. This tight coupling needs to be technically and organisationally possible. Organisationally, this tight coupling is possible in projects which are carried out by a single team combining all relevant disciplines; in the remainder of this chapter it is assumed that the organisational requirement is fulfilled. Technically, the economic optimisation routine needs to be able to dynamically call the EAD estimation function during its optimisation process. However, optimisation routines typically expect a pre-calculated set of data, which means an optimisation routine will need to be modified in order to support 'lazy evaluation'. One such optimisation routine that can be easily implemented in a general programming language and adapted to use lazy evaluation is the shortest-path approach.

In the following section the shortest-path approach is further investigated in order to solve the problem of an economic optimisation for multiple interdependent flood defences. The aim of this chapter is to develop a generic, computationally efficient approach for finding the economically optimal configuration of a flood defence system with an arbitrary number of interdependent flood defences which, for example, influence each other's EAD. The reliability and performance (in terms of number of EAD calculations) of finding economically optimal targets will be tested by comparing the results of the proposed method with a number of benchmark studies. This is accomplished using the following approach:

- Computational efficiency will be primarily obtained by minimising the number of (time-consuming) Expected Annual Damage (EAD) computations in the algorithm until they are actually required (i.e. 'lazy evaluation')

- A generically applicable, flexible representation of the problem space will be presented which is able to use an arbitrary number of defences. Specifically, this en-

tails generating a graph in an automated way based on an arbitrary number of interdependent flood defences

In section 4.2, a description of the application and a description of the applied algorithm are given. Implementation details, focused on the computational efficiency of the algorithm, are discussed in Section 4.3, as well as a list of potential future improvements to the algorithm. Next, the proposed approach is applied to some simplified case studies in Section 4.4, and is followed by a discussion (Section 4.5) regarding the relevance of the proposed approach. Finally, the results and experiences are concluded in Section 4.6.

4.2. AN ALGORITHM FOR FLOOD DEFENCE SYSTEMS WITH MULTIPLE INTERDEPENDENT FLOOD DEFENCES

4.2.1. PROGRAMMATIC REPRESENTATION OF THE SOLUTION SPACE

A common choice to present optimisation problems is to use graph algorithms [56]. Regarding the economic optimisation of flood defences, this choice was also made in [46]. An example of a graph for a single flood defence is shown in Figure 4.4. The graph shows the possible investments over time for a single flood defence. In this graph the vertices (dots) are the possible heights the flood defence can have at a certain point in time. In order to go the next point in time, edges are drawn which connect a vertex to all the possible vertices in the next point of time.

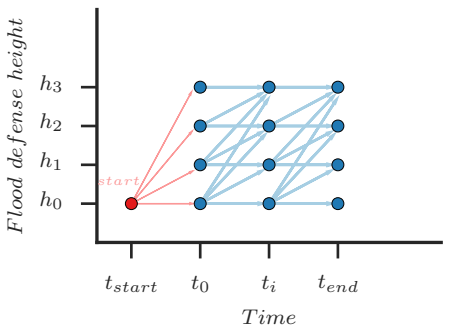

Figure 4.4: Graph where the vertices (dots) at each time step are connected via edges (arrows) to the next time step.

These points in time are not fixed; the amount and position can be altered to the needs of a particular problem. In practice, these points in time can be related to the (political) decision process of a particular problem: if the relevant flood defences are reviewed and (if necessary) reinforced every five years, it would make sense to have a graph that corresponds to these points in time.

Generally speaking, edges in a graph can be directed or undirected. However, steps backwards in time do not make sense for investment schemes. Therefore, only edges

directed forward in time are used. The edge cost (or weight) of an edge is the total cost (EAD plus investment cost) of moving between the connected vertices. Furthermore, it is assumed that flood defences will not be intentionally decreased to a lower level, which is why, for example, there are no edges running from h_1 to h_0. The starting point of the graph is denoted with start in Figure 4.4 at time t_{start} at a height equal to the current height (h_0).

In case of multiple flood defences, the proposed method takes into account that flood defences can be interdependent and interact with each other hydrodynamically. This means that the EAD of the system of defences can potentially be influenced by each defence, which also means that each combination of flood defence levels has to be considered relevant. For a graph with multiple interdependent flood defences, these combinations replace the height of a single flood defence on the y-axis in Figure 4.4. These combinations of heights for multiple flood defences can be obtained by computing the Cartesian product of the flood defence levels of all the involved defences. For n flood defences, the Cartesian product equation for determining the combinations is shown in Eq. 4.3:

$$\prod_{i=1}^{n} \vec{X}_i = \vec{X}_1 \times \ldots \times \vec{X}_n = \left\{(x_1, \ldots, x_n) \,|\, x_1 \in \vec{X}_1, \ldots, x_n \in \vec{X}_n\right\} \tag{4.3}$$

where $\vec{X}_i$ is a vector containing all the flood defence levels of flood defence i, and x_i is a realisation of vector $\vec{X}_i$ (i.e. a flood defence level for flood defence i). If all vectors $\vec{X}_i$ are of the same length y, the total number of combinations will be y^n.

The number of relevant system combinations reduces significantly if each flood defence can be optimised independently of the other flood defences in the system. The assumption of independence can be made if none of the flood defences in a system have a (significant) influence on the EAD estimates of the other flood defences. The total number of system configurations under the independence assumption is $n \cdot y$, as each flood defence could then be optimised separately (e.g. using a graph per flood defence similar to the graph shown in Figure 4.4. If only some defences are independent from other flood defences in the system, this is considered a special case of the proposed approach. In that case, using the Cartesian product is still valid and applicable, although it will result in larger than necessary graph. In case of some independent elements, a possible approach to reduce the size of the graph is discussed in Section 4.3.4.

Figure 4.5 shows an example of the Cartesian product for two flood defences where each flood defence has two possible heights. The graph in Figure 4.5 resembles the graph in Figure 4.4 for a single flood defence. Similar to Figure 4.4, edges in Figure 4.5 are only drawn to vertices containing sets of heights equal or greater than the set of heights in the vertex at the origin of the edge. However, because Figure 4.5 has two defences instead of one, the outgoing edges are slightly different when compared to Figure 4.4. For example, the height combination h_{A0}, h_{B1} is never connected to h_{A1}, h_{B0} (since that would correspond to a reduction in height for defence B).

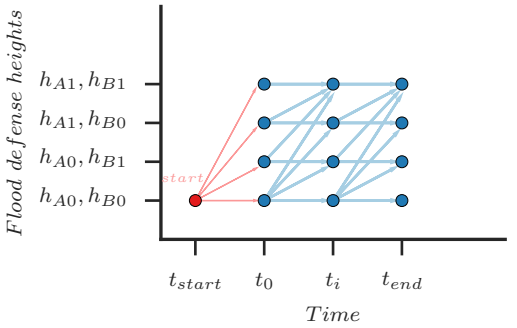

Figure 4.5: Graph with vertices (dots) and edges (arrows) for two defences (A and B). Each defence has two possible heights.

4

4.2.2. IMPLEMENTATION OF A GRAPH ALGORITHM

In general terms, a graph algorithm will iterate over vertices in a graph in an effort to find the path with the lowest costs between a given start and end vertex. However, in the graphs of Figure 4.4 and Figure 4.5 t_{end} contains a number of possible end points, which means that the algorithm will need to find as many optimal paths as there are end points in the graph. In order to only have to run the algorithm once, a stop vertex is added; the graph of Figure 4.5 with an additional stop vertex is shown in Figure 4.6. The edges running towards this stop vertex are all given a weight of zero. Now, the algorithm only has to find a single optimal path between t_{start} and t_{stop}. Why this is an efficient contribution is illustrated in Section 4.2.4.

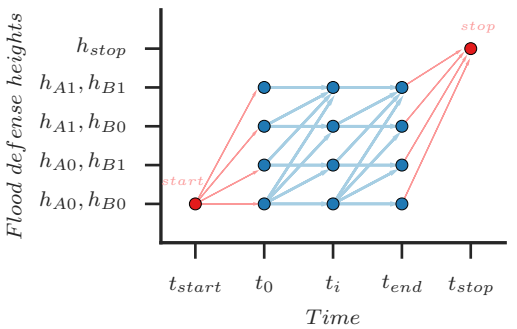

Figure 4.6: The graph of Figure 4.5 with an additional stop vertex.

The graph as shown in Figure 4.6 is a graph with directed non-negative edges. For this kind of graph, a number of algorithms can be used to find the shortest (optimal) path in a graph, for example: the Dijkstra algorithm [57], the A* algorithm [58], and the Uniform Cost Search (e.g. [59]). All three can be considered to be part of the family of

best-first search algorithms, where both the Dijkstra and the Uniform Cost Search (UCS) algorithms can be seen as a special case of the A* algorithm.

Typically, the best-first search algorithms are implemented with a min-priority queue. A min-priority queue holds a sorted list of vertices, where the sorting is based on the cost of reaching that vertex from the start vertex; the vertex with the lowest cost is at the top of the queue. This list of vertices in the priority queue constitutes of, depending on the implementation, either all vertices in the graph (Dijkstra as implemented in [56]), or only the vertices already visited by the graph algorithm (UCS). A comparison between the two algorithms can be found in [60], where the priority queue as implemented by UCS was found to be faster and using less memory. This is consider a relevant advantage, as the number of vertices can be large when using the Cartesian product of flood defence levels (Section 4.2.1). For this reason, the UCS algorithm is implemented.

In [22], a dynamic programming approach was used, which is related to the shortest-path algorithms discussed thus far. However, the Dijkstra algorithm (and by extension the UCS and A* algorithms) are seen in [56] as a part of the *greedy* shortest-path algorithms family, which in [56] is clearly defined as a different type of algorithm than dynamic programming. Greedy algorithms are typically much faster than dynamic programming approaches, at the expense of not always finding the optimal solution (because less possible solutions are considered). The optimality condition is further discussed in Section 4.2.4. Nevertheless, because less possible solutions are considered in a greedy algorithm, this can also lead to a part of the graph never being visited by a greedy algorithm. Combined with 'lazy evaluation', this can lead to a significant reduction in the number of EAD calculations which are actually executed; see also Section 4.3.3.

Applying the UCS algorithm to a graph such as shown in Figure 4.6 begins with creating a priority queue which only contains the start vertex. After this initialization, the iteration process is started. Each iteration starts with taking out the vertex with the lowest cost known thus far from the priority queue (which is the top entry in the queue). Taking out means the optimal route (lowest cost) from the start vertex to this vertex now known. The vertex that has just been taken out of the priority queue is then queried in the graph to find all the connecting vertices in the next time step. Each connecting vertex is added to the priority queue if the vertex is not already in the queue. If the vertex already exists in the queue, the weight is only updated if the newly proposed cost is lower than the known cost so-far. Iteration continues until at the start of an iteration the stop vertex is the top entry in the priority queue. An actual example of the application of this algorithm will be elaborated in Section 4.2.3.

4.2.3. EXAMPLE APPLICATION OF THE ALGORITHM IN AN ECONOMIC OPTIMISATION

This section shows a simple example of an economic optimisation for a single flood defence. While this example uses a single flood defence for simplicity, the same principles apply for multiple flood defences. Regarding the investment costs and EAD estimates,

if a vertex at t_1 is connected to another vertex with a larger height at t_2, it is assumed that the actual heightening occurs at t_1. This leads to a slightly different graph than the conceptual implementation shown in Section 4.2.1 & 4.2.2, and is emphasized by drawing the edges of the figures in this example (i.e. Figures 4.7, 4.8 & 4.9) in a way which is visually more consistent with the timing of the investment decision.

The result of the first two iterations is shown in Figure 4.7, where the start vertex is labelled with the number 1. In this example, the start vertex is associated with a height of 4.25 meter and starts at $t = 0$, identical to vertex 2. Because the path to vertex 2 is the only possible path, vertex 2 is the only addition to the priority queue. In the next iteration, vertex 2 is taken out of the priority queue as it is the vertex with the lowest total cost. The total cost to reach vertex 2 is 0, because there was no heightening (height remains at 4.25 meter) and no time expired ($t_{start} = 0$); the EAD is zero because time needs to expire for risk to occur. From vertex 2, the number of possible next steps and associated total costs are computed and added to the priority queue, as illustrated in Figure 4.7. Note that the total costs to reach for example vertex 12 consists of the total cost from t_{start} to $t = 100$, not just the cost from $t = 50$ to $t = 100$.

The algorithm will continue for a while, until the situation of Figure 4.8 is reached where vertex 24 is taken out of the priority queue. The new found total costs for vertex 29, 30 and 31 are not lower than the total cost for vertex 25, which means the algorithm takes a step back and continues from vertex 25. From vertex 25, vertex 30 and 31 are re-evaluated in Figure 4.9, where only vertex 30 results in lower costs than the existing options. This means that only vertex 30 is updated with the new, lower, total cost in the priority queue. Additionally, if hypothetically vertex 31 is the vertex with the lowest cost, the optimal path would revert back to using vertex 24 instead of vertex 25 (because the path from vertex 25 to 31 has higher costs than the path from vertex 24 to 31).

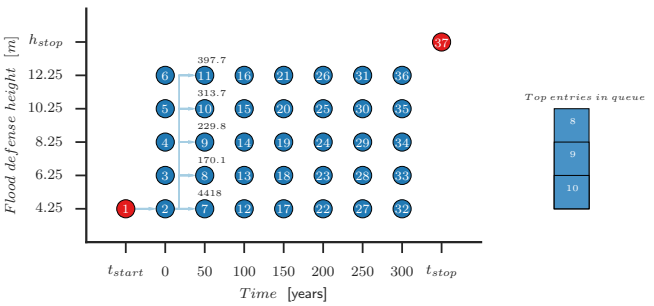

Figure 4.7: The first two iterations of the graph algorithm with a min-priority queue. The vertices available in the priority queue are those which have total costs above their respective vertices, and the first three entries are shown in the column on the right. Note that because the choice was made to connect the start vertex to vertex 2, vertices 3 - 6 will not be visited.

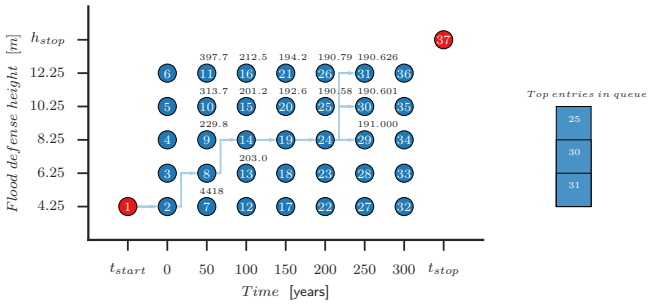

Figure 4.8: After six iterations with the graph algorithm, vertices 29, 30 and 31 are added to the priority queue. However, in this case the algorithm makes a step back in time, because vertex 25 is the item with the lowest total cost in the priority queue.

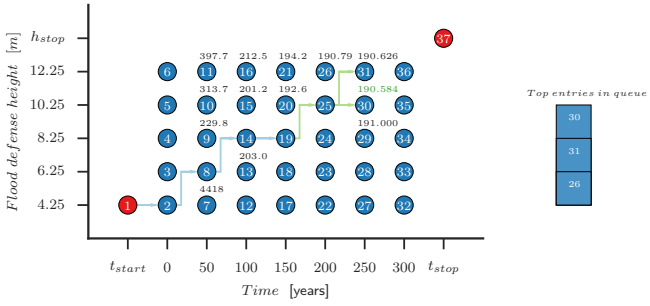

Figure 4.9: During iteration seven, the old path is abandoned, and an alternative path with vertex 25 instead of vertex 24 is taken. Vertices 30 and 31 are already in the priority queue (calculated from vertex 24), and will only get updated if the total costs from vertex 25 are lower (which is the case for vertex 30).

4.2.4. GLOBAL OPTIMAL SOLUTION

The UCS algorithm finds the shortest path in a graph, see for example [60] for a recent elaboration regarding the 'correctness' of the UCS algorithm or [61] for a proof regarding A* (UCS can be considered a special case of A*). What remains is whether the additional stop vertex of Section 4.2.2 leads to a potential heuristic solution or still to the optimal path. However, assuming that the optimal path towards the stop vertex is found, whichever vertex at t_{end} is part of that optimal path has to be the optimal choice. Otherwise, the path towards the end vertex is not optimal, which contradicts the earlier mentioned proofs. In order to further test the performance of the proposed method, Section 4.4 will compare numeric results from the proposed method to other approaches. These approaches are known to give global optimal results.

4.2.5. OVERVIEW OF THE APPROACH

A general overview of the approach discussed in the previous sections is shown in Figure 4.10. The method is composed of four steps: input, pre-processing, processing and post-processing. Of these steps, user interaction is only required at the input step. The rest of the steps run automatically. Specifically, the user needs to supply vectors of flood defence levels per flood defence, a time vector and a function which can calculate the cost of an edge in the graph. In the following steps, the graph is created (pre-process), the optimal path is found (process), and the optimal path is shown (post-process).

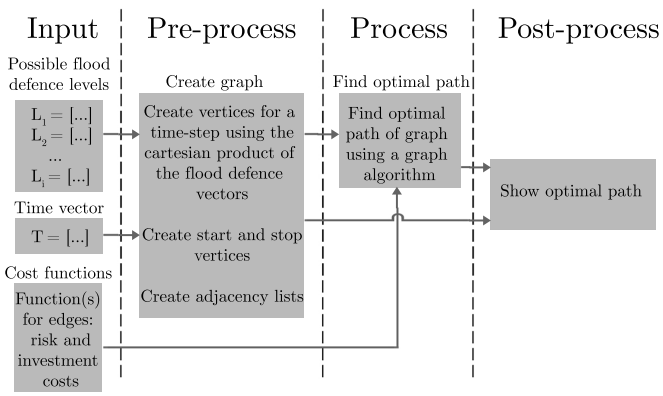

Figure 4.10: Overview of the approach using a graph and graph algorithm. In the proposed approach, the graph algorithm is the UCS algorithm. The input column is the only part what the user should provide, the other steps run automatically.

4.3. EFFICIENCY IMPROVEMENTS

The economic optimisation of multiple interdependent flood defences, implemented in a graph using Section 4.2, can potentially lead to large numbers of vertices and even

larger numbers of edges. For example, for eight interdependent flood defences with six possible heights the number of vertices per time step is approximately 1.68 million (6^8), while the number of edges per time step is even larger at approximately 35 billion. For large problems such as these, storing all the possible vertices and edges would lead to huge data structures and a huge number of EAD calculations. This requires both an efficient implementation of the graph, and an efficient evaluation of EAD calculations (i.e. as few as possible). An efficient graph implementation is discussed in Sections 4.3.1 & 4.3.2, while the efficient evaluation of EAD calculations is discussed in Section 4.3.3. Potential further efficiency improvements are discussed in Section 4.3.4.

4.3.1. REPETITIVENESS IN LISTS OF VERTICES

Even though the graphs of Section 4.2.1 can be classified as sparse graphs (number of edges is much smaller than the number of vertices squared, [56]), the number of edges is still much larger than the number of vertices. Therefore, focus was first placed on data structures related to the edges of a graph. For sparse graphs, these are the adjacency lists: a group of vertices connected via edges stemming from a source vertex in a previous time step. In these adjacency lists, repetitiveness can be found with respect to two aspects.

The first repetitive aspect is the similarity of adjacency lists for the same combination of flood defence levels at different time steps (except for the adjacency lists at t_{end}). In Figure 4.7, vertices with the same combination of flood defence levels at different time steps are for example vertices 2, 7 and 12. The adjacency lists for these vertices are shown in Figure 8, where it is apparent that the adjacency list for the next time step can be found by adding an offset to the elements of the adjacency list of the current time step. For example, the adjacency list of vertex 2 can be turned into the adjacency list of vertex 7 by adding the total number of combinations in each time step (which is five in Figure 4.11)

The second repetitive aspect is for adjacency lists between vertices in the same time step. Because the lowest vertex in each time step (e.g. vertices 2, 7, 12, 17, 22 and 27 in Figure 4.7) has outgoing edges running to each and every vertex in the next time step, higher vertices (e.g. in Figure 4.7, vertex 8 is 'higher' than vertex 7) contain a subset of the adjacency list of the lowest vertex. In other words, outgoing edge lists in a single time step can be generated dynamically by shrinking the adjacency list of the lowest vertex in a time step. This is shown in Figure 4.12.

The combination of these two repetitive characteristics results in that only a single adjacency list needs to be stored in memory (i.e. the adjacency list of the lowest vertex in the first time step). This single adjacency list can be adapted to most vertices in the graph by means of offsetting and shrinking the stored adjacency list. Notable exceptions are the adjacency lists for the vertices at t_{end}, but the adjacency lists for these vertices are already known and only contain the stop vertex.

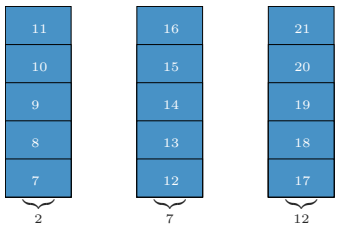

Figure 4.11: The adjacency lists for vertices 7 and 12 of Figure 4.7 can be obtained by adding an offset to the adjacency list of vertex 2.

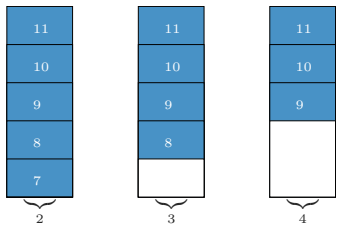

Figure 4.12: The adjacency lists for vertices 3 and 4 of Figure 4.7 are reduced sets of the adjacency list for vertex 2.

4.3.2. CONDITIONALLY REMOVING EDGE CONNECTIONS

Besides reducing the size of the data structures associated with a graph, the adjacency list associated with a vertex can also be reduced under certain conditions. Typically, the time between improvements in flood defences is large (in the order of 50 years), due to either high (fixed and variable) costs associated with investments in flood defences, or long planning periods [46]. Therefore, if one or multiple flood defences have been strengthened recently, the adjacency list can be reduced to only contain vertices that keep the recently strengthened flood defence(s) at the current level(s). However, this so called 'waiting time' before new investments are considered has to be chosen with care, because the waiting time should not influence the optimal time between investments. Nevertheless, a correctly chosen waiting time can greatly improve the run time of the algorithm, because of the significant reduction in number of edges that need to be evaluated. This reduction is shown in Figure 4.13, where the total number of visited vertices is plotted as a function of the 'waiting time'; the underlying problem that is solved by the algorithm is the same problem as shown in Section 4.4.3.

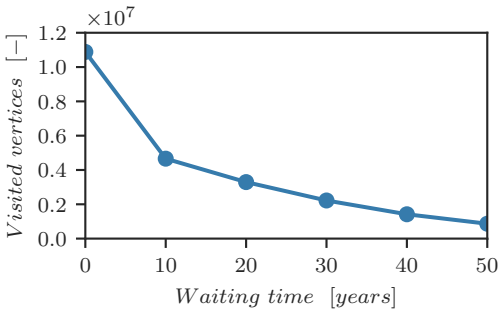

Figure 4.13: Total number of visited vertices as a function of the waiting time for the example of Section 4.4.3.

4.3.3. REDUCING THE NUMBER OF EAD CALCULATIONS

In the overview of Figure 4.10 it is implied that the EAD calculations belonging to an edge are only carried out when that edge is visited by the graph algorithm. Provided that a graph algorithm does not visit all vertices, delaying EAD calculations belonging to an edge until that edge is visited leads to less EAD calculations than the total number of possible EAD calculations in a particular graph. In contrast, if EAD (or more generally, cost) calculations are done before a graph algorithm is initialised, all possible EAD calculations need to be calculated beforehand.

As an example, Figure 4.14 shows the number of times each vertex is visited is in the example of Section 4.2.2. The majority of the vertices in Figure 4.14 get visited once, but a significant proportion is never visited by the graph algorithm; these vertices have a zero above their indices. A small proportion of the vertices, specifically vertices 30 and 31, are visited twice; the reason for this re-visiting can be seen in Figure 4.9. To avoid completely re-doing cost calculations upon a revisit, parts of a calculation can be cached in order to reduce the computational penalty incurred by revisiting vertices. The total number of possible EAD calculations is the number of years multiplied with the number of options on the y-axis; for Figure 4.14 this leads to a total number of EAD calculations of 1505 (or $301 \cdot 5$). Because a number of vertices do not get visited by the algorithm, the number of actual executed EAD calculations goes down to 1000, or approximately 66% of all possible EAD calculations.

Furthermore, the number of EAD calculations can be further reduced by using the 'waiting time' of Section 4.3.2. In Section 4.3.2, it was found that a minimum waiting time between investments will lead to less edges being evaluated by the algorithm. This also implies that less EAD calculations will be executed. Using the same example as in Figure 4.13, the reduction in the percentage of actual executed EAD calculations is given as a function of the waiting time in Figure 4.15. Between using a waiting of 0 years (i.e. no minimum waiting time at all) and a waiting time of 50 years the number of EAD calculations goes down from approximately 60% to 40% for the example of Section 4.4.3.

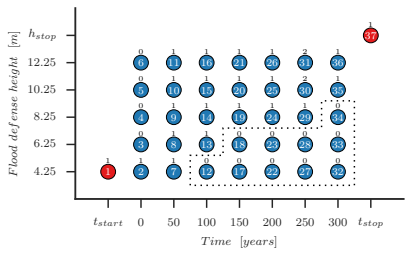

Figure 4.14: Number of times each vertex is visited by the algorithm for the example in Section 4.2.2. The dotted area emphasizes that a part of the graph is never visited, while vertex 30 and 31 get visited twice.

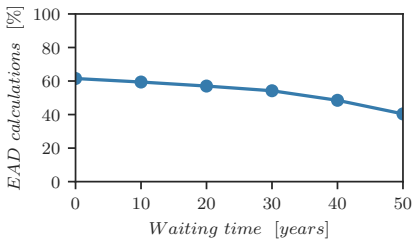

Figure 4.15: Percentage of actual executed EAD calculations as a function of the waiting time for the example of Section 4.4.3.

4.3.4. POTENTIAL IMPROVEMENTS AND SPECIAL CASES

Further improvements can be made both to the graph implementation and to the implementation of the algorithm. The algorithm was implemented as a single process; a performance improvement might be found by utilizing parallel programming. The first place where parallel programming could be beneficial is the loop over an adjacency list. This is because the potentially expensive EAD calculations are done as part of determining an edge weight. Therefore, parallelising the loop over an adjacency list over multiple computational nodes can lead to significant performance improvements.

Furthermore, regarding the graph implementation, a special case is a flood defence system which has independent flood defences. Section 4.2.1 uses the Cartesian product of flood defence options, which has the underlying notion that all flood defences are interdependent. If some flood defences are independent (i.e. the defences protect different, independent areas), this leads to an inefficient graph. The independency of flood defences can be used in an adapted graph representation in order to get an efficient graph. While this is not implemented in this chapter, a way to solve this inefficiency for the system in Figure 4.16 is shown conceptually in Figure 4.17, which uses 'subgraphs' to reduce the number of combinations.

These subgraphs are small graphs which only contain the number of strengthening options for a single defence for a single time period (e.g. in Figure 4.17, from t_{i-1} to t_i). Additionally, the subgraphs take into account what the level is of the influential defences (e.g. in Figure 4.17, the front defence B is the only influential defence for the rear defences). The use of subgraphs leads to a smaller number of combinations, as the Cartesian product would have resulted in a total number of 5120 ($5 \cdot 4^5$) vertices per time step. With subgraphs, the number of vertices per time step is reduced to 100 ($5 \cdot 5 \cdot 4$).

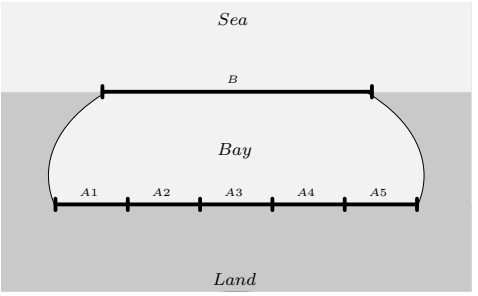

Figure 4.16: A top view of a system with a front line defence (B, five possible safety levels) and five rear defences ($A1 - A5$, each has four possible safety levels). The front defence influences the rear defences, but the rear defences do not influence each other.

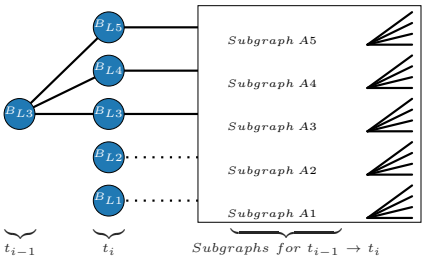

Figure 4.17: Part of the graph belonging to the system of Figure 4.16 for the period t_{i-1} to t_i. Because the rear defences do not influence each other, subgraphs are used for the rear defences.

4.4. RESULTS FOR SIMPLIFIED FLOOD DEFENCE SYSTEMS

In order to test the performance of the proposed algorithm versus some existing approaches, three cases are investigated. For simplicity, these three cases will be based upon a common set of investment and EAD relations, as well as a common set of input values. The values and symbols used in this section are largely copied from [20, page 34] and reproduced in Table 4.1, with only minimal changes. These EAD and investment cost relations consist of simple formulations which were specifically chosen for exhibiting the approach, for ease of reproducibility, and for showing the efficiency regarding the number of EAD calculations. In practice, EAD estimates can be quite complex and/or have a high computational burden, especially when flood defences are modelled to have hydrodynamic interactions with each other. For example, a single EAD estimate for a complex flood defence system with interdependencies can take hours [15] or even days [14].

Table 4.1: Variables and values taken from [20] for the EAD and investment equations in this section. NLG refers to the currency used in the Netherlands prior to the euro.

Name	Unit	Symbol	Value
Height above mean sea level, base	cm	H_0	425
Annual exceedance probability belonging to H_0	-	P_0	0.0038
Parameter exponential distribution water level	1/cm	α	0.026
Increase water level	cm/year	η	1
Damage by flooding in 1953	10^6 NLG	V_0	20000
Economic growth	1/year	γ	0.02
Rate of interest (real)	1/year	δ	0.04
Variable costs of investment	10^6 NLG/cm	C_v	0.42
Fixed costs of investment	10^6 NLG	C_f	61.7
Heightening of the flood defence at time t	cm	u_t	-
Height of the flood defence at time t	cm	H_t	-

The common set of investment (I) and EAD (or flood risk cost, R) relations are similar to the relations used with the data of Table 4.1 in [20]. The sum of the investment cost and EAD is the total cost, which needs to be minimised in order to get economically optimal safety targets:

$$\text{Total Cost} = \int_0^\infty R(t)\,dt + \sum_{t=0}^{\infty} I(t) \tag{4.4}$$

$$R(t) = P_0 e^{-\alpha(H_t - H_0 - \eta t)} V_0 e^{\gamma t} e^{-\delta t} \tag{4.5}$$

$$I(t) = \left(C_v u_t + C_f \text{sign}(u_t)\right) e^{-\delta t} \tag{4.6}$$

where $\text{sign}(u_t)$ is used to prevent fixed costs in case there is no heightening u_t. This

sign(u_t) function returns zero if the heightening u_t is equal to zero, and returns one when the heightening u_t is larger than zero.

4.4.1. SINGLE FLOOD DEFENCE

For a single flood defence, with the values of Table 4.1, an analytical solution can be found in [20, page 35]. This solution consists out of an initial dike height increase coupled with a periodical, constant dike increase over an infinite time horizon. The numerical results were re-calculated with the solution listed in [22], and resulted in an immediate initial increase of 235 centimetres with a periodical increase of 129 centimetres every 73 years.

Because the approach introduced in this chapter is a numerical approach, a finite time period had to be used instead of an infinite time horizon. Similar to [46], a time period of 300 years was used with, for this application, steps of one year. The possible heights were discretized using a range starting from 425 to 1225 cm, with steps of one centimetre. Note that these step sizes (and dimensions) were deliberately chosen to be on par with the accuracy level of the analytical solution. In practice, these step sizes would probably be too detailed for the practical attainable accuracy in flood defence construction (see also [46]). Furthermore, the total number of possible EAD calculations in this problem is 241,101 (or $801 \cdot 301$). Of these, 137,971 were actually executed by the UCS algorithm, which corresponds to using only 57% of all possible EAD calculations. Increasing the 'waiting time' to 50 years did not affect the solution but did reduce the percentage of executed EAD calculations down to 43%.

A comparison of the results found using the algorithm and the analytical solution is shown in Figure 4.18. The algorithm found an initial increase of 235 cm, with three additional increases in height at 73 years apart. These three were found to be 129 cm, 130 cm, and 132 cm. The last increase is different from the analytical solution, and can be attributed to being close to the end of the time horizon. A finite time horizon implies that there is no EAD beyond the time horizon, which explains why there is no investment found by the algorithm in year 292. To compensate for the lack of an investment in year 292, the investment in year 219 is slightly larger. This explanation is supported by results with a time horizon of 400 years, where the heightening in year 219 changes to an expected 129 centimetres. These deviations near to the time horizon underline that if a certain point in time is considered relevant, the used time horizon should stretch significantly beyond that point in time. However, this is a general problem with all numerical methods, because of the required finite time horizon, and not a specific issue related to the approach proposed in this chapter. Furthermore, in practice this problem can be circumvented by setting the time horizon used in the algorithm to sufficiently exceed the practically required time horizon.

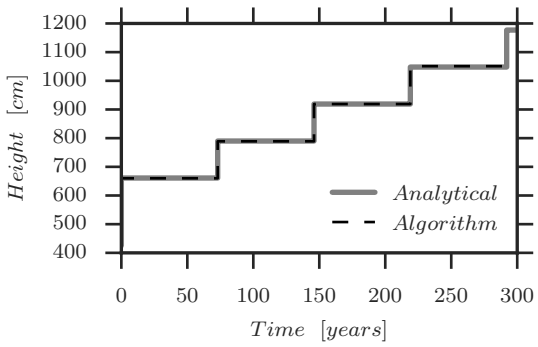

Figure 4.18: The investment scheme found using the algorithm is almost identical to the analytical solution.

4.4.2. TWO INDEPENDENT FLOOD DEFENCES

In the next example two defences are investigated using the graph algorithm, both with the same characteristics as the single flood defence in the previous section. However, the step size for the heights is increased to 20 cm in order to test the response of the algorithm to larger step sizes. Expected is that, despite the less detailed step size, the investment scheme for both defences should be identical to each other and close to the analytical solution provided in the previous section.

Indeed, the results of the algorithm, illustrated in Figure 4.19, show that both defences are initially increased with 240 cm, while in both year 75 and 143 the defences are increased with 120 cm, and finally in year 212 with 140 cm. Clearly, the larger step size in height leads to larger differences when compared to the analytical solution. Nevertheless, any overshoot/undershoot of the height is 'repaired' in the duration between investments, keeping the solution of the optimal path stable and close to the analytical solution. Furthermore, the total number of possible EAD calculations in this problem is 24,682 (or $2 \cdot 41 \cdot 301$). Of these, 14,510 were actually executed by the UCS algorithm, which corresponds to using only 59% of all possible EAD calculations. If a 'waiting time' of 50 years is used, the solution is unaffected but the percentage of executed EAD calculations goes down to 48%.

4.4.3. TWO DEPENDENT FLOOD DEFENCES

The final case is similar to the case with two independent flood defences, however the second defence is now dependent on the performance of the first defence. This dependency is illustrated in Figure 16, and is a simplified version of the case discussed in [26] and Chapter 3.

The dependency between the defences in Figure 4.20 is implemented by adapting

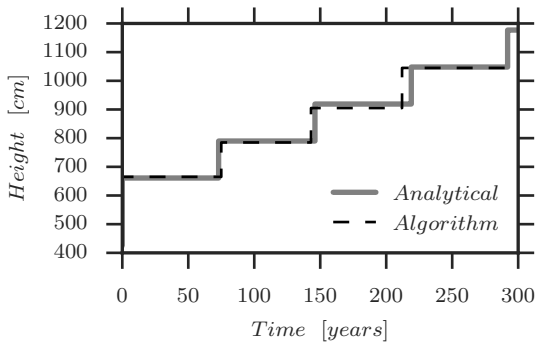

Figure 4.19: The two (independent) flood defences have an identical solution with the approach proposed in this chapter, and are (even with the usage of larger step sizes) good approximations of the known analytical solution.

Figure 4.20: A coastal system with two lines of defence. This figure is an adaption from an illustration found in [26].

the EAD equation of Eq. 4.5 as follows:

$$R(t) = \left(P_1 P_{2|1} + (1 - P_1) P_{2|\bar{1}}\right) V_0 e^{\gamma t} e^{-\delta t} \tag{4.7}$$

$$P_i = P_0 e^{-\alpha_i (H_{i,t} - H_0 - \eta t)} \tag{4.8}$$

where P_i is a generic formulation used for the failure probabilities P_1, $P_{2|1}$ and $P_{2|\bar{1}}$. The probabilities and are the failure probabilities of the second defence, dependent on the failure ($P_{2|1}$) or non-failure ($P_{2|\bar{1}}$) of the first defence, where the failure probability of the first defence is denoted by P_1. Similarly, the investment equation in Eq. 4.6 is expanded to include different costs for the two lines of defence:

$$I(t) = \left(C_{v1} u_1 + C_f \operatorname{sign}(u_1)\right) e^{-\delta t} + \left(C_{v2} u_2 + C_f \operatorname{sign}(u_2)\right) e^{-\delta t} \tag{4.9}$$

The new variables used in Eqs. 4.7, 4.8 & 4.9 are listed in Table 4.2. The solution found with the approach proposed in this chapter was checked with the method proposed in [27]; the outcomes of both methods were found to be identical and are shown in Figure 4.21. Furthermore, the total number of possible EAD calculations in this problem is 505,981 (or $41^2 \cdot 301$). Of these, 311,190 were actually executed by the UCS algorithm, which corresponds to using only 62% of all possible EAD calculations. If a 'waiting time' of 50 years is used, the solution is unaffected but the percentage of executed EAD calculations goes down to 40%.

Table 4.2: Additional variables used in Eqs. 4.7, 4.8 & 4.9, complementary to Table 4.1.

Name	Unit	Symbol	Value
Annual exceedance probability belonging to H_o	-	P_0	0.01
Exponential parameter for defence 1	1/cm	α_1	0.026
Exponential parameter for defence 2 for $P_{2\|\bar{1}}$	1/cm	$\alpha_{1\|\bar{2}}$	0.052
Exponential parameter for defence 2 for $P_{2\|1}$	1/cm	$\alpha_{1\|2}$	0.026
Variable costs of investment for defence 1	10^6 NLG/cm	C_{v1}	0.21
Variable costs of investment for defence 2	10^6 NLG/cm	C_{v2}	0.42

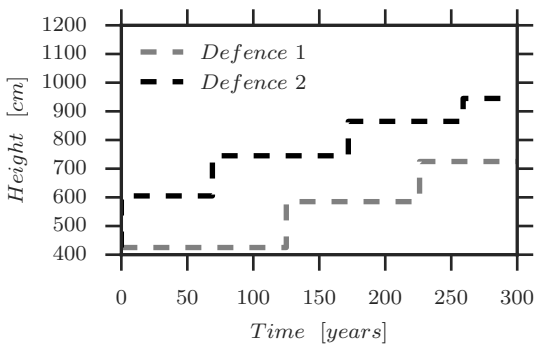

Figure 4.21: Optimal investment schemes for the case with two interdependent flood defences.

4.5. DISCUSSION

The proposed approach (see also Figure 4.10) in this chapter is based on a best-first graph algorithm, which is relatively easy to implement in most general or scientific programming languages. This can be considered to be a significant advantage over linear programming algorithms, especially for those who are not familiar with the implementations of linear programming as proposed by [27]. Although the application area is the same as for [27], notable differences are present between the two approaches. The approach of [27] is capable of including both interdependent & independent flood defences and focused on finding the proven economically optimal solution quickly given pre-calculated EAD estimates and investment costs. The proposed approach focuses on flood defence systems with mostly interdependent flood defences (though Section 4.3.4 does discuss a possible efficient extension to mostly independent flood defences) and computational costly EAD calculations. Therefore, the focus of the proposed approach is on reducing the number of actually executed EAD calculations (compared to pre-calculating all possible EAD estimates).

An inherent problem of working with flood defence systems where most, if not all, elements are dependent on each other, is that the number of system combinations grows exponentially with the number of interdependent flood defences. The sheer number of combinations means that the total number of interdependent flood defences should probably be kept below ten. This is nothing more than a rule of thumb based on the experience running the best-first graph algorithm on a consumer laptop. The true maximum depends on a number of factors: the number of height options per defence, the performance of the particular implementation of the proposed approach, the computational cost of the associated EAD functions and the computational power of the computer used.

Even though all examples in this chapter make use of flood defence heights, this was only done to illustrate the approach. Other measures besides flood defences can be incorporated as well in the graph that is used to find the optimal solution. While this is not a unique feature of the proposed approach (i.e. any graph-based approach can do this), it is a relevant point for the viability of practical applications. For example, if a retention area is considered (as illustrated in Figure 4.22), a list with possible sizes of the retention area could also be used in the approach of Figure 4.10: in principle, as long as a measure has a number of options or levels in increasing order that can be quantified and monetised, it can be included in the approach. This makes the actual application range much wider than flood defence systems with only height-dependent flood defences such as levees or (storm surge) barriers.

The proposed approach works best if the type of each flood defence is known and singular. In the case that a number of different defence types are considered for the same flood defence, it would be better to do an optimisation run per type of defence. An example of this would be the choice between a closure dam or a storm surge barrier at the same location. In this case, the algorithm should be run twice, first with a closure

dam and then with a storm surge barrier. This should result in two optimal configurations (one with a closure dam, the other with a storm surge barrier), which can then be compared using the same metric, for example their benefit-cost ratios.

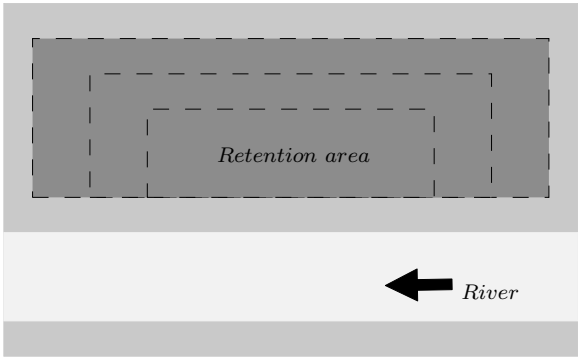

Figure 4.22: A retention area can also be optimised using the approach proposed in this chapter. In this example, the surface area of the retention basin is used instead of the height of a flood defence.

4.6. CONCLUSIONS

This chapter presented a generic, computationally efficient approach for finding the economically optimal configuration of a flood defence system with an arbitrary number interdependent flood defences. Computational efficiency was achieved by delaying EAD (Expected Annual Damage) calculations until they are actually needed in an optimisation routine (i.e. 'lazy evaluation'), which leads to a reduction in the number of EAD calculations that need to be done. In the examples shown in this paper, the reduction in number of EAD calculations was at least 40%. This is a significant and relevant reduction, as the EAD calculations relevant for this approach often have a high computational cost. This is especially the case when multiple flood defences interact with each other hydrodynamically in a larger flood defence system.

The approach presented in this chapter uses a best-first graph algorithm, which is simple to implement and advances existing shortest-path implementations for economic optimisation of interdependent flood defence systems. Furthermore, the approach is flexible towards the number and type of flood defences because the graph representation shown in this chapter can trivially accommodate an arbitrary number of interdependent flood defences. The proposed approach utilizes the repetitive properties of the graphs in order to efficiently store the representation of the graph in memory. In case independent flood defences are present in a system, the proposed approach of generating a graph can be adapted to a more efficient method which makes use of the attractive properties of independence. To that end, a concept has been proposed which reduces the size of the graphs.

Assuming that the graph and combinations of flood defences are portrayed correctly,

the best-first graph algorithm has been proven in literature to return the shortest (or optimal) path in a graph. To corroborate this for the proposed implementation and intended application, the method was tested on a number of benchmark problems with known solutions. The tests show that indeed the optimal path is found with the approach proposed in this chapter, which justifies the conclusion that the implementation was done correctly.

5

IMPACT OF INCLUDING INTERDEPENDENCIES BETWEEN MULTIPLE RIVERINE FLOOD DEFENCES ON THE ECONOMICALLY OPTIMAL FLOOD SAFETY LEVELS

In risk analysis of riverine flood defence systems, sections of flood defences are often considered separately, herewith ignoring their interdependence, e.g. due to the hydraulic response following dike breaches in the system. In previous studies it has been found that such interdependence can have a significant influence on flood risk estimates and the spatial distribution. In this chapter a method is proposed for the economic optimisation of riverine flood defence safety levels from a river system perspective. In order to deal with the computational challenge of integrating the hydraulic interactions in an economic optimisation, a surrogate model was developed. Despite the many simplifications, this model yields reasonably accurate results within acceptable time. The application of the model to a case study in the Netherlands has shown that taking into account interactions between flood defences has significant influence on optimal long term strategies for flood defences. The results suggest that accounting for interdependence in setting safety standards and reinforcement prioritisation yields a significant return on investment both in terms of lower investment cost and in terms of more effective risk reduction.

The contents of this chapter have been published in [62].

5.1. INTRODUCTION

Settlements and industry along rivers are often protected against flooding by flood defences such as dikes and hydraulic structures. Multiple flood defences in the same river basin area can be considered as a system of riverine flood defences. In The Netherlands, flood defence systems are used to protect a major part of the country against flooding. The safety level of these systems is assessed periodically and policies are in place to meet the safety standard in 2050 for all primary flood defences.

A common way of determining how safe a flood defence system currently is, is by analysing for each flood defence separately how it performs under loading. In case of a riverine flood defence system, the loading could be a high river discharge. However, recent literature shows how multiple flood defences interact with each-other hydrodynamically as a system during an extreme event [e.g. 12–16]. These studies found significant differences in case a system as a whole was studied instead of as separate, independent elements.

The required safety of a flood defence can be (and, for the Netherlands, is) based on criteria for acceptable risk [2, 63]. One of the acceptable risk metrics used in the Netherlands is an economic cost-benefit analysis, which is used to determine the optimal protection level of a flood defence (e.g. see as early as [9]). In this chapter such an economic optimisation of protection levels is considered. Other acceptable risk criteria such as societal risk and individual risk (life safety) are not considered here but are important nonetheless. Examples of other criteria for acceptable risk can be found in for example [29], as well as in the context of Integrated Flood Risk Management (IFRM, e.g. see [64]). However, in this chapter only the economic acceptable risk by means of an economic optimisation is considered.

'Optimal' is defined in this context as where the total costs, which is the sum of investment costs and expected annual damages, is at a minimum. The Expected Annual Damages (EAD) of flood defences are defined in an economic optimisation as the expected loss in an arbitrary year, and can be found as a function of the annual probabilities of flooding and the expected damages due to flooding ([1]); an overview of this approach as followed in the Netherlands can be found in [17]. These EAD estimates change in time by effects such as economic growth and climate change. The results of following the general approach as described in [17] can be displayed as a series of (economically optimal) investments to adjust the safety level of a flood defence over time (Figure 5.1).

In an economic optimisation, the probability of flooding can be estimated using reliability analysis. In order to include interdependencies between flood defences in an economic optimisation, not only the reliability analysis need to be able to include these interdependencies, but the economic optimisation approach as well. In the economic optimisation methods mentioned in for example [17], interdependencies between multiple flood defences are not present. An economic optimisation method which is able to handle these interdependencies (which was applied to a case study in the Netherlands) can be found in [27]. However, this method used pre-calculated EAD estimates and fo-

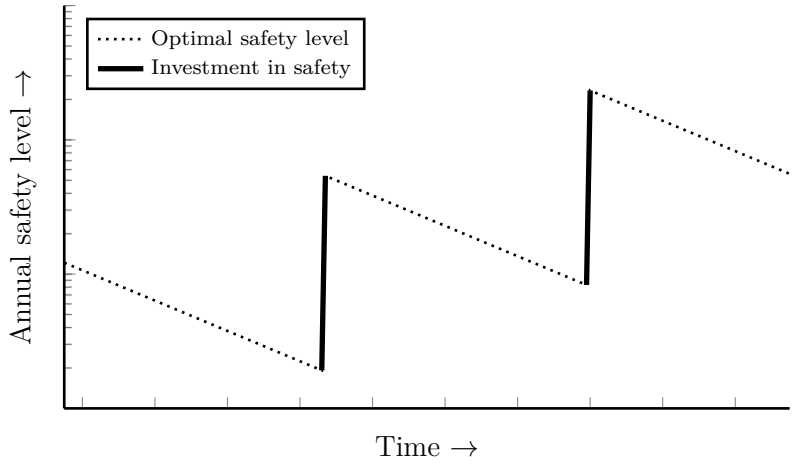

Figure 5.1: Schematic view of the result of an economic cost-benefit analysis for a flood defence (e.g. as described in [17]). A series of investments are needed to make sure that the defence remains at an optimal level from an economic point of view due to (over time) changing expected annual damages. Image reproduced from [53].

cused on an application for a coastal system. For riverine systems, this method needs to be evolved further as pre-calculating EAD estimates is not always feasible.

Generally speaking, each flood defence in a riverine system can be interdependent on any other flood defence in that same system by means of hydrodynamic interactions. A straightforward example of this is a river along which flood defences exist. If an upstream flood defence breaches, a part of the river discharge will flow through the breach, leading to less discharge downstream. Less discharge downstream means that the load on the downstream defences will be reduced. The fact that each flood defence in a riverine system can be interdependent on any other flood defence in that same system, makes a riverine flood defence system more complex than a coastal flood defence system. Furthermore, obtaining a single EAD estimate for a riverine flood defence system with hydrodynamic interactions can be computationally expensive: it can take hours [15] or even days [14]. In the context of an economic optimisation, where a large number of EAD estimates need to be evaluated, this can quickly become infeasible.

In this chapter a cost-benefit analysis is carried out for a riverine flood defence system with multiple interdependent flood defences, in a computational tractable manner. This economic cost-benefit analysis will then be used to compare the impact of including the effect of hydrodynamic interactions of multiple flood defences on the economically optimal investment scheme in a case study (compared to not including these interactions). The term interdependency, instead of the more generic (statistical) term dependency, is used here to express the dependent behaviour (i.e. hydraulic interactions) between different flood defences.

While analytical derivations are interesting for simple (riverine) cases, as is demonstrated in Appendix C, these are heavily simplified cases and therefore interesting mostly from an academic point of view. The case presented in this chapter is more complicated and complex than the cases in Appendix C, which would result in either overly long and obfuscated analytical equations or overly simplified equations.

The work presented here builds upon previous work done in [26, 53, 65]. The general idea of performing an economic optimisation with EAD estimates based on hydrodynamic interactions between flood defences was also used [26], but with less types of hydrodynamic interactions and applied to a (different, simpler) coastal system. [65] discusses some fundamental impacts of including riverine hydrodynamic interactions on an economic optimisation, but does this using an analytical economic optimisation and hypothetical, small riverine systems. The economic optimisation method discussed in [53] is applied here as part of the case study.

5.2. CASE DESCRIPTION

The case study used in this research is based on the area in the Netherlands where the river Rhine enters the Netherlands, see also Figure 5.2. This area has been the subject of a number of recent studies regarding the impact of hydrodynamic interactions on flood risk estimates in the area (see for example [14–16]). Instead of using these existing models, a simplified model was developed in order to reduce the model run time. This model is similar to the existing models with respect to the fact that it represents the impact of hydrodynamic interactions on EAD estimates. The underlying model is primarily based on the work in [15], but with simplified hydrodynamics (in order to reduce model run time). Section 5.3 contains further details regarding the model and how it is used in an economic optimisation. An overview of the case area is shown with two illustrations in Figure 5.3.

In Figure 5.3, the flood prone areas are 'D48', 'D49', 'D50' and 'D51'. All these areas can experience damage due to flooding (the areas are indicated with striped rectangles). Breach flows can occur due to breaches at nine locations, which represent potential breach locations and their impacts anywhere in the system. These breach locations are indicated with stars in Figure 5.3, while the arrows originating from the breaches represent the breach flows. The breach flows represent the hydrodynamic interactions in the model. Breaches can occur, depending on the breach location, external and/or internal. External breaches occur at the river-facing side of a breach location due to a local extreme river discharge. On the other hand, internal breaches occur due to a load at the polder-facing side due to water levels of an already flooded area.

The breach location 'GER', if it breaches, has two breach flows: one flow connects to the flood prone area D48 (10% of the breach volume Q_{GER}), while the second flow forms a shortcut to the river IJssel (90% of the breach volume Q_{GER}). Furthermore, the breach locations B49i and B50i can form internal shortcuts between the flood prone areas D49 & D50 and D50 & D51, respectively. The breach flows associated with the breach locations

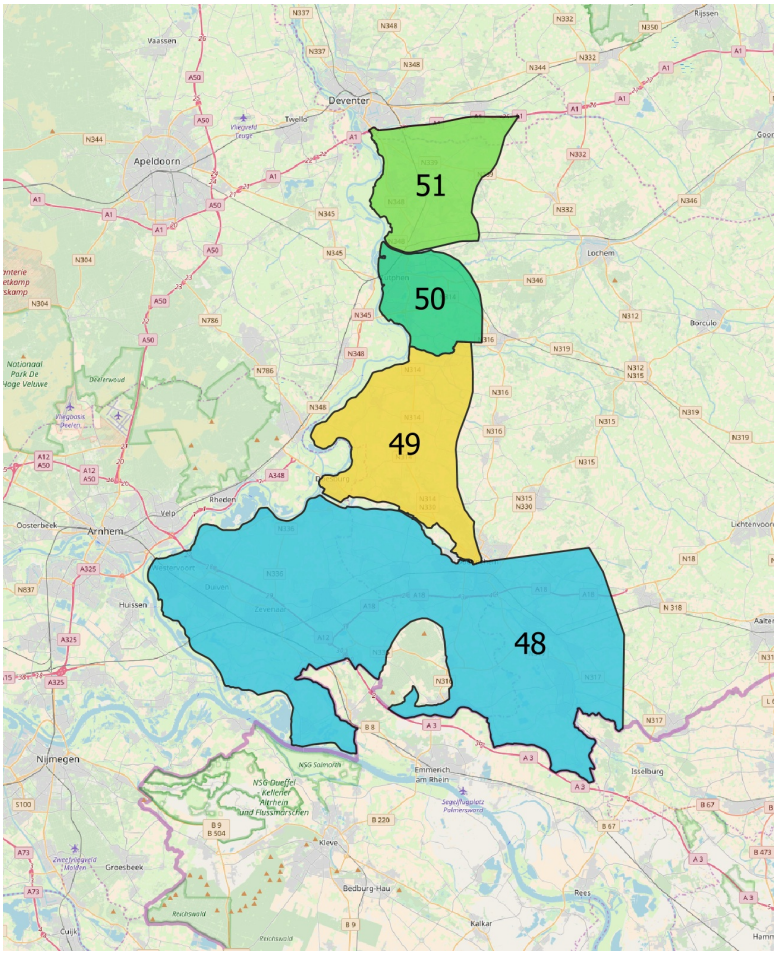

Figure 5.2: The actual area in the Netherlands upon which the case in this section is based. The numbered surfaces are dike ring areas, which are areas that are protected by flood defences (which are typically dikes). Map data © OpenStreetMap.

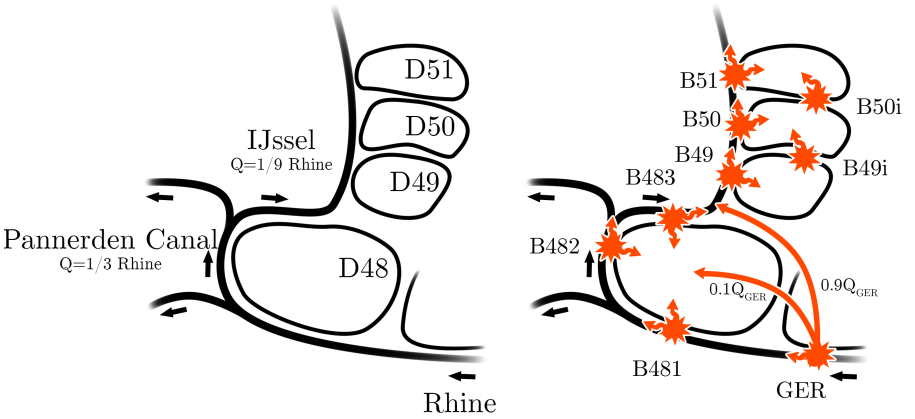

Figure 5.3: Overview of the simplified case study area. The illustration on the left shows the names and flow directions of the river branches in the study area, as well as the numbers of the areas prone to flooding. The illustration on the right shows the same area, but now with the locations & names of breaches and the resulting breach flows.

B49i & B50i are purposefully directed downstream, as the area along the river IJssel is sloping downwards in the downstream direction of the river.

To provide a benchmark for results with hydrodynamic interactions, the model can be run without hydrodynamic interactions as well. This means that the hydrodynamic interactions are removed from the hydrodynamic model. Practically, 'no hydrodynamic interactions' has the following implications:

- The breach location GER will not form a shortcut from the Rijn to the IJssel;
- If a breach occurs, the downstream river discharge is unaltered;
- The internal breach locations B49i and B50i never breach, which means that internal shortcuts cannot be formed;
- The four breach locations GER, B481, B482 and B483 can all still influence the flood damage at D48 together.

5.3. APPROACH

5.3.1. GENERAL APPROACH

In principle, an economic optimisation of a flood defence system is a cost-benefit analysis which attempts to minimize the Net Present Value (NPV) of the total cost, where the

total cost is the sum of the Expected Annual Damage (EAD) estimates (Section 5.3.3) and the accompanying investment costs (Section 5.3.4); see also for example [9, 22]. In this case, the EAD estimates are determined by means of hydrodynamic simulations and impact assessments of (potential) flood events while taking into account the performance of the flood defence systems in place (Section 5.3.2). Practically, this means that the economic optimisation evaluates various system configurations (in terms of the reliability levels of the individual flood defence sections) in order to find an optimal investment scheme for the considered time period. A system configuration is defined here as a unique combination of flood defence levels. For example, in a flood defence system with two flood defences A and B, where both flood defences have five possible levels (labeled here as 1 to 5), a single system configuration (out of a total of $5^2 = 25$ possible configurations) would be flood defence A at level 1 and flood defence B at level 2.

Usually, an economic optimisation of flood defences requires repeated investments (see e.g. [21, 22]) as time dependent changes such a economic growth in a flood-prone area, reduced dike strength due to subsidence and increasing river discharges due to climatic changes increase the EAD. This means that, at some point in time, it will become economically attractive to (re)invest in reinforcing flood defences, which is incorporated in the optimisation routine through the Present Value (PV) of cash flows.

Figure 5.4 shows an overview of the approach. Starting from a current system configuration, the hydraulic interactions are implemented in hydrodynamic simulations and damage estimations (Section 5.3.2), which are used to estimate the EAD (Section 5.3.3). An optimisation algorithm then determines, based on a cost-benefit analysis, the optimal system configuration per time step for the considered time period (economic optimisation, Section 5.3.5). This collection of optimal system configurations in time can then be used to determine the accompanying optimal investment scheme.

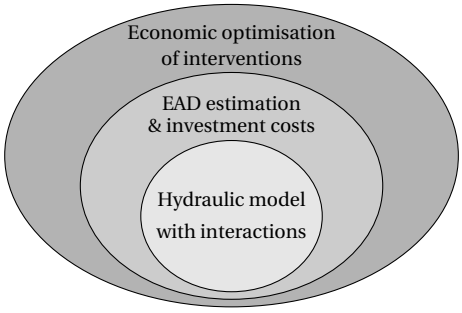

Figure 5.4: Overview of an economic optimisation with hydraulic interactions, as further described in Section 5.3.2 - 5.3.5.

5.3.2. HYDRAULIC SIMULATIONS AND DAMAGE ESTIMATIONS

If a flood defence breaches, flood damage due to the inflow of water can be expected. In order to estimate these (economic) flood damages, two primary elements need to be determined for a flood-prone area: the extent and severity of a flood, and the damage due to this flooding. The first can be simulated with a wide range of methods, for example with 1D models [e.g. as in 15], 2D models [e.g. as in 14], or flood cell storage methods [e.g. as in 12]. After estimating the extent and severity of the flood, typically in terms of flood depth and for some purposes also in terms of flow velocities, the information is combined with vulnerability characteristics (e.g. stage-damage curves) to obtain damage estimates. In The Netherlands, the HIS-SSM method can do this based on land use and damage functions [15, 66].

The hydraulic simulations for the case study are done with a (simplified) hydrodynamic model that describes the propagation of a (peak) discharge wave through the river branches. Once a breach occurs at a breach location, breach flows can occur toward flood-prone areas or form a shortcut between river branches (as described in Chapter 5.2). A more detailed description of the hydrodynamic model can be found in D.1. A single model run yields information regarding which flood defence has breached and what the inundation depths are at flood prone areas. Figure 5.5 shows an example of a time series of inundation depths with a time step size of two hours.

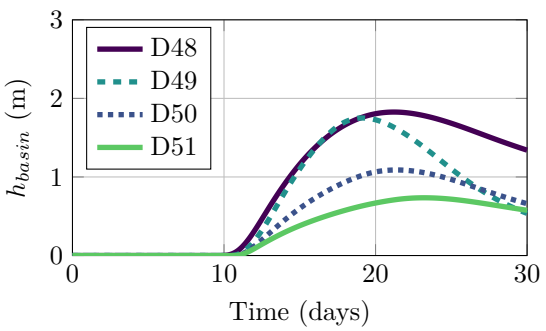

Figure 5.5: Example of inundation depths for the flood prone areas of Figure 5.3 for a single model run with a peak discharge of 16,000 m^3/s.

The damage (D) in the flood prone areas of the case study is assumed to follow a logarithmic relation that depends on the inundation depth (i.e. h_{basin}) and is shown in Eq. 5.1. The maximum damage (D_{max}) is reached at the inundation level d_{max}, as shown in Figure 5.6. The values for the maximum damage and the maximum inundation depth are shown in Table 5.1. The values for the maximum damage (D_{max}) are based on data listed in [22] which represent a monetary valuation of material and non-material loss in case of a flood. Furthermore, the maximum damage is assumed to increase over time (t, in years). In accordance with [22], the annual economic growth rate (γ) is set to 0.02.

$$D(h_{basin}, t) = \begin{cases} D_{max} \frac{\ln(1+h_{basin})}{\ln(1+d_{max})} e^{\gamma t} & \text{if } h_{basin} \leq d_{max} \\ D_{max} e^{\gamma t} & \text{if } h_{basin} > d_{max} \end{cases} \tag{5.1}$$

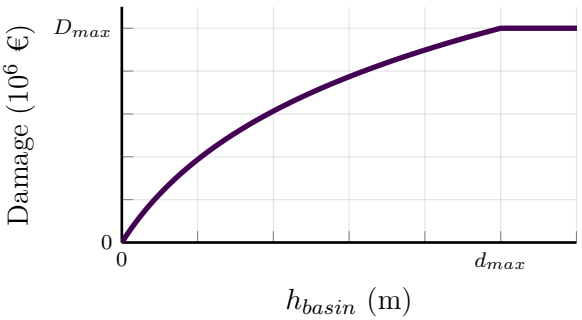

Figure 5.6: Damage at a flood prone area grows logarithmically to a maximum damage value D_{max}, which coincides with an inundation level at d_{max}.

Flood prone area	D_{max} (10^6)	$d_{max}(m)$
D48	7046	5.0
D49	82	5.0
D50	2119	5.0
D51	57	5.0

Table 5.1: D_{max} and d_{max} values for the flood prone areas of Figure 5.3. The D_{max} values are based on data listed in [22].

5.3.3. EAD ESTIMATION

On an abstract level, the likelihood of flooding depends on the ratio between the strength and the load of the flood defences. This is shown in the reliability equation Z in Eq. 5.2.

$$Z = Strength - Load \tag{5.2}$$

In this chapter the load is the water level at the defence and the strength is the critical height of the flood defence, which is uncertain due to the nature of most flood defence failure mechanisms (e.g. shear resistance of the soil in and under a dike). The evaluation of the limit state function results in an estimation of the probability of failure (of that breach location).

Eq. 5.2 is evaluated for each breach location in the case study. Various methods are available to estimate the probability of failure with this equation, of which Monte Carlo simulation is a frequently used method; regarding (Dutch) riverine flood defence systems with hydrodynamic interactions, see for example [14] and [16]. A similar Monte

Carlo method with Importance Sampling is used as mentioned in [67]. This method (including contributing distributions) is further specified for the case study in D.1.3.

The Expected Annual Damage (EAD) estimates in the case study are determined with the Monte Carlo method as well. These estimates are calculated by determining (for each Monte Carlo sample) the maximum water depth in a flood prone area and the accompanying flood damage (i.e. Section 5.3.2). By incorporating the likelihood of the Monte Carlo sample (and hence the likelihood of the flood damage), a flood loss curve can be constructed as shown in Figure 5.7. The area under this flood loss curve represents the EAD estimate for that specific flood prone area. By using this approach, the EAD estimate can be influenced by any breached breach location ((or multiple breach locations) that leads to a damage at the flood prone area. This is essential in order to determine the effects of hydrodynamic interactions on the EAD estimates.

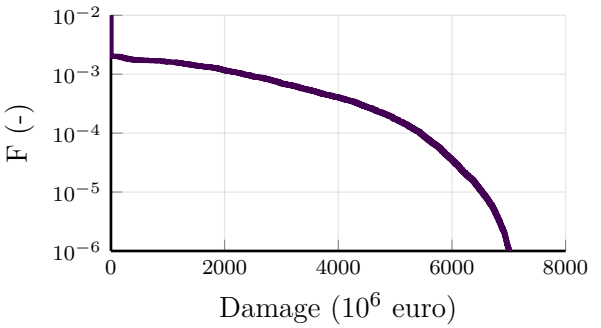

Figure 5.7: Example of a flood loss curve for D48 with hydrodynamic interactions, which plots the annual exceedance probability F versus the damage. In this example, all breach locations were set to an annual failure probability of 1/1000.

5.3.4. INVESTMENT COSTS

The investment costs represent the cost of increasing the safety level of a flood defence. These costs can be determined based on actual design studies for specific locations, but can also be approached by more general relations. Specifically for dikes, a number of relations were discussed in, for example, [22]. The exponential, dike-height dependent relation proposed in [22] is shown in Eq. 5.3. In Eq. 5.3, u is defined as the height increase from height h_1 to height h_2, C_f is the fixed investment cost, C_v is the variable investment cost, and λ is an exponential scaling factor. This equation will be used in the case study of this chapter.

$$I(u, h_2) = \begin{cases} 0 & \text{if } u = 0 \\ \left(C_f + C_v u\right) e^{\lambda h_2} & \text{if } u > 0 \end{cases} \tag{5.3}$$

Investment costs and time dependent parameters for the case study are associated with each breach location, and are shown in Table 5.2. Similar to the maximum damage

values (Section 5.3.2), the values in Table 5.2 are based on data found in [22]. The parameters C_f, C_v and λ are to be used with the exponential investment relation (Eq. 5.3). Parameter η has been interpreted as a proxy for degradation of strength over time in [22]. Therefore, it was implemented as a reduction on the mean critical height of the associated breach location. Furthermore, the yearly discount rate δ is set to 0.04 (in accordance with [22]).

A slight modification from [22] is made for D48, as it has only a single value and contains three breach locations in this case study (see Figure 5.3). Therefore the values for investment cost related parameters C_f and C_v are distributed equally over the breach locations B481, B482 and B483. Furthermore, the breach location GER has been given the same investment and time dependent characteristics as B481 (and therefore B482 & B483).

Because of the time dependent parameters, the number of possible decisions to be evaluated in the economic optimisation (Section 5.3.5) is influenced not only by the number of system configurations, but also by the considered reinforcement moments in time. Specifically for the number of EAD calculations, the considered reinforcement moments in time increase the number of EAD calculations as the EAD estimates differ each year.

Breach	$C_f\ (10^6)$	$C_v\ (10^6)$	λ (-)	$\eta\ (m/year)$
GER	11.9	47.7	0.63	0.00496
B481	11.9	47.7	0.63	0.00496
B482	11.9	47.7	0.63	0.00496
B483	11.9	47.7	0.63	0.00496
B49	20.0	80.0	0.46	0.00304
B50	8.13	33.0	0.00	0.00320
B51	15.0	60.0	0.71	0.00294

Table 5.2: Investment and time dependent parameter values for the breach locations of Figure 5.3. The values mentioned for C_f, C_v and λ are input for the investment function discussed in Section 5.3.4 and based on data in [22]. η denotes the degradation of strength over time.

5.3.5. OPTIMISATION ROUTINE

Finding the economically optimal investment scheme can be done analytically for simple systems (e.g. see [22]). For larger (or more complex) flood defence systems numerical methods are more convenient. A recent numerical method that is capable of optimising flood defence systems with multiple interdependent defences can be found in [27] and [55]. The study in [53] uses a similar approach as in [27] to optimise flood defence systems with multiple interdependent defences, but attempts to reduce the number of EAD calculations required by the numerical optimisation method.

The optimisation process can be conveniently visualized with the help of graphs [46].

This is shown conceptually in Figure 5.8. In this plot, each dot represents a system configuration at a certain moment in time. The lines between the dots represent a change in system configuration (if the dot later in time is at a higher position on the y-axis). The lines are given weights based on the sum of investment costs and EAD between, for example, t_0 and t_i, in order to obtain the optimal system configuration. Even if the system configuration does not change, the EAD can change due to temporal changes (see also Section 5.3.3 & 5.3.4).

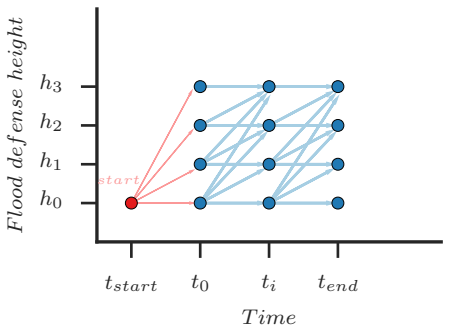

Figure 5.8: Conceptual image of a graph for a single flood defence, which helps to visualize the optimisation process. Image reproduced from [53].

Using the numerical optimisation method of [53], the number of EAD calculations is reduced by only executing the calculation of the necessary estimates which are used by the optimisation routine (i.e. 'lazy evaluation'). This method was shown to reduce the number of required EAD calculations by not having to calculate EAD estimates at lower safety levels in the distant future. Based on the examples in [53], the expected reduction is roughly a factor two.

For the case study, five different levels are considered per defence, in accordance with levels currently considered in Dutch safety standards (e.g. see [2]) and are associated with the failure probabilities per breach location. These five levels are called L1 to L5 and are related to the current ($t = 0$) annual failure probabilities of 1/300, 1/1000, 1/3000, 1/10,000 and 1/30,000 for each breach location separately *without* interactions. The number of system configurations for Figure 5.3, with the three internal breach locations linked to the levels of the external breach locations (see D.1.3), is equal to 5^7 or 78,125.

The total time horizon used in the economic optimisations for the case study spans 300 years in the future (similar to the choice in e.g. [45]), with 58 moments marked as potential reinforcement times. These 58 moments are concentrated mostly in the near future. This is because decisions in the near future are considered as more important than decisions in the distant future (i.e. weigh more heavily on the total cost estimate due to discounting). The first 20 years have a possible decision each year (including

one at $t = 0$), while the next 80 years have a possible decision every five years, while the remaining 200 years have a possible decision every ten years.

5.3.6. COMPUTATIONAL EFFICIENCY

Numerical modelling of hydrodynamic interactions, especially in a Monte Carlo setting, can be computationally expensive, see for example [14]. This computational burden will be amplified in the context of an economic optimisation, which investigates multiple system configurations (see also Section 5.3.5). Each system configuration needs an EAD estimate; which means multiple Monte Carlo simulations. The number of system configurations is dependant on the underlying system, but can easily reach hundreds or thousands system configurations.

Without hydrodynamic interactions (see also Section 5.2), the economic optimisation can be done independently for each flood prone area. Practically, this means that for D48 there are 625 possible system configurations per time step (5^4), while for the other flood prone areas (D49, D50 and D51) there are only five possible system configurations per time step.

If hydrodynamic interactions are included, the number of potential system configurations increases to 78,125 per time step (Section 5.3.5). This results in more than 23 million potential EAD calculations in a period of 300 years. If only 50% of these 23 million EAD calculations actually need to be computed and each EAD calculation takes about one second, the resulting computational time would be approximately 68 days on a single CPU core. If these calculations can be distributed with perfect efficiency over multiple cores, 100 cores would be done in less than a day. However, during this study a computer cluster was not available which meant that computing the EAD estimates were considered a high computational burden. This burden would be even larger if a more complex hydrodynamic model was used (e.g. in [15] it took hours to compute a single EAD estimate).

Because of this high computational burden, it was first checked whether or not including hydrodynamic interactions leads to significantly different results. To that end, Spearman's correlation coefficients were calculated between the input (critical heights of the breach locations) and output (EAD per flood prone area) for all 78,125 system configurations at $t = 0$ with hydrodynamic interactions in Table 5.3.

Table 5.3 shows that the breach locations upstream of a flood prone area (see also Figure 5.3) have a significant correlation with the EAD in that flood prone area. These correlation coefficients show that the hydrodynamic interactions cannot be disregarded a-priori and that an economic optimisation with hydrodynamic interactions will most likely produce different results than an economic optimisation without hydrodynamic interactions. Therefore, surrogate modelling was applied to reduce the calculation time.

Surrogate modelling is an approximation method where computationally expensive models are replaced with more efficient surrogates; a review of surrogate modelling can be found in [68]. In this review, two types of surrogate models are distinguished: phys-

Breach location	D48	D49	D50	D51
GER	0.01	-0.54	-0.49	-0.39
B481	-0.65	0.05	0.05	0.05
B482	-0.47	0.09	0.09	0.08
B483	-0.31	0.16	0.13	0.12
B49	0.00	-0.75	0.07	0.17
B50	0.00	0.00	-0.78	-0.02
B51	0.00	0.00	0.00	-0.82

Table 5.3: Spearman's correlation coefficients for the critical heights of breach locations (rows), versus the EAD of the flood prone areas (columns).

ically based models with lower numerical complexity (e.g. going from a 2D model to a 1D model), and response surface surrogates (e.g. fitting a polynomial function through results obtained from a 2D model). Surrogate modelling can therefore help in relieving the computational burden, at the cost of returning an approximation of the results of a model with higher numerical complexity rather than running the actual model over and over again. Circumventing computationally expensive Monte Carlo simulations has been done before (e.g. see the list of applications in [68]). Either way, it is here considered as an important part of fulfilling the aim of this chapter because of the necessary computational savings.

In this chapter, an Artificial Neural Network (ANN) was chosen to approximate the EAD calculations, as the case study already uses a hydrodynamic model with a low numerical complexity. An ANN was used as the response of the underlying data was unknown; neural nets are perceived to have a high flexibility towards emulating the response of underlying data. A more detailed description of the basic structure and training of neural network can be found in for example [69].

In order to train the neural network, all 78,125 possible system configurations at time step $t = 0$ were calculated. This data size could be calculated in a couple of hours because of the relatively simple hydrodynamic relations in the case study. Within the training data set, it was observed that the response type seems to be non-linear, as shown in the plots of Figure 5.9. This justifies the usage of a neural net instead of using, for example, a simpler linear regression analysis. Further details regarding the implementation and performance of the neural networks are described in D.2. In D.2, the correlation coefficients of Table 5.3 are well approximated using the surrogate model. With the help of the surrogate models, the economic optimisation takes minutes instead of weeks.

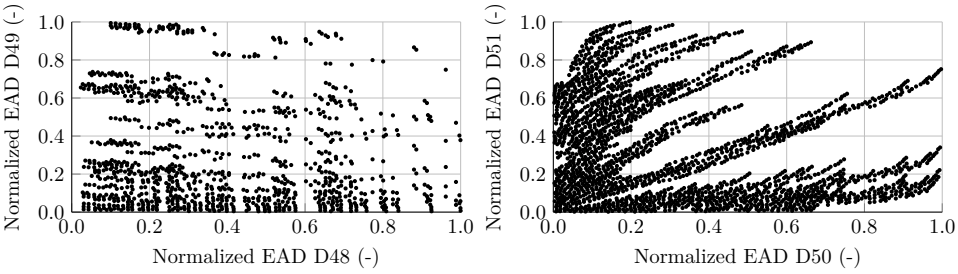

Figure 5.9: Normalized EAD scatter plots for identical system configurations at $t = 0$; all possible 78,125 system configurations are used. Two possible combinations of flood prone areas are shown, D48 versus D49 and D50 versus D51. The response seems to be weak non-nonlinear in D48 versus D49, while there seems to be a strong non-linear response in D50 versus D51. If the areas were hydrodynamically independent, the plots would be expected to be an evenly distributed field of dots.

5.4. RESULTS

In this section, the approach of Section 5.3 is applied to the case as described in Section 5.2 to estimate the impact of including hydrodynamic interactions in a riverine flood defence system with multiple dike sections. This is done by comparing EAD estimates and optimal system configurations with and without accounting for hydrodynamic interactions. Based on literature, a significant difference is expected to be found in the flooding probabilities and associated EAD estimates for simulations with and without interactions; see for example [14–16, 65].

In order to check whether or not the model with interactions yields different results than the model without interactions, a qualitative check is made for area D48, with all breach locations set to an annual failure probability of 1/1000. The cumulative probability distribution of flood damage (flood loss curve) for both models is shown in Figure 5.10. This figure shows a clear difference for flood prone area D48 where between the two model runs from about 3 billion euros up until the maximum flood damage. The tails of the flood loss curves converge because in both curves the maximum damage in D48 is reached (Table 5.1).

5.4.1. OPTIMISATION WITHOUT HYDRODYNAMIC INTERACTIONS

To provide a benchmark for an economic optimisation with hydrodynamic interactions, also an economic optimisation without hydrodynamic interactions was done. The resulting optimal investment schemes for the seven breach locations are shown in Figure 5.11 & 5.12. The expected behavior per flood defence is a gradual increase of the level over time. This is explained by economic growth (i.e. larger potential damages) and a higher probability of a flood defence failing (e.g. due to flood defence degradation or climate change). Breach location B50 in Figure 5.12 is the only location that does not show a gradual increase in level. Apparently, flood prone area D50 is attractive for investment (i.e. investment costs are relatively low regarding the achievable EAD reduction),

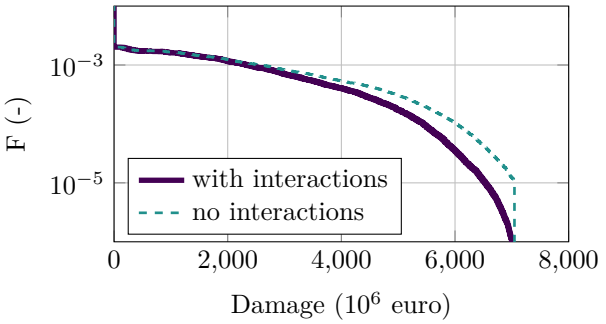

Figure 5.10: Example of flood loss curve for D48 with and without hydrodynamic interactions, which plots the annual exceedance probability F versus the damage. All breach locations were set to an annual failure probability of 1/1000.

and the initial level L1 is too low. The maximum level of L5 is already reached around year 60, which indicates that the chosen safety levels are possibly limiting the economic optimisation for B50; in the following years a higher level than L5 might, economically, be a better optimal choice. Other locations hit their maximum level later: around year 200, or not at all (i.e. B51).

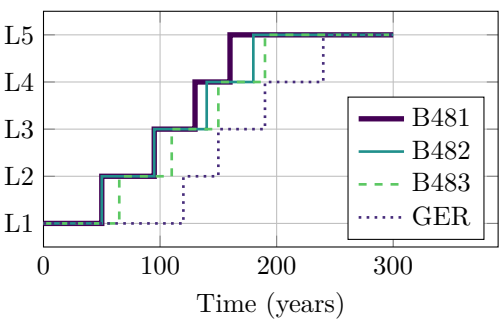

Figure 5.11: Optimal investment schemes assuming no hydrodynamic interactions for the four breach locations of D48 (GER, B481, B482 and B483).

The flood prone areas can be optimised separately as hydrodynamic interactions are not included in these optimisations, which reduces the number of EAD calculations. Because the EAD over a period of multiple years is approximated as the sum of EAD estimates for that period, the maximum number of EAD calculations for D48 is approximately the number of years plus one (301) times the number of system configurations (625), which equals 188,125 potential EAD calculations. By using the lazy evaluation feature of the used economic optimisation routine (see Section 5.3.5), 52% of these EAD calculations were actually executed.

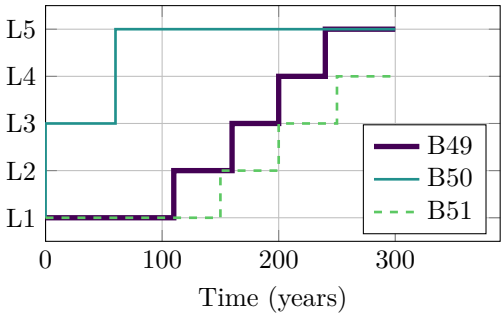

Figure 5.12: Optimal investment schemes assuming no hydrodynamic interactions for the three breach locations for D49, D50 and D51 (B49, B50 and B51).

5.4.2. OPTIMISATION WITH HYDRODYNAMIC INTERACTION

With the help of the surrogate models as described in Section 5.3.6, the economic optimisation takes minutes instead of weeks. Even though the surrogate model reduces the computational impact of acquiring EAD estimates considerably, this was further reduced by the lazy execution of the used optimisation routine (see Section 5.3.5): about 60% of all potential EAD calculations was actually used.

The economic optimisation with hydrodynamic interactions is carried out in two variants: one with breach location GER at a constant level (L1), and one with breach location GER as any other breach location, free to be optimised. This was done as the breach location GER in the case study represents a breach location in Germany. Therefore, this breach location may not, or cannot, be subjected to an investment strategy as desired by the Dutch part of the system.

Figure 5.13 shows the temporal development of the total EAD on a system level for the two strategies and the case without interactions. This shows that the development of the EAD under the assumption of 'no interactions' and 'with interactions and GER free' is roughly the same.

For 'GER fixed', the EAD clearly deviates after about 150 years. It is likely that, because GER is fixed at a low level, the economic optimisation routine is not able to 'control' the growth of the EAD elsewhere as investments here are no longer cost-efficient. Also the growth in EAD might not be contained because the highest available level for breach locations (L5) is simply not high enough.

Figure 5.14 shows the development of the annual flooding probabilities over time for the optimal investment schemes found with and without hydrodynamic interactions, using the model *with* hydrodynamic interactions. Especially the development of D50 using the investment scheme without interactions can be seen as too conservative (i.e. these flooding probabilities are significantly lower than the investment scheme with interactions). This is further supported by Figure 5.15, which shows the cumulative discounted investment costs of the three investment schemes: the investment costs for the

scheme based on the case without interactions are significantly higher than the investment costs for both schemes determined with interactions.

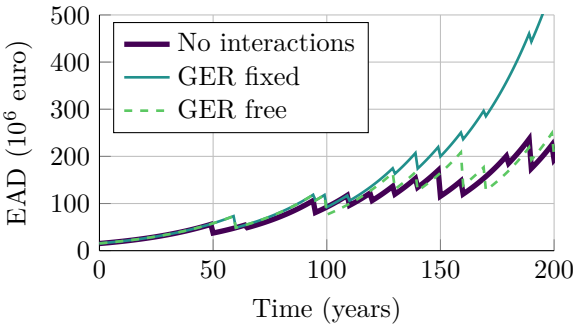

Figure 5.13: System EAD (i.e. summed EAD of all flood prone areas) over time for the three optimal investment paths as done in this section: one with no interactions (Section 5.4.1) and two with interactions (one with breach location GER fixed at level L1 and one with GER free to be optimised).

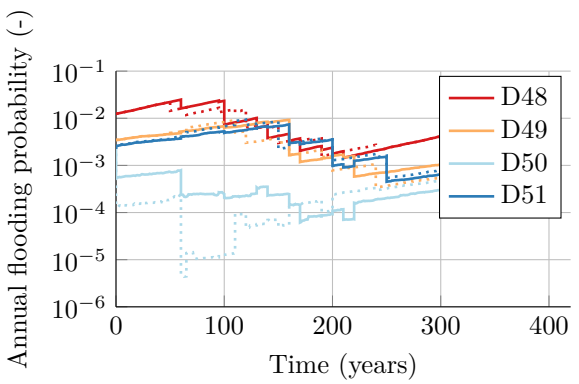

Figure 5.14: Annual flooding probability over time using the optimal investment scheme which was determined *with* interactions (solid lines, 'GER free') and *without* interaction (dotted lines). The flooding probabilities are in both cases calculated *with* interactions.

The optimal investment schemes for the optimisation without hydrodynamic interactions, with interactions and with interactions but with GER fixed are shown in Figures 5.16, 5.17 & 5.18, respectively. When compared to the situation without interactions, it is clear that both optimisations with interactions have a significantly different investment strategy. In the first 100 years, investments in B481 and B482 are only slightly delayed when compared to the optimisation without interactions, as the discharge reduction from upstream breaches is small compared to the Rijn/Nederrijn discharge. For the locations at the IJssel (B483, B49, B50 and B51), investments are delayed significantly and (initial) investments are reduced as well, as the effect of upstream breaches

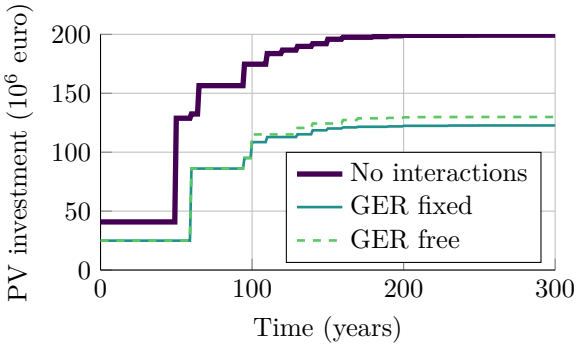

Figure 5.15: Cumulative sum (over time) of the present value of the system investment costs using the optimal investment schemes which were determined in this section.

and shortcutting is larger due to the smaller discharge capacity of the IJssel. The fact that for 'GER free' investment at these three locations is reduced further compared to 'GER fixed' highlights the importance of reinforcing dike section GER in order to manage downstream flood risks: a low level for dike section GER leads to higher risk at B49, B50 and B51 caused by higher water levels due to shortcutting.

Furthermore, Figure 5.18 with breach location GER fixed at L1 shows a peculiar large jump in safety level for B51 around year 230. This can be explained by the fact that all other options except increasing B49 from L4 to L5 are exhausted. However, as B49 also reduces the flood probability of B50 (where the potential damage is much higher) that investment might only increase the risk further, meaning that investment in B51 is the only option to (slightly) mitigate the exponential growth in EAD shown in Figure 5.13.

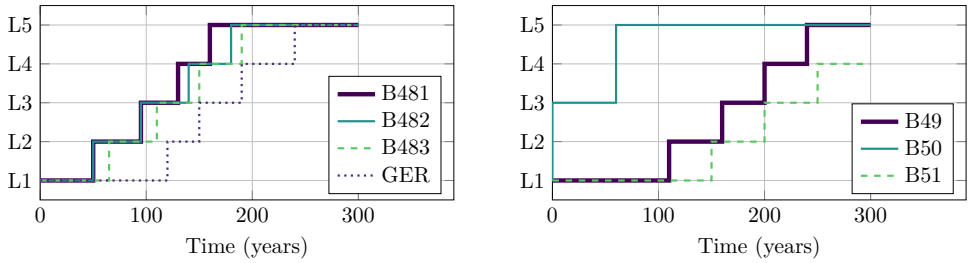

Figure 5.16: Investment schemes for the seven breach locations that follow from the economic optimisation without hydrodynamic interactions (Section 5.4.1, copies of Figure 5.11 & 5.12).

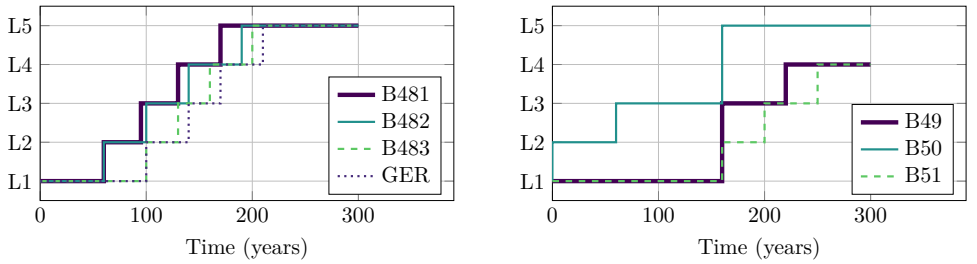

Figure 5.17: Investment schemes for the seven breach locations for an economic optimisation with hydrodynamic interactions and breach location GER free to be optimised as well.

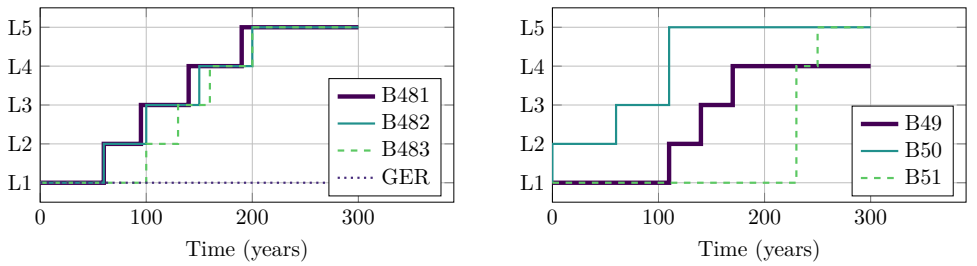

Figure 5.18: Investment schemes for the seven breach locations for an economic optimisation with hydrodynamic interactions and breach location GER fixed at its L1 level.

5.5. DISCUSSION

In this chapter a case was presented where interdependence between riverine flood defences has been taken into account in the context of an economic cost-benefit optimisation. Whereas past studies on this topic, such as the ones by [15], [14] and [13] only considered the phenomenon itself, here the perspective of optimal decision making and investment patterns was added. Previous studies on optimal investments for riverine flood defences (e.g. [17]) also did not consider these interdependencies.

As the computational complexity of these calculations is large it was necessary to simplify some aspects of the model, such as the hydrodynamic model. Despite the simplification of the hydrodynamic model the general behaviour of the system is still very much in line with the model used by [15] who used a calibrated quasi-2D model. Nevertheless it could be valuable to use a more complex calibrated model in an optimisation context as it will also improve assumptions such as the constant discharge fractions of the various river branches (see Figure D.3).

Incorporating such a more complex model in this context would however significantly increase computation times of the optimisation model. A possible avenue to mitigate this could be to calibrate a simple model such as described in Section 5.2 using the complex model. This would still improve computation time, and would in essence be a replacement of a model with high numerical complexity with a surrogate model of lower numerical complexity (see also Section 5.3.6). At the same time, it might be more efficient to train a response surface surrogate model directly on the output of a more complex model, without the intermediate step of a model with lower numerical complexity.

For more complex models, defining a proper training data set poses some additional issues. In Section 5.4.2, all system configurations at a single time step are used as the training data set. Especially for more complex models and larger systems calculating all system configurations might become infeasible. To that end, using smaller training data sets might be feasible as well (e.g. see [70]), or Latin hypercube sampling could be used to optimise the size of the training dataset while still achieving a good fit; see also [68].

Even though the framework applied provided reasonably accurate results in acceptable calculation times, modelling choices made in this chapter could be altered for other cases. This involves the choice of surrogate model type and which parts of the calculation to include in the surrogate model. Such choices should always be based on a consideration of required accuracy versus computational tractability.

It is found from the results that whether or not interdependencies are included in the model makes a large difference for the investment pattern, especially for the more downstream flood defence sections. This is in line with the findings by [15] on the same area, where it was found that the influence of interdependencies on risk levels was larger for more downstream locations. Up to now these influences have not been included in quantitative analysis of optimal safety standards [17] or investment patterns. The most prominent reason for this is the computational complexity, however techniques such

as the neural networks used here are promising in tackling such complex optimisation problems [68].

Where optimal investment patterns were studied in this chapter, another potentially promising application of the modelling approach is the prioritisation of reinforcement measures under budget constraints. As shown in this study, the investment costs can change significantly if hydrodynamic interactions are included. For example, if the estimate of a flooding probability decreases by including interdependencies, a reinforcement (investment) of that flood defence section can be postponed in favour of other more urgent defences. This is particularly relevant for large flood defence infrastructure investment programs such as the Flood Protection Program in the Netherlands.

The case study considers an area close to the border with Germany. In this area dike breaches in Germany can cause significant damage in the Netherlands, meaning that the optimisation of the German flood defences should also be considered in the optimisation for the Dutch system. This chapter therefore included the cases 'GER free' and 'GER fixed'. From a comparison of these cases it was found that especially on the long term the EAD skyrocketed, as the EAD is dominated by breaches in Germany. This illustrates the importance of looking past administrative borders in order to achieve appropriate flood risk management strategies.

In the case study in this chapter it was shown that interdependencies can have a large influence on flood risk management strategies. In order to fully exploit the model set-up outlined in this chapter for decision making on safety standards, prioritisation and cross-border risk analysis it is specifically important that there is a shared trust towards the underlying models. This interest potentially conflicts with simplifying the model in order to keep the computational burden of these calculations in check. Therefore it is important that future developments focus on connecting the outlined approach to calibrated models, for which some suggestions have been presented in this section.

5.6. CONCLUSIONS

In this chapter a modelling framework that enables an economic cost-benefit analysis of a riverine flood defence system with multiple interdependent flood defences was presented. This economic cost-benefit analysis was then used to compare the impact of including the effect of multiple interdependent flood defences and their hydrodynamic interactions on the economically optimal investment scheme in a case study (versus not including these interactions).

Using a simple hydrodynamic model in a Monte Carlo simulation with Importance Sampling enabled economic optimisation with limited or no hydrodynamic interactions (as described in Section 5.4.1). However, to be able to take into account the increasing number of system configurations when accounting for hydrodynamic interactions, a neural network was used as a surrogate model. It was shown that for the case study in this chapter, the used surrogate model provides a reasonable approximation for the simple hydrodynamic model whilst significantly reducing the computational burden. For

the case study, significant differences were found both in terms of the timing of the optimal investments, as well as the magnitude of the required investments.

It was shown that for efficient flood risk management strategies in the case study area interdependencies have to be taken into account as there are significant differences in investment patterns. Therefore relaxing the assumptions of independence will likely lead to more optimal investment strategies and thus more cost-effective protection of flood prone areas. As there are several options for coping with the typically significant computational burden of including hydrodynamic interactions it is expected that the research costs towards including hydrodynamic interactions will be significantly outweighed by the potential cost-savings that can be achieved by having a better, more optimal, investment scheme.

6

CONCLUSION

This thesis presented an approach to explicitly include the (hydrodynamic) interactions between flood defences in an economic optimisation of a system of flood defences. The explicit incorporation of hydrodynamic interactions was done by modelling the hydrodynamic interactions in risk estimates. Next, the influence of interactions on economic optimisation was analysed by means of analytical derivations, and by more elaborate numerical economic optimisation approaches. Furthermore, it was shown and discussed how these improvements can influence economically optimal safety targets and flood risk management practice.This chapter combines the detailed conclusions and recommendations in the previous chapters into the main findings (Section 6.1) and recommendations (Section 6.2). Furthermore, some extensions to other areas of interest are discussed in Section E.

6.1. FINDINGS

The aim of this thesis was to investigate the influence of interdependence in a system of flood defences on the associated economically optimal safety targets and the associated investment and risk costs. This was done by investigating three subjects. First, a framework was developed in order to incorporate the effect of interdependence in a flood defence system with interdependent flood defences in a cost-benefit analysis. Secondly, insight was developed into when interdependence between flood defences leads to a significant difference on the associated economically optimal safety targets (compared to not accounting for interdependence). Thirdly, the impact and computational performance (i.e. by reducing the computational burden) of including interdependence between flood defences is tested in case studies with numerical economic optimisations.

These three subjects were discussed in the context of two types of flood defence systems: coastal and riverine systems. Coastal systems are characterized as systems with multiple lines of defence. A simple but representative coastal system consists of a front defence (i.e. storm surge barrier), separated by a body of water from rear defences (i.e. levees) which protect the hinterland. For coastal systems, the load increases for the rear defences if the front defence fails. On the other hand, riverine systems are considered in this thesis as a collection of flood defences (or flood defence sections, typically levees) which are adjacent to one or more river streams. For riverine systems, mostly load decreases can be expected (i.e. discharge reduction downstream due to storage behind a breached flood defence), though load increases can occur as well (e.g. formation of a shortcut between two river flows).

The research aim was posed as an overall research question as well, with three accompanying sub-questions in Section 1.4:

> *What is the influence of hydrodynamic interactions on the economically optimal safety targets, and the associated investment and risk costs of a system of flood defences?*
>
> i. How can hydrodynamic interactions be incorporated within an economic cost-benefit analysis in a computationally efficient manner?
>
> ii. What are the expected changes due to incorporating hydrodynamic interactions on an economic optimisation of a system of flood defences?
>
> iii. How are coastal and riverine flood defence systems affected by hydrodynamic interactions, and what are the differences between the two types in the context of an economic optimisation?

The findings of Chapters 2 - 5 are combined and organised per sub-question in the following sections.

HOW CAN HYDRODYNAMIC INTERACTIONS BE INCORPORATED WITHIN AN ECONOMIC COST-BENEFIT ANALYSIS IN A COMPUTATIONALLY EFFICIENT MANNER?

Hydrodynamic interactions were incorporated in an economic cost-benefit analysis as part of the flood probability and, hence, flood risk estimates. The incorporation in the flood probability estimates was done in two ways. The first (numerical) approach used hydrodynamic simulations where hydrodynamic interactions are incorporated. These simulations were then used to derive annual flood probability estimates and expected annual damage estimates. These damage estimates (which now include hydrodynamic interactions) are then used in a cost-benefit analysis. This is an intuitive physics approach, albeit computationally expensive as it requires numerous hydrodynamic simulations.

The second (analytical) approach utilized flood probability relations where the expected behaviour with hydrodynamic interactions was incorporated. This was done by using conditional flood probability relations (Chapters 3&5, where these relations are conditional on the failure (i.e. breaching) or functioning of other flood defences which are part of the same flood defence system. These conditional flood probability relations were then used to derive conditional expected annual damage estimates, which were combined into expected annual damage estimates per flood defence. These estimates were then used in the optimisation of an economic cost-benefit analysis. This approach is more abstract (i.e. a statistical approach based on the underlying physics) and less accurate, but computationally more efficient approach as the underlying relations were expressed using relatively simple mathematical relations.

The optimisation of an economic cost-benefit analysis was done both analytically and numerically in this thesis. An analytical analysis gives insight into the behaviour of the economically optimal solution, using (simplified) mathematical relations and expressions. Mathematical (simplified) relations were found in the second approach (i.e. numerical analysis with conditional flood probability relations with hydrodynamic interactions incorporated). Therefore, an analytical cost-benefit analysis needs the second (analytical) approach in order to be able to solve the optimisation and end up with analytical results. Analytical solutions do tend to become overly complex as the flood defence system itself has a lot of interdependent flood defences.

On the other hand, a numerical cost-benefit analysis can use both (numerical) hydrodynamic models and analytical relations, and can therefore use both approaches. However, computational tractability becomes an issue, as an economic optimisation of a complex flood defence system lead to numerous expected annual damage calculations, because there were many possible system configurations. To overcome computational limitations, computational efficiency was improved in two areas: in the expected annual damage calculations and in the economic optimisation routine:

- The expected annual damage calculations were estimated more quickly by using hydrodynamic simulations to calibrate computationally fast flood probability relations and/or flood damage relations, for example with a meta model. Essentially,

this combines the first and second approach of incorporating hydrodynamic interactions in an economic cost-benefit analysis. Typically this sped up expected annual damage calculations by an order (or even several orders) of magnitude.

- An economic optimisation routine was set up in such a way that it required only the expected annual damage calculations it actually needed (Chapter 4). Typically, the number of actually needed expected annual damage calculations was half of all calculations that could have been made by the optimisation routine.

WHAT ARE THE EXPECTED CHANGES DUE TO INCORPORATING HYDRODYNAMIC INTERACTIONS ON AN ECONOMIC OPTIMISATION OF A SYSTEM OF FLOOD DEFENCES?

The expected changes due to hydrodynamic interactions can be explained by consecutively discussing the impact of including hydrodynamic interactions on flood events, annual flooding probabilities, economically optimal annual flooding probabilities and finally economically optimal investment schemes.

In case a breach occurs in an upstream flood defence as part of a larger flood defence system, the result is either an increased or decreased load on downstream flood defences. This statement looks at a *flood event*. If events are impacted, so are the annual probabilities of flooding. Generally speaking, an increased load leads to a higher annual probability of flooding, while a decreased load leads to a lower annual probability of flooding downstream. However, how often these hydrodynamic interactions are expected to occur depends on the protection levels of the flood defences in the system: if the protection levels are relatively high, breaches and therefore hydrodynamic interactions are rarely expected to occur. In other words, the impact on the system flood risk depends on the existing (target) flood protection levels within a flood defence system.

Annual probabilities of flooding are used in an economic optimisation. Within an economic optimisation, the effect of hydrodynamic interactions on the economically optimal (annual) probabilities of flooding were found to be typically limited when compared to those found without hydrodynamic interactions. These results were found with both analytical and numerical methods. Significant differences were only found in a case with large differences in the optimal probabilities of flooding without hydrodynamic interactions (e.g. see Chapter 3 and specifically Appendix B.3).

However, a much more pronounced effect was found in the investment schemes resulting from an economic optimisation (which show when and how much a flood defence should be strengthened). The investment schemes showed that including hydrodynamic interactions lead to postponed or advanced investments (compared to investment schemes found without interactions). An example of this is if a flood defence system has existing protection levels which are higher than what the economic optimisation would result in. Investments are then postponed until the risk cost of the system can be cost-efficiently reduced by strengthening (i.e. investing in) one or more flood defences in the flood defence system.

Another difference in the investment schemes with hydrodynamic interactions that was found is that the size of the investments for flood defences changed. Due to hydrodynamic interactions, the effect of strengthening a flood defence had a wider (system) impact than just a risk reduction for the flood-prone area associated with that particular flood defence. A (seemingly straightforward) example was found both in the coastal and riverine flood defence system cases with an upstream flood defence and a potentially load-increasing breach for the rest of the flood defence system. Typically, this leads to increased investments in that upstream defence and decreased investments in the downstream defences.

Both the change in investment size and timing also served as an explanation for why the impact on the economically optimal (annual) probabilities of flooding were found to be typically limited. For example, if due to a load reduction the expected annual flooding probabilities decrease, a delay in investment leads (over time) to an increased expected annual flooding probability.

Including hydrodynamic interactions in an economic optimisation also leads to different system configurations than an optimisation without interactions. A prime example of this was shown in the coastal flood defence system chapter where the construction of a storm surge barrier is contemplated. The failure of a storm surge barrier in a coastal flood defence system will lead to an increased load on the rear defences. As such, the decision to build a storm surge barrier, from an economic point of view, depends wholly on its cost-effectiveness with which it is able to reduce the hydraulic loads at rear defences. An economic optimisation with interactions provides insight into *how much* protection a storm surge barrier will offer.

HOW ARE COASTAL AND RIVERINE FLOOD DEFENCE SYSTEMS AFFECTED BY HYDRODYNAMIC INTERACTIONS, AND WHAT ARE THE DIFFERENCES BETWEEN THE TWO TYPES OF SYSTEM IN THE CONTEXT OF AN ECONOMIC OPTIMISATION?

An example of a coastal flood defence system, as defined and used in this thesis, is that of a storm surge barrier and rear flood defences. These rear flood defences are typically assumed to protect flood-prone areas which can flood independent of each-other. Therefore, the primary hydraulic interaction is between the storm surge barrier and the rear defences; in case the storm surge barrier fails, the load increases for the rear defences. The storm surge barrier acts as a 'gatekeeper', which means in the context of an economic optimisation that, provided a storm surge barrier is cost-effective, investments in the storm surge barrier reduce the expected annual damages associated with the rear defences.

A riverine flood defence system, as defined and used in this thesis, was not as straightforward as a coastal flood defence system. A riverine system was assumed to consist of flood defences which, if flooded, can affect the probability of flooding of the other (downstream) flood defences. This is due to the fact that it was assumed that these flood defences are along the one or more common rivers. Furthermore, depending on where and how the flooding pattern evolves in the system, a breach lead to downstream flood

defences experiencing a load increase or a load decrease. For larger riverine flood defence systems, it therefore became hard to predict a-priori how the system as a whole is affected by the incorporated hydrodynamics interactions. Furthermore, the aforementioned aspects also made the economic optimisation harder to solve due to the sheer number of possible system configurations in a riverine system. For the riverine flood defence system case study, the general conclusion was that the effect of hydrodynamic interactions was predominantly seen in the timing and size of investments. In which direction the timing and size of these investments shifted depends on the dominant hydrodynamic interaction: load reductions generally lead to postponed and reduced investments, load increase to advanced and increased investments.

6.2. RECOMMENDATIONS

FUTURE RESEARCH

The focus of this thesis was on including the impact of hydrodynamic interactions on the flood risk estimates within an economic optimisation. Other terms within an economic optimisation were even used deterministically, while terms such as the discount rate and investment costs do have a significant impact on the optimization result. Therefore it would make sense to replace these point estimates with random variables.

One step further would be to consider all terms of an economic optimisation as random variables and evaluate the economic optimisation within a probabilistic framework (e.g. using a Monte Carlo simulation). This will result in an economic optimisation result where the uncertainty of that result can also be quantified. However, treating these factors as explicitly uncertain within an optimisation will lead to a further growth of the computational cost, which already increased due to the implementation of hydrodynamic interactions. This is because a probabilistic framework around an economic optimisation requires (many) repeated economic optimisations in order to quantify the uncertainty of the random variables.

While the flood risk estimates were estimated probabilistically, only the expected value is actually used in the economic optimisations as used in this thesis. This implicitly assumes a risk-neutral behaviour (as discussed in [71]). An extension to include other risk preferences (e.g. risk-aversity) should be straightforward.

The flood defence resistance has been modelled as a probability distribution of the critical water level of a flood defence. In practice, the failure probability of a flood defence is determined by evaluating a number of failure mechanisms, of which some are only partially (or even only marginally) affected by the height of a flood defence. Examples of such mechanisms are piping or macro-stability. In the Netherlands, quite a lot of data is already available how various failure mechanisms affect current Dutch flood defences. A more detailed estimation can be made that utilizes these existing data to obtain more accurate estimate of a flood defence failure probability. This can be done for example by combining fragility curves of separate failure mechanisms.

The number of possible flood defence system configurations (i.e. the possible combinations of protection levels of flood defences in a flood defence system) was shown to rapidly increase for larger systems. The number of configurations can increase to such an amount that solving the economic optimisation is no longer feasible, especially if all flood defences are considered as interdependent. To that end, the number of possible combinations can be limited by offering less protection levels as options for flood defences (i.e. a coarser discretization). These limitations can be based on practical information, such as an existing decision that a flood defence will be strengthened to protection level X in year Y.

FLOOD RISK MANAGEMENT PRACTICE & PRIORITY ASSESSMENT

An economic optimisation, as used in the Netherlands, is one of the instruments in the determination of the safety standards (or norms) for flood defences. However, with some adaptation, it can also be used to prioritise investments in flood defences under budget constraints and/or existing standards. As shown in this thesis, the estimated annual flooding probabilities per flood prone area can differ significantly once hydrodynamic interactions are included. A valid reason to constrain an economic optimisation is a minimally acceptable safety level (which is recorded in Dutch law). If the economic optimisation is constrained by forcing the current standard as the minimum and higher standards as a possibility for the flood defences, the result of this optimisation will mostly adhere to the current standards. Flood defences where a higher standard is found than the current standard can then be advocated as defences that need additional funding to be strengthened (beyond the current standard). Similarly, additional funding can also be advocated for a flood defence if a strengthening in an economic optimisation for that flood defence with interactions is found sooner than without interactions. For the Dutch practice, this could be supplementary to the 'distance to standard' criterium (ratio of actual flood probability divided by the acceptable flood probability) which is used among others to prioritise flood defence investments.

A direct result of using interdependent flood defences in a flood defence system is that more emphasis is put on the 'system' part of flood defences. Especially in the case of riverine flood defence systems, it was argued that all flood defences along a river should be considered as part of a large system. However, this needs a change in the current common way of thinking: flood risk management is still very much a national affair, despite initiatives such as the EU Floods Directive. Hydrodynamic interdependencies are a vital argument for initiatives such as the EU Floods Directive. In order to integrally implement system behaviour the system itself, not national borders, should be defining flood risk management.

The methods in this thesis can also be used as a design instrument for a flood defence system which contain a part that only functions as 'load-relieving' for the rest of the system (e.g. a storm surge barrier or a retention area). By incorporating such a flood defence system in an economic optimisation with hydrodynamic interactions, the economically optimal performance of such a 'load-relieving' part (and all other defences in

the system) can be found. This approach can then be used to set design targets for the 'load-relieving' part and the other defences in the system. Some initial work for two applications (a retention area and a flood defence with multiple functions) can be found in Appendix E. For a retention area, the economic viability was investigated for a retention area upstream of a flood defence, where the additional cost of constructing a retention area is incorporated together with an expected load reduction on a downstream flood defence. For a flood defence with a secondary function, the benefits of a synchronised maintenance schedule and (yearly) benefits were included in an economic optimisation of a flood defence and that secondary function.

REFERENCES

[1] B. Gouldby and P. Samuels, *Language of Risk. Project definitions,* FloodSite (2009).

[2] M. Kok, R. Jongejan, M. Nieuwjaar, and I. Tanczos, *Fundamentals of Flood Protection*, Tech. Rep. (Expertise Netwerk Waterveiligheid (ENW), 2017).

[3] L. M. Bouwer, *Have disaster losses increased due to anthropgenic climate change?* American Meteorological Society **BAMS**, 39 (2011).

[4] D. Paprotny, A. Sebastian, O. Morales-Napoles, and S. Jonkman, *Trends in flood losses in Europe over the past 150 years,* Nature Communications (2018), 10.1038/s41467-018-04253-1.

[5] T. Rijcken, *EMERGO: The Dutch flood risk system since 1986*, Ph.D. thesis, Delft University of Technology (2017).

[6] A. Maris, V. de Blocq van Kuffeler, W. Harmsen, P. Jansen, G. Nijhoff, J. Thijsse, R. Verloren van Themaat, J. de Vries, and L. van der Wal, *Rapport Deltacommissie. Deel 3. Bijdragen 2: Beschouwingen over stormvloeden en getijbeweging*, Tech. Rep. (Mathematisch Centrum, 1961).

[7] M. Faber and M. Stewart, *Risk assessment for civil engineering facilities: critical overview and discussion,* Reliability Engineering & System Safety **80**, 173 (2003).

[8] M. H. Faber, J. D. Sørensen, and A. C. W. M. T. Vrouwenvelder, *On the regulation of life safety risk,* (2015).

[9] D. Van Dantzig, *Economic Decision Problems for Flood Prevention,* Econometrica **24**, 276 (1956).

[10] R. Jongejan, B. Maaskant, W. ter Horst, F. Havinga, N. Roode, and H. Stefess, *The VNK2-project: a fully probabilistic risk analysis for all major levee systems in the Netherlands,* in *Floods: From Risk to Opportunity (IAHS Publ. 357)*, Vol. 2005 (IAHS Press, Wallingford, 2013) pp. 75–85.

[11] CEIWR-HEC, *EAD - Expected Annual Flood Damage Computation - User's Manual,* , 53 (1989).

[12] S. Vorogushyn, B. Merz, K.-E. Lindenschmidt, and H. Apel, *A new methodology for flood hazard assessment considering dike breaches,* Water Resources Research **46** (2010), 10.1029/2009WR008475.

[13] S. Vorogushyn, K.-E. Lindenschmidt, H. Kreibich, H. Apel, and B. Merz, *Analysis of a detention basin impact on dike failure probabilities and flood risk for a channel-dike-floodplain system along the river Elbe, Germany,* Journal of Hydrology **436-437**, 120 (2012).

[14] W. Courage, T. Vrouwenvelder, T. van Mierlo, and T. Schweckendiek, *System behaviour in flood risk calculations,* Georisk: Assessment and Management of Risk for Engineered Systems and Geohazards **7**, 62 (2013).

[15] W. Klerk, M. Kok, K. de Bruijn, S. Jonkman, and P. van Overloop, *Influence of load interdependencies of flood defences on probabilities and risks at the Bovenrijn/IJssel area, The Netherlands,* in *Proceeding of the 6th international conference on flood management - ICFM6, 1-13.* (Brazilian Water Resources Association and Acquacon Consultoria, 2014).

[16] K. M. De Bruijn, F. L. M. Diermanse, and J. V. L. Beckers, *An advanced method for flood risk analysis in river deltas, applied to societal flood fatality risks in the Netherlands,* Natural Hazards and Earth System Sciences Discussions **2**, 1637 (2014).

[17] J. Kind, *Economically efficient flood protection standards for the Netherlands,* Journal of Flood Risk Management **7**, 103 (2014).

[18] V. Tsimopoulou, *Economic optimisation of flood risk management projects*, Dissertation, Delft University of Technology (2015).

[19] R. Custer, *Hierarchical Modelling of Flood Risk for Engineering Decision Analysis*, Dissertation, Technical University of Denmark (2015).

[20] C. Eijgenraam, *Optimal safety standards for dike-ring areas*, Tech. Rep. 62 (CPB, The Hague, 2006).

[21] J. Vrijling and I. van Beurden, *Sealevel rise: a probabilistic design problem,* Coastal Engineering Proceedings , 1160 (1990).

[22] C. Eijgenraam, R. Brekelmans, D. den Hertog, and K. Roos, *Optimal Strategies for Flood Prevention,* Management Science (2016), 10.1287/mnsc.2015.2395.

[23] I. van Beurden, *Probabilistische berekening overslag veiligheid van zeeweringen & de invloed van de onzekerheid in de relatieve zeespiegelrijzing hierop*, Master thesis, Delft University of Technology (1988).

[24] J. Vrijling, *Multi layer safety,* in *Safety, Reliability and Risk Analysis* (CRC Press, 2013) pp. 37–43.

[25] C. Eijgenraam, *Protection against flooding: Cost-benefit analysis for Space for the River, Part 1*, Tech. Rep. 82 (The Hague, 2005).

[26] E. Dupuits, T. Schweckendiek, and M. Kok, *Economic Optimization of Coastal Flood Defense Systems,* Reliability Engineering & System Safety **159** (2016).

[27] P. Zwaneveld and G. Verweij, *Economisch optimale waterveiligheid in het IJsselmeergebied*, Tech. Rep. 10 (CPB, The Hague, 2014).

[28] C. Small and R. J. Nicholls, *A Global Analysis of Human Settlement in Coastal Zones,* Journal of Coastal Research **19**, 584 (2003).

[29] S. Jonkman, P. van Gelder, and J. Vrijling, *An overview of quantitative risk measures for loss of life and economic damage,* Journal of Hazardous Materials **99**, 1 (2003).

[30] M. J. Lickley, N. Lin, and H. D. Jacoby, *Analysis of coastal protection under rising flood risk,* Climate Risk Management **6**, 18 (2014).

[31] T. van der Pol, E. van Ierland, and H.-P. Weikard, *Optimal dike investments under uncertainty and learning about increasing water levels,* Journal of Flood Risk Management **7**, 308 (2014).

[32] H. Voortman, *Risk-based design of large-scale flood defence systems,* Dissertation, Delft University of Technology (2003).

[33] K. T. Lendering, S. N. Jonkman, P. van Gelder, and D. J. Peters, *Risk-based optimization of land reclamation,* Reliability Engineering & System Safety **144**, 193 (2015).

[34] J. C. J. H. Aerts, W. Botzen, A. van der Veen, J. Krywkow, and S. Werners, *Dealing with Uncertainty in Flood Management Through Diversification,* Ecology and Society **13** (2008).

[35] B. Kolen, *Certainty of uncertainty in evacuation for threat driven response. Principles of adaptive evacuation management for flood risk planning in the Netherlands*, Phd, Radboud Universiteit Nijmegen (2013).

[36] J. R. Lund, *Floodplain planning with risk-based optimization,* Journal of Water Resources Planning and Management **127**, 202 (2002).

[37] T. Zhu and J. Lund, *Up or out? - Economic-engineering theory of flood levee height and setback,* Journal of Water Resources Planning and Management **135**, 90 (2009).

[38] E. Dupuits and T. Schweckendiek, *Flood risk and economically optimal safety targets for coastal flood defense systems,* in *ICASP12: 12th International Conference on Applications of Statistics and Probability in Civil Engineering, Vancouver, Canada, 12-15 July 2015*, edited by T. Haukaas (Vancouver, 2015).

[39] P. Bedient and J. Blackburn, *Lessons from Hurricane Ike* (Texas A&M University Press, Houston, 2012).

[40] CIRIA, CUR, and CETMEF, *Ciria CUR* (C683, CIRIS, London, 2006) pp. 0–8.

[41] A. Vrouwenvelder, *Normstelling b-keringen,* (2014), private communication, TNO note.

[42] J. W. van der Meer, W. L. A. ter Horst, and E. H. van Velzen, *Calculation of fragility curves for flood defence assets,* in *Flood Risk Management: Research and Practice* (CRC Press, London, 2008) pp. 567–573.

[43] T. Schweckendiek, A. Vrouwenvelder, E. Calle, W. Kanning, and R. Jongejan, *Target Reliabilities and Partial Factors for Flood Defenses in the Netherlands,* in *Modern Geotechnical Codes of Practice - Code Development and Calibration*, edited by P. Arnold, G. Fenton, M. Hicks, and T. Schweckendiek (IOS Press, 2013) pp. 311–328.

[44] S. N. Jonkman, M. M. Hillen, R. J. Nicholls, W. Kanning, and M. van Ledden, *Costs of Adapting Coastal Defences to Sea-Level Rise New Estimates and Their Implications,* Journal of Coastal Research **290**, 1212 (2013).

[45] R. Brekelmans, D. Den Hertog, K. Roos, and C. Eijgenraam, *Safe Dike Heights at Minimal Costs: The Nonhomogeneous Case,* Operations Research **60**, 1342 (2012).

[46] P. J. Zwaneveld and G. Verweij, *Safe Dike Heights at Minimal Costs*, Tech. Rep. (CPB, The Hague, 2014).

[47] SSPEED, *H-GAPS Houston-Galveston Area Protection System*, Tech. Rep. (Rice University, Houston, 2015).

[48] K. Stoeten, *Hurricane Surge Risk Reduction For Galveston Bay*, M.sc. thesis (2013).

[49] T. Schweckendiek, A. Vrouwenvelder, and E. Calle, *Updating piping reliability with field performance observations,* Structural Safety **47**, 13 (2014).

[50] U.S. Department of Commerce, *Bureau of Economic Analysis,* (2015), [Online; accessed 17-September-2015].

[51] U.S. Department of the Treasury, *Resource Center,* (2015), [Online; accessed 17-September-2015].

[52] National Oceanic and Atmospheric Administration, *Tides and Currents,* (2015), [Online; accessed 17-September-2015].

[53] E. J. C. Dupuits, F. L. M. Diermanse, and M. Kok, *Economically optimal safety targets for interdependent flood defences in a graph-based approach with an efficient evaluation of expected annual damage estimates,* Natural Hazards and Earth System Sciences **17**, 1893 (2017).

[54] G. Verweij, *Safe dike heights at minimal costs - an integer programming approach,* (2014).

[55] B. Yüceoglu, *Branch-and-cut algorithms for graph problems,* Ph.D. thesis, Maastricht University (2015).

[56] T. H. Cormen, *Introduction to Algorithms, 3rd Edition:* (MIT Press, 2009).

[57] E. W. Dijkstra, *A Note on Two Probles in Connexion with Graphs,* Numerische Mathematik **1**, 269 (1959).

[58] P. Hart, N. Nilsson, and B. Raphael, *A Formal Basis for the Heuristic Determination of Minimum Cost Paths,* IEEE Transactions on Systems Science and Cybernetics **4**, 100 (1968).

[59] B. J. H. Verwer, P. W. Verbeek, and S. T. Dekker, *An Efficient Uniform Cost Algorithm Applied to Distance Transforms,* IEEE Transactions on Pattern Analysis and Machine Intelligence **11**, 425 (1989).

[60] A. Felner, *Position paper: Dijkstra's algorithm versus uniform cost search or a case against dijkstra's algorithm,* in *Fourth Annual Symposium on Combinatorial Search* (2011).

[61] D. Gelperin, *On the optimality of A*,* Artificial Intelligence **8**, 69 (1977).

[62] E. Dupuits, W. Klerk, T. Schweckendiek, and K. de Bruijn, *Impact of including interdependencies between multiple riverine flood defences on the economically optimal flood safety levels,* Reliability Engineering & System Safety (2019), 10.1016/J.RESS.2019.04.028.

[63] J. Vrijling, W. van Hengel, and R. Houben, *Acceptable risk as a basis for design,* Reliability Engineering & System Safety **59**, 141 (1998).

[64] P. Samuels, M. Morris, P. Sayers, J. Creutin, A. Kortenhaus, F. Klijn, E. Mosselman, A. Van Os, and J. Schanze, *A framework for integrated flood risk management,* (2010).

[65] E. Dupuits, K. de Bruijn, F. Diermanse, and M. Kok, *Economically optimal safety targets for riverine flood defence systems,* E3S Web Conf. **7**, 20004 (2016).

[66] M. Kok, *Standaardmethode 2004 : schade en slachtoffers als gevolg van overstromingen* (Ministerie van Verkeer en Waterstaat, Rijkswaterstaat, Den Haag, 2004).

[67] F. L. M. Diermanse, K. M. Bruijn, J. V. L. Beckers, and N. L. Kramer, *Importance sampling for efficient modelling of hydraulic loads in the Rhine–Meuse delta,* Stochastic Environmental Research and Risk Assessment **29**, 637 (2015).

[68] S. Razavi, B. A. Tolson, and D. H. Burn, *Review of surrogate modeling in water resources,* Water Resources Research **48**, n/a (2012).

[69] A. A. Chojaczyk, A. P. Teixeira, L. C. Neves, J. B. Cardoso, and C. Guedes Soares, *Review and application of Artificial Neural Networks models in reliability analysis of steel structures,* Structural Safety **52**, 78 (2015).

[70] J. P. Aguilar-López, J. J. Warmink, R. M. J. Schielen, and S. Hulscher, *Piping erosion safety assessment of flood defences founded over sewer pipes,* European Journal of Environmental and Civil Engineering , 1 (2016).

[71] H. van Erp, *A Bayesian framework for risk perception*, Ph.D. thesis, Delft University of Technology (2017).

[72] W. Van der Wiel, *Probabilistic risk assessment of a system of dike ring areas*, Master thesis, Delft University of Technology (2004).

[73] H. Verheij, *Aanpassen van het bresgroeimodel in HIS-OM: Bureaustudie*, Tech. Rep. (Deltares, Delft, 2003).

[74] P. Kamrath, M. Disse, M. Hammer, and J. Köngeter, *Assessment of Discharge through a Dike Breach and Simulation of Flood Wave Propagation,* Natural Hazards **38**, 63 (2006).

[75] F. D. Foresee and M. T. Hagan, *Gauss-Newton approximation to Bayesian learning,* in *Neural Networks,1997., International Conference on*, Vol. 3 (1997) pp. 1930–1935 vol.3.

[76] M. Kok, J. W. Stijnen, and W. Silva, *{U}ncertainty analysis of river flood management in the {N}etherlands,* Safety and Reliability: Proceedings of the ESREL 2003 Conference, Swets & Zeitlinger, Lisse, the Netherlands. ISBN 90-5809-551-7 **1**, 927 (2003).

[77] J. P. Aguilar Lopez, *Probabilistic safety assessment of multi-functional flood defences*, Ph.D. thesis (2016).

A

SUPPORTING ECONOMIC OPTIMISATION EQUATIONS

A

A.1. EXPONENTIAL PROBABILITY OF EXCEEDANCE

Vrijling and van Beurden use in [21] a different form of probability of exceedance compared to Van Dantzig in [9]. Van Dantzig uses:

$$P_f(X) = P_0 e^{-\alpha(X-\eta t)} \qquad P_0 = c_0 e^{-\alpha H_0} \tag{A.1}$$

While Vrijling and van Beurden use:

$$P_f(X) = e^{-\frac{X+H_0-\eta t-A}{B}} \tag{A.2}$$

These equations are equivalent to each-other; this can be shown by multiplying Eq. A.2 by $e^{\frac{H_0-H_0}{B}}$:

$$\begin{aligned} P_f(X) &= e^{\frac{H_0-H_0}{B}} e^{-\frac{X+H_0-\eta t-A}{B}} \\ &= e^{\frac{A-H_0}{B}} e^{-\frac{1}{B}(X-\eta t)} \\ &= e^{\frac{A}{B}} e^{-\frac{1}{B}H_0} e^{-\frac{1}{B}(X-\eta t)} \end{aligned} \tag{A.3}$$

The rewritten form in Eq. A.3 shows that indeed Eq. A.1 & A.2 are equal, if α, c_0 and P_0 in Eq. A.1 are taken to be equal to respectively $\frac{1}{B}$, $e^{\frac{A}{B}}$ and $e^{\frac{A-H_0}{B}}$.

A.2. OPTIMAL PERIODIC INCREASE AND PERIOD

The optimal periodic increase $\hat{u}$ follows from recursively solving the following equation from [22], where $\hat{u}$ is the only unknown parameter:

$$0 = \frac{C_v\left(e^{(\alpha-\zeta)\hat{u}}-1\right)}{C_f + C_v\hat{u}} + \left(\lambda\left(e^{(\alpha-\zeta)\hat{u}}-1\right) - \frac{(\alpha-\zeta)\,r}{\alpha\eta+\gamma-r}\left(e^{((\alpha-\zeta)-q)\hat{u}}-1\right)\right)\frac{1}{1-e^{-q\hat{u}}} \tag{A.4}$$

with:

$$q = \frac{r(\alpha-\zeta) - (\alpha\eta+\gamma-r)\lambda}{\alpha\eta+\gamma} \tag{A.5}$$

Once the optimal periodic increase $\hat{u}$ is known, the optimal periodic time between increases can be found with Eq. 2.14, which is shown again in Eq. A.6.

$$\hat{T} = \frac{\alpha-\zeta+\lambda}{\alpha\eta+\gamma}\hat{u} \tag{A.6}$$

B

Expanded derivations and illustrations for a simplified coastal system

B.1. SIMPLIFIED ECONOMIC OPTIMISATION

The total costs for the simplified system of Section 3.3 are defined in Eq. B.1. The optimal safety targets, in this case the height of the front and rear defence (h_A and h_B) can be found by minimising the total cost equation. This can be done by taking the partial derivatives of the total cost with respect to the two heights, and equating these derivatives to zero. The partial derivates are shown in Eqs. B.2 & B.3.

$$TC = \sum PV(C_R) + \sum PV(C_I) \tag{B.1}$$
$$\sum PV(C_R) = P_A \frac{D_A}{r} + P_B \frac{D_B}{r}$$
$$\sum PV(C_I) = C_{f,A} + C_{v,A} h_A + C_{f,B} + C_{v,B} h_B$$

$$\frac{\partial TC}{\partial h_B} = C_{v,B} + \frac{\partial P_B}{\partial h_B}\left(\frac{D_B}{r} + \frac{D_A}{r}\left(P_{A|B} - P_{A|\overline{B}}\right)\right) + \frac{D_A}{r}\left(P_B \frac{\partial P_{A|B}}{\partial h_B} + P_{\overline{B}} \frac{\partial P_{A|\overline{B}}}{\partial h_B}\right) \tag{B.2}$$

$$\frac{\partial TC}{\partial h_A} = C_{v,A} + \frac{D_A}{r}\left(P_B \frac{\partial P_{A|B}}{\partial h_A} + P_{\overline{B}} \frac{\partial P_{A|\overline{B}}}{\partial h_A}\right) \tag{B.3}$$

The probabilities of exceedance are all assumed to have a similar (exponential) form, but with potentially different parameters. This makes it possible to replace the derivates of the probabilities of exceedance with the following equations:

$$\frac{\partial P_{A|B}}{\partial h_A} = \frac{\partial}{\partial h_A} e^{-\frac{h_A - \alpha_{A|B}}{\beta_{A|B}}} = \frac{P_{A|B}}{-\beta_{A|B}} \tag{B.4}$$

$$\frac{\partial P_{A|\overline{B}}}{\partial h_A} = \frac{\partial}{\partial h_A} e^{-\frac{h_A - \alpha_{A|\overline{B}}}{\beta_{A|\overline{B}}}} = \frac{P_{A|\overline{B}}}{-\beta_{A|\overline{B}}} \tag{B.5}$$

$$\frac{\partial P_B}{\partial h_B} = \frac{\partial}{\partial h_B} e^{-\frac{h_B - \alpha_B}{\beta_B}} = \frac{P_B}{-\beta_B} \tag{B.6}$$

Substituting the results of Eqs. B.4, B.5 & B.6 in Eqs. B.2 & B.3 and equating the latter two equations to zero leads to the following two equations, where the probabilities are now *optimal* probabilities (indicated by adding a circumflex, e.g. $P_B \rightarrow \widehat{P}_B$):

$$\beta_B C_{v,B} r = \widehat{P}_B\left(D_B + D_A\left(\widehat{P}_{A|B} - \widehat{P}_{A|\overline{B}}\right)\right) - \beta_B D_A\left(\widehat{P}_B \frac{\partial \widehat{P}_{A|B}}{\partial h_B} + \widehat{P}_{\overline{B}} \frac{\partial \widehat{P}_{A|\overline{B}}}{\partial h_B}\right) \tag{B.7}$$

$$\frac{C_{v,A} r}{D_A} = \left(\widehat{P}_B \frac{\widehat{P}_{A|B}}{\beta_{A|B}} + \widehat{P}_{\overline{B}} \frac{\widehat{P}_{A|\overline{B}}}{\beta_{A|\overline{B}}}\right) \tag{B.8}$$

Eq. B.7 can be further rewritten into a direct expression for $\widehat{P}_B$:

$$\widehat{P}_B = \frac{\beta_B C_{v,B} r + \beta_B D_A\left(\widehat{P}_B \frac{\partial \widehat{P}_{A|B}}{\partial h_B} + \widehat{P}_{\overline{B}} \frac{\partial \widehat{P}_{A|\overline{B}}}{\partial h_B}\right)}{D_B + D_A\left(\widehat{P}_{A|B} - \widehat{P}_{A|\overline{B}}\right)} \tag{B.9}$$

B.2. RELATION WITH DERIVATIONS IN AN EARLIER PUBLISHED CONFERENCE PAPER

In [38], a similar derivation as shown in Section B.1 was published. The derivation in [38] can be shown to be a simpler form of what was shown in Section B.1. This can be done by assuming the following: $D_B = 0$, $\frac{\partial \widehat{P}_{A|\overline{B}}}{\partial h_B} = 0$, $\frac{\partial \widehat{P}_{A|B}}{\partial h_B} = 0$. This simplifies Eqs. B.8 & B.9 to the following equations:

$$\widehat{P}_B = \frac{\beta_B C_{v,B} r}{D_A\left(\widehat{P}_{A|B} - \widehat{P}_{A|\overline{B}}\right)} \tag{B.10}$$

$$\frac{C_{v,A} r}{D_A} = \left(\widehat{P}_B \frac{\widehat{P}_{A|B}}{\beta_{A|B}} + \widehat{P}_{\overline{B}} \frac{\widehat{P}_{A|\overline{B}}}{\beta_{A|\overline{B}}}\right) \tag{B.11}$$

Furthermore, in [38] the exceedance probability of a single rear defense (i.e. without a front defence) was used to express the influence of a front defence on the rear defence: $P_{A|B} = mP_A$ and $P_{A|\overline{B}} = nP_A$. These expressions can be shown to be a modification of the α parameter of the exponential exceedance:

$$mP_A = me^{-\frac{h_A - \alpha_A}{\beta_A}} = e^{\ln(m)} \cdot e^{-\frac{h_A - \alpha_A}{\beta_A}} = e^{-\frac{h_A - (\alpha_A + \beta_A \ln(m))}{\beta_A}} \tag{B.12}$$

Because Eq. B.12 shows that only the α parameters of the exponential exceedance distributions are affected, this means that following substitution can be made: $\beta_{A|\overline{B}} = \beta_{A|B} = \beta_A$. This substitution, and $P_{A|B} = mP_A$ & $P_{A|\overline{B}} = nP_A$ change Eqs. B.10 & B.11 to the following:

$$\widehat{P}_B = \frac{\beta_B C_{v,B} r}{D_A\left(m\widehat{P}_A - n\widehat{P}_A\right)} \tag{B.13}$$

$$\frac{\beta_A C_{v,A} r}{D_A} = \left(\widehat{P}_B m\widehat{P}_A + \widehat{P}_{\overline{B}} n\widehat{P}_A\right) \tag{B.14}$$

In [38], Eq. B.11 was rewritten in terms of $\widehat{P}_A$. However, this expression is a contradiction: this expression would express what the optimal exceedance probability is of a single rear defence (i.e. without a front defence), given the influence of a front defence. The correct expression for the rear defence influenced by a front defence is already given in Eq. B.11. The left hand side shows that the optimal exceedance probability of a rear defence influenced by a front defence, under the given assumptions, is the same as the optimal exceedance probability of a single rear defence (see also Eq. 3.10). Nevertheless, the height of the rear defence is influenced by the performance of a front defence, and a expression for this height can be found:

$$\begin{aligned} e^{-\frac{\widehat{h}_A - \alpha_A}{\beta_A}} &= \frac{\beta_A C_{v,A} r}{D_A\left(\widehat{P}_B m + \widehat{P}_{\overline{B}} n\right)} \\ \rightarrow \widehat{h}_A &= \alpha_A - \beta_A \ln\left(\frac{C_{v,A}\beta_A r}{D_A\left(\widehat{P}_B (m-n) + n\right)}\right) \end{aligned} \tag{B.15}$$

B.3. EXAMPLE APPLICATION

In order to illustrate the predicted effects of including load reduction, a synthetic example is given, using the input of Tables B.1 & B.2. In Table B.1 a load reduction is simulated by a reduction in the α parameter (see also the previous Section B.2), while in Table B.2 a load reduction is simulated by changing the exponential scale parameter (β). The exceedance probabilities for the two tables are plotted in Figures B.1 & B.2.

Parameter	Value	Unit
$\alpha_{A\|B}$	2.0	m
$\beta_{A\|B}$	0.4	m
$\alpha_{A\|\overline{B}}$	0.8	m
$\beta_{A\|\overline{B}}$	0.4	m
α_B	2.0	m
β_B	0.5	m
$C_{v,A}$	10000.0	$\$/m$
$C_{v,B}$	1000.0	$\$/m$
D_A	1000000.0	$
D_B	30.0	$
r	0.04	–

Table B.1: Input values for the synthetic application of the simplified economic optimisation of a double flood defence system. The potential flood risk reduction is achieved with the α parameter.

Parameter	Value	Unit
$\alpha_{A\|B}$	2.0	m
$\beta_{A\|B}$	0.4	m
$\alpha_{A\|\overline{B}}$	2.0	m
$\beta_{A\|\overline{B}}$	0.1	m
α_B	2.0	m
β_B	0.5	m
$C_{v,A}$	10000.0	$\$/m$
$C_{v,B}$	1000.0	$\$/m$
D_A	1000000.0	$
D_B	30.0	$
r	0.04	–

Table B.2: Input values for the synthetic application of the simplified economic optimisation of a double flood defence system. The potential flood risk reduction is achieved with the β parameter.

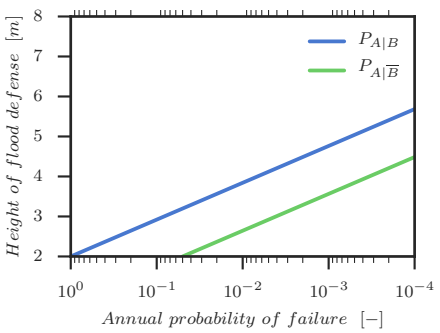

Figure B.1: Exponential failure probability distributions of the rear defence of Table B.1, conditional on a failed or functioning front defence.

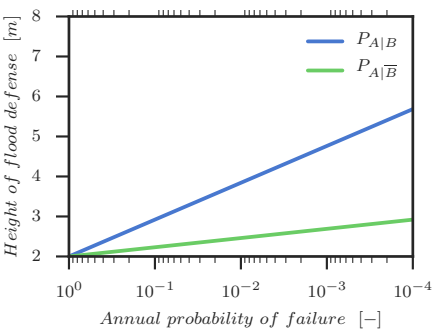

Figure B.2: Exponential failure probability distributions of the rear defence of Table B.2, conditional on a failed or functioning front defence.

In case of no hydrodynamic interactions, a straightforward expression exists for the

economically optimal safety target of a flood defence. This expressions was given in Eq. 3.10. However, the equations for the double flood defence system (Eqs. B.10 & B.11) are not that straightforward to interpret: both equations have an iterative nature, and Eq. B.11 does not contain a direct expression for P_A. In order to give more insight into these expressions, a range of P_B and P_A values are plotted against the results of using these values in the partial derivatives of the total costs in Figure B.3.

These graph show a number of things. For Figures B.3a & B.3c, it can be seen that indeed P_A is equal to $P_{A,single}$ (as was already shown in Eq. B.14). Furthermore, in Figure B.3a the optimal solution for the exceedance probabilities is identical to the single solutions for $P_{A,single}$ and $P_{B,single}$. This changes in Figure B.3c, where a lower D_B leads to a difference between P_B and $P_{B,single}$. The same type of behavior (i.e. larger differences between the single system values and double defence system) can be detected in Figures B.3b & B.3d. Furthermore, Figures B.3b & B.3d show that P_A can deviate from $P_{A,single}$ in case the load reduction is done via the exponential scale parameter β.

The previous focused on the impact on the exceedance probabilities. It is also relevant to see what the impact on the optimal height of the flood defences ($\widehat{h}_B$ and $\widehat{h}_A$) is. This is shown in Figure B.4, where both the optimal values for the exceedance probabilities and the optimal values for the heights are shown and compared to the single flood defences (i.e. no hydrodynamic interactions). Compared to the single defence heights, it can be seen that the optimal heights for the rear defence in the double defence system differ significantly, even in the cases where the differences in the rear defence exceedance probabilities are small or even equal to eachother (i.e. Figures B.4a & B.4b).

B

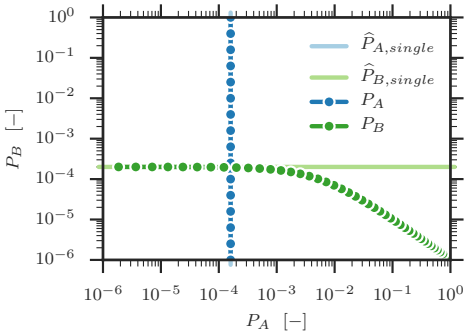

(a) Optimal solution behavior for Table B.1.

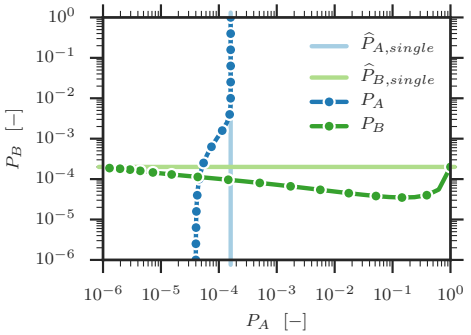

(b) Optimal solution behavior for Table B.2.

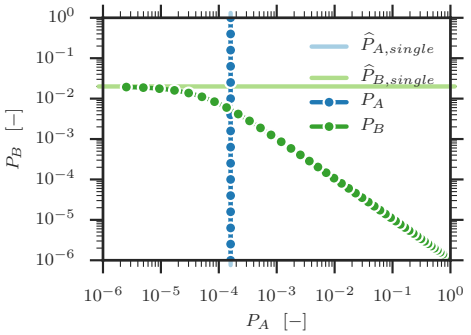

(c) Optimal solution behavior for Table B.1, except with D_B lowered to 1000.

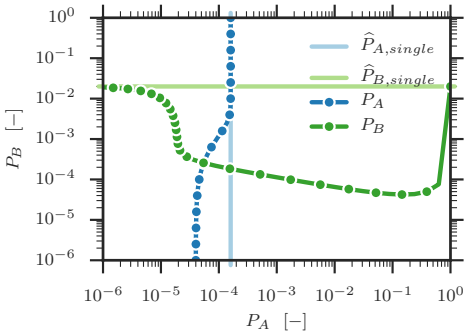

(d) Optimal solution behavior for Table B.2, except with D_B lowered to 1000.

Figure B.3: Optimal solution behavior for a single (i.e. no hydrodynamic interactions, Eq. 3.10) and double optimisation. Optimal values including load reduction are located at the intersection of the dotted lines. The solution of P_A in Figures B.3a & B.3c is based on Eq. B.14, while in Figures B.3b & B.3d it is based on Eq. B.11. The solution for P_B in all four figures is based on Eq. B.10. For $P_{A,single}$, the same values are used as for a rear defence with a failed front defence.

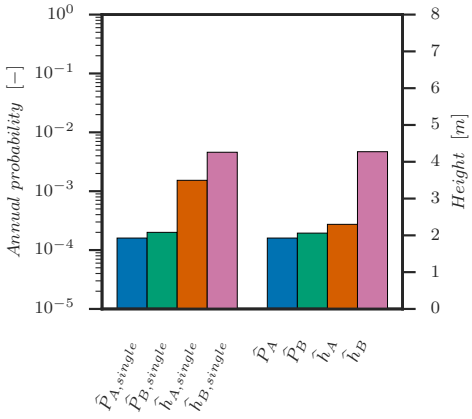

(a) Optimal solution for Table B.1.

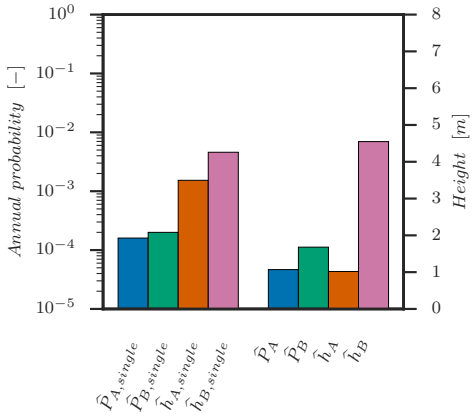

(b) Optimal solution for Table B.2.

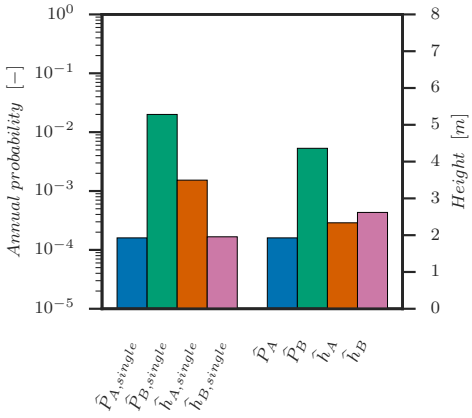

(c) Optimal solution for Table B.1, except with D_B lowered to 1000.

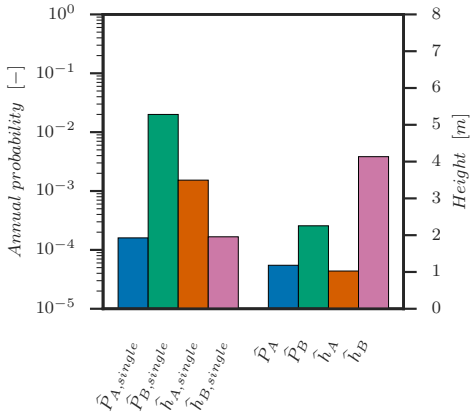

(d) Optimal solution for Table B.2, except with D_B lowered to 1000.

Figure B.4: Optimal solution behavior for a single (i.e. no hydrodynamic interactions, Eq. 3.10) and double optimisation. The solution of P_A in Figures B.3a & B.3c is based on Eq. B.14, while in Figures B.3b & B.3d it is based on Eq. B.11. The solution for P_B in all four figures is based on Eq. B.10. For $P_{A,single}$, the same values are used as for a rear defence with a failed front defence.

C

Analytical economic optimisation for a simplified riverine system

A riverine flood defence system can be defined as a series of multiple flood defences alongside rivers in a riverine system. An example of such a series of flood defences can be found in the form of dike rings in the Dutch Rhine and Meuse river delta. If one of the flood defences breaches, the water levels downstream of the breach can change, which will affect the failure probability. To determine the flood risk of the system, the effect of breaches on failure probabilities downstream need to be addressed. An upstream breach in a riverine flood defence system can either lead to a load increase or load decrease for the downstream defences elsewhere in the system; an example of a load increase is shown in Figure C.1a while a load decrease is shown in Figure C.1b. The load increase in Figure C.1a behaves similarly to the (simple) coastal system with multiple lines of defence described in Chapter 3.

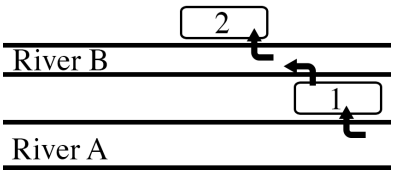

(a) Loads can be increased on defence 2 if, for example, flood defence 1 breaches and forms a short from river A to river B.

(b) Loads can be decreased on defence 2 if, for example, flood defence 1 breaches and stores some of the (peak) discharge in river A.

Figure C.1: Riverine system layouts which in case of failure of the upstream defence 1, either increase (Figure C.1a) or decrease (Figure C.1b) the load on the downstream defence 2.

Regarding the economically optimal safety targets, this appendix follows the identical approach described in Chapter 3, in particular Sections 3.2 & 3.3. Summarising, exponential failure probabilities are assumed (Eq. C.1), which are used to determine the expected annual damages in Eq. C.2. These expected annual damages are added to the investment costs (Eq. C.3) and together form the total costs. Minimisation of the total costs (Eq. C.4) is where the economically optimal safety targets can be found.

$$P_i = 1 - F(h_i) = \exp\left(-\frac{h_i - \alpha_i}{\beta_i}\right) \tag{C.1}$$

$$C_R = P_i D_i \tag{C.2}$$

$$C_{I,i} = C_{f,i} + C_{v,i} h_i \tag{C.3}$$

$$\min\{TC\} = \min\left\{\sum PV(C_R) + \sum PV(C_I)\right\} \tag{C.4}$$

For a single flood defence, the optimal failure probability is described in Eq. 3.10, and is shown here again in Eq. C.5. In this equation, $\widehat{P}_{i,single}$ is the optimal failure probability of single defence i. This optimal failure probability is influenced by the exponential scale parameter β_i, the variable investment cost $C_{v,i}$, the flood damage D_i and discount rate r.

$$\widehat{P}_{i,single} = \frac{\beta_i C_{v,i} r}{D_i} \tag{C.5}$$

C.1. RIVERINE FLOOD DEFENCE SYSTEM WITH TWO DEFENCES

The analytical solution in Eq. C.5 was expanded in Chapter 3 to two, interdependent flood defences. For a riverine system with two flood defences, the expanded formulas describing the economically optimal safety targets of a (simplified) coastal system of Section 3.3 can be re-used. Specifically, Eqs. 3.8 & 3.9 are re-used. A description and derivation of these equations can be found in Sections 3.2 & 3.3. As Figure C.1 uses the names 'Defence 1' and 'Defence 2' instead of 'Defence B' and 'Defence A', Eqs. 3.8 & 3.9 are updated in Eqs. C.6 & C.7 to use the nomenclature of Figure C.1.[1] In this section, attention will be solely given to the economically optimal failure probability of flood defences. The optimal heights or (in case of repeated investments) investment schemes are discussed as part of a case study in Chapter 5.

$$\frac{C_{v,2}\, r}{D_2} = \left(\widehat{P}_1 \frac{\widehat{P}_{2|1}}{\beta_{2|1}} + \widehat{P}_{\bar{1}} \frac{\widehat{P}_{2|\bar{1}}}{\beta_{2|\bar{1}}} \right) \tag{C.6}$$

$$\widehat{P}_1 = \frac{\beta_1 C_{v,1}\, r}{D_1 + D_2 \left(\widehat{P}_{2|1} - \widehat{P}_{2|\bar{1}} \right)} \tag{C.7}$$

OPTIMAL FAILURE PROBABILITY OF DEFENCE 1: LOAD INCREASE

For the load increasing situation, Eq. C.7 can be simplified by using the approximation that the probability of failure of defence 2 given a failed defence 1 is much larger than with a functioning defence 1. This approximation (Eq. C.8) changes Eq. C.7 into Eq. C.9. Eq. C.9 shows that the contribution of the flood damage near defence 2 is contained in the second part of the denominator: the flood damage at defence 2 multiplied with the probability of failure at defence 2 given a breach at defence 1 ($D_2 \widehat{P}_{2|1}$).

$$\widehat{P}_{2|1} \gg \widehat{P}_{2|\bar{1}} \quad \rightarrow \quad \widehat{P}_{2|1} - \widehat{P}_{2|\bar{1}} \approx \widehat{P}_{2|1} \tag{C.8}$$

$$\widehat{P}_1 \approx \frac{\beta_1 C_{v,1}\, r}{D_1 + D_2 \widehat{P}_{2|1}} \tag{C.9}$$

Assuming that probability of failure at defence 2 given a breach at defence 1 ($\widehat{P}_{2|1}$) is 1/1000, the flood damage D_2 would need to be 1000 times larger to be in the same order of the contribution of defence 1 (which is D_1). However, this assumption does not hold if the system of flood defences behave like dominos (i.e. cascading failures).[2] In that case, the probability of failure at defence 2 given a breach at defence 1 ($\widehat{P}_{2|1}$) is much larger or even close to one. Therefore, the damage at defence 2 only needs to be in the same order as the damage at defence 1 for it to have an impact at the optimal failure probability at defence 1.

[1] Another reason to use different naming is to separate the coastal formulations from the riverine formulations.

[2] An example of this domino behavior can be found with flood defences which are joined to each-other with relatively weak inner levees. If a river-facing upstream defence breaches, the inner levees will almost certainly also breach, leading to cascading failures downstream.

A large discrepancy between the flood damages of defence 1 (D_1) and defence 2 (D_2) can be expected in a coastal system. This is based on the assumption that defence 1 is typically a storm surge barrier, while defence 2 represents for example a dike ring area. While storm surge barriers are expensive to construct, the potential economic damage of the area behind defence 2 is usually much larger than the potential economic damage of defence 1: $D_2 \gg D_1$. The damage caused by a failed defence 1 due to inundation will typically be low, as a storm surge barrier separates 'water from water'. Therefore, the damage costs will be governed by more indirect costs. For example, repair costs and the economic damage due to loss of functionality (e.g. a road on top of the barrier). In this situation, where $D_2 \gg D_1$, it is likely for the optimal failure probability of the front defence $\widehat{P}_1$ to be significantly influenced (i.e. reduced) by the rear defence.

However, for riverine flood defence systems the potential flood damage associated with defence 1 and 2 does not have to follow the previous expectation of $D_2 \gg D_1$. In fact, if defences 1 and 2 are both dike ring areas, the flood damages near defence 1 and 2 might also be approximately equal to each-other ($D_2 \approx D_1$) or the damage near defence 1 might be much greater than near defence 2 $D_2 \ll D_1$. In both these cases, it is much less likely for the optimal failure probability of the upstream defence $\widehat{P}_1$ to be significantly influenced by the downstream defence. Nevertheless, an earlier mentioned exception to this is when a domino effect between flood defences can be expected (i.e. $\widehat{P}_{2|1} \approx 1$). In this case, a significant influence *can* be expected if the flood damages near defence 1 and 2 are approximately equal to each-other ($D_2 \approx D_1$); see also section C.4.

OPTIMAL FAILURE PROBABILITY OF DEFENCE 1: LOAD DECREASE

For the load decreasing situation, Eq. C.7 can be simplified by using a similar approximation as in Eq. C.8. Only in this case, the assumption will be that the probability of failure of defence 2 given a failed defence 1 is much smaller than with a functioning defence 1. This approximation (Eq. C.10) changes Eq. C.7 into Eq. C.11:

$$\widehat{P}_{2|1} \ll \widehat{P}_{2|\bar{1}} \quad \rightarrow \quad \widehat{P}_{2|1} - \widehat{P}_{2|\bar{1}} \approx -\widehat{P}_{2|\bar{1}} \tag{C.10}$$

$$\widehat{P}_1 \approx \frac{\beta_1 C_{v,1} r}{D_1 - D_2 \widehat{P}_{2|\bar{1}}} \tag{C.11}$$

The first thing that stands out in Eq. C.11 is that the contribution of defence 2 is now subtracted from the flood damage for defence 1. Effectively, this leads to a potential *increase* of the optimal failure probability. Regarding the significance of the impact of defence 2 on the optimal failure probability of defence 1, the same analysis as made for the load increasing situation still holds for the load decreasing situation: a significant impact is likely in case $D_2 \gg D_1$, but much less likely in case $D_2 \approx D_1$ or $D_2 \ll D_1$.[3]

[3] The earlier mentioned domino-effect (i.e. cascading breaches) is not applicable in a load-decreasing scenario, because this effect is by definition load-increasing.

OPTIMAL FAILURE PROBABILITY OF DEFENCE 2

The optimal failure probability of defence 2 can be examined using Eq. C.6. The optimal failure probability of defence 2 ($\widehat{P}_2$) was already found in Section 3.3 to be bound between the optimal conditional probabilities $\widehat{P}_{2|\overline{1}}$ and $\widehat{P}_{2|1}$. In Eq. 3.2, an expression was given for the non-optimal failure probability of defence 2. This expression is updated for the nomenclature of Figure C.1, and used to express the optimal failure probability of defence 2:

$$\widehat{P}_2 = \widehat{P}_1 \widehat{P}_{2|1} + \widehat{P}_{\overline{1}} \widehat{P}_{2|\overline{1}} \tag{C.12}$$

It can be assumed that the optimal failure probability of defence 1 ($\widehat{P}_1$) will be a (very) small, positive number. As a simplification, $\widehat{P}_1$ can even be approximated as being zero; this also means that the optimal probability of defence 1 *not* failing ($\widehat{P}_{\overline{1}}$) is approximately one (as $\widehat{P}_{\overline{1}}$ was defined as $1 - \widehat{P}_1$). These approximations can be used in both Eq. C.12 & C.6, which changes them into Eq. C.13 & C.14:

$$\widehat{P}_2 \approx \widehat{P}_{2|\overline{1}} \tag{C.13}$$

$$\frac{C_{v,2} r \beta_{2|\overline{1}}}{D_2} \approx \widehat{P}_{2|\overline{1}} \tag{C.14}$$

The result of Eq. C.13 can be substituted in Eq. C.14 to get an approximate result for the optimal failure probability of defence 2:

$$\widehat{P}_2 \approx \frac{C_{v,2} r \beta_{2|\overline{1}}}{D_2} \tag{C.15}$$

If the approximation of the optimal failure probability of defence 1 ($\widehat{P}_1$) being a very small number holds, the effect of the upstream defence 1 on the optimal failure probability of defence 2 is limited to the conditional exponential scale parameter $\beta_{2|\overline{1}}$. The analysis of the impact of defence 1 on defence 2 then becomes straightforward, as the exponential scale parameter is conditional on defence 1 *not* failing. In other words, this is the same situation as when the effect of upstream breaches is completely ignored. However, this analysis depends on the approximation that the optimal failure probability of defence 1 is approximately equal to zero ($\widehat{P}_1 \approx 0$). The cases where this approximation does *not* hold can be found with help of the earlier made analyses of the optimal failure probability of defence 1. For example, a likely case where the optimal failure probability can be relatively large is when the flood damage in case defence 1 breaches (D_1) is approximately zero.

C.2. ILLUSTRATION OF RIVERINE CONDITIONAL FAILURE PROBABILITIES

The analyses described in the previous sections depend on approximations regarding the conditional failure probabilities of defence 2. The assumption in the previous is that

the ratio between these two probabilities is large (Eqs. C.8 & C.10). In this section, the ratio will be investigated based on a simple example.

Generally speaking, a breach will lead to some discharge being diverted. This diverted discharge will then either lead to a load increase or a load decrease downstream of the breached flood defence. Therefore, the simple example will be based on what a change in discharge volume in a river means for the occurring water levels. For this example, the river Rhine in the Netherlands will be used. A representative (peak) discharge distribution for the river Rhine can be found in [67], which is a Gumbel distribution and is shown in Figure C.2. The discharges can be converted to (equilibrium) water levels with the help of a representative cross-section of the river Rhine. This was done in [72], which also lists a function which approximates the conversion from discharge to water level directly, and a similar equation is listed here in Eq. C.16:

$$h_r = 0.0335 Q_r^{0.617}, \tag{C.16}$$

where h_r is the water level in the river and Q_r is the discharge in the river. A simple simulation of an upstream breach would be a constant reduction of the occurring discharge. The effect of reducing the discharge by 10% and 20% is shown in Figure C.3. These water level relations are approximated with manually fitted exponential exceedance relations (exponential exceedance relations are imposed by the simplifications in the used economic optimisation).

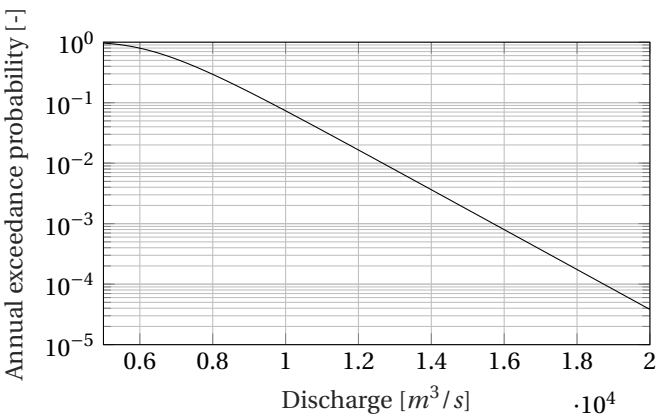

Figure C.2: Annual exceedance probabilities using a Gumbel distributed discharge for the river Rijn (Gumbel parameters are taken from [67]).

With the help of these lines, the conditional failure probabilities of defence 2 can be illustrated. The goal of this illustration is to indicate when these two conditional probabilities (conditional on whether or not defence 1 has failed) differ significantly: $\widehat{P}_{2|1} \ll \widehat{P}_{2|\overline{1}}$ (load reduction) or $\widehat{P}_{2|1} \gg \widehat{P}_{2|\overline{1}}$. For a load reduction, this is illustrated in Table C.1.

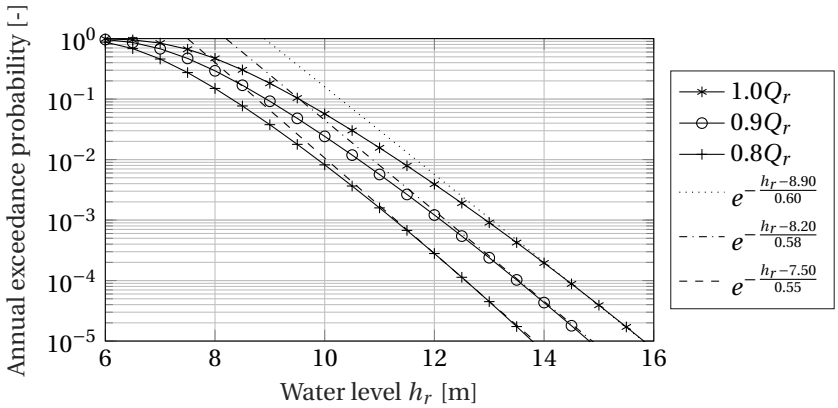

Figure C.3: Annual exceedance probabilities for water levels based on Eq. C.16. The solid lines with markers represent the water levels belonging to a discharge reduction of 20% ($0.8Q_r$), 10% ($0.9Q_r$) or no reduction ($1.0Q_r$). These three relations are approximated with manually fitted exponential exceedance distributions, which are shown in the plot as well.

reduction	$\widehat{P}_{2\|1}$	$\widehat{P}_{2\|\overline{1}}$	$\frac{\widehat{P}_{2\|\overline{1}}}{\widehat{P}_{2\|1}}$	$\widehat{P}_{2\|1} \ll \widehat{P}_{2\|\overline{1}}$
10%	$0.9Q_r$	$1.0Q_r$	≈ 4	~
20%	$0.8Q_r$	$1.0Q_r$	≈ 20	+

Table C.1: Illustration of the effect of a load reduction on the conditional probabilities of defence 2.

Table C.1 illustrates that, in case Figure C.3 represents the conditional probabilities for a load reduction, it can be assumed that line $1.0Q_r$ represents the downstream defence without an upstream breach ($\widehat{P}_{2|\bar{1}}$), while line $0.9Q_r$ (or line $0.8Q_r$) represents the downstream defence *with* an upstream breach ($\widehat{P}_{2|1}$). From Figure C.3, it can be seen that the ratio between the two probabilities (calculated as $\widehat{P}_{2|\bar{1}} \Big/ \widehat{P}_{2|1}$) at a water level of 12 meters is either a factor of four (if line $0.9Q_r$ is used) or twenty (if line $0.8Q_r$ is used). The factor of four is not really sufficient to use the approximation of Eq. C.10, but the factor of twenty certainly is. For a load increase, the analysis is similar, only the water level relations used for the conditional probabilities need to be switched around.

In case of a load increase due to a shortcut between two rivers, another reason to be able to use that the probability of defence 2 given a breach at defence 1 is much larger than the probability of defence 2 given no breach at defence 1 ($\widehat{P}_{2|1} \gg \widehat{P}_{2|\bar{1}}$, Eq. C.8) would be if the shortcut is formed between two different-sized rivers. Specifically, if the breach flow is routed from a large river to a small river. In that case, even a small breach at the large river can result in a relatively big load increase at the small river. For example, the relative impact of adding a discharge of $500 m^3/s$ to an existing discharge of $1500 m^3/s$ has a more profound impact than adding the same discharge to an existing discharge of $15{,}000 m^3/s$. Consequently, the ratio between the two conditional failure probabilities for defence 2 will then be large ($\widehat{P}_{2|1} \gg \widehat{P}_{2|\bar{1}}$).

C.3. LOAD REDUCTION IN A SYSTEM OF THREE FLOOD DEFENCES

The previous analyses were limited to two flood defences. It is expected that if more defences are added, the effect of a load reduction at defence 1 becomes stronger. To investigate this further, the load reduction displayed in Figure C.1 is expanded to three defences in Figure C.4.

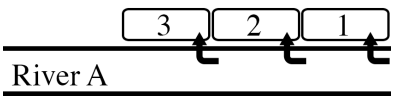

Figure C.4: Loads can be decreased on defence 2 and defence 3 if, for example, flood defence 1 breaches and stores some of the (peak) discharge in river A.

In order to derive analytical economically optimal safety targets for the system shown in Figure C.4, the economic optimisation shown in Appendix B.1 needs to be expanded in order to take flood defence 3 into account. The main governing equation is shown in Eq. C.17. In this equation, both the expected annual system risk cost and the system investment cost are now defined as the sum of the contributions of the three flood defences.

$$TC = \sum PV(C_R) + \sum PV(C_I) \tag{C.17}$$
$$\sum PV(C_R) = P_1 \frac{D_1}{r} + P_2 \frac{D_2}{r} + P_3 \frac{D_3}{r}$$
$$\sum PV(C_I) = C_{f,1} + C_{v,1} h_1 + C_{f,2} + C_{v,2} h_2 + C_{f,3} + C_{v,3} h_3$$

The failure probabilities of defence 2 and 3 are expanded into conditional probabilities using the chain rule for probability and the law of total probability as follows:

$$P_2 = P_1 P_{2|1} + P_{\bar{1}} P_{2|\bar{1}} \tag{C.18}$$
$$P_3 = P_{2\cap 1} P_{3|2\cap 1} + P_{\bar{2}\cap 1} P_{3|\bar{2}\cap 1} + P_{2\cap \bar{1}} P_{3|2\cap \bar{1}} + P_{\bar{2}\cap \bar{1}} P_{3|\bar{2}\cap \bar{1}} \tag{C.19}$$

ECONOMICALLY OPTIMAL DEFENCE 1

The economically optimal level for defence 1 can be found by taking the partial derivative of the total cost equation with respect to the height of flood defence 1 and equating it to zero:

$$\frac{\partial TC}{\partial h_1} = 0 \tag{C.20}$$
$$\frac{\partial P_1}{\partial h_1} = \frac{\partial}{\partial h_1} e^{-\frac{h_1 - \alpha_1}{\beta_1}} = \frac{P_1}{-\beta_1} \tag{C.21}$$
$$\begin{aligned} C_{v,1}\beta_1 r = {} & \widehat{P}_1 D_1 + \left(\widehat{P}_1 P_{2|1} - \widehat{P}_1 \widehat{P}_{2|\bar{1}}\right) D_2 \\ & + \left(\widehat{P}_1 P_{2|1} \widehat{P}_{3|2\cap 1} - \widehat{P}_1 \widehat{P}_{\bar{2}|\bar{1}} \widehat{P}_{3|\bar{2}\cap \bar{1}}\right) D_3 \\ & + \left(\widehat{P}_1 \widehat{P}_{\bar{2}|1} \widehat{P}_{3|\bar{2}\cap 1} - \widehat{P}_1 \widehat{P}_{2|\bar{1}} \widehat{P}_{3|2\cap \bar{1}}\right) D_3 \end{aligned} \tag{C.22}$$

Rewriting Eq. C.22 in terms of $\widehat{P}_1$ results in an expression describing the economically optimal exceedance probability for defence 1:

$$\widehat{P}_1 = \frac{C_{v,1}\beta_1 r}{D_1 + D_2\left(\widehat{P}_{2|1} - \widehat{P}_{2|\bar{1}}\right) + D_3\left(\widehat{P}_{2|1}\widehat{P}_{3|2\cap 1} - \widehat{P}_{\bar{2}|\bar{1}}\widehat{P}_{3|\bar{2}\cap \bar{1}} + \widehat{P}_{\bar{2}|1}\widehat{P}_{3|\bar{2}\cap 1} - \widehat{P}_{2|\bar{1}}\widehat{P}_{3|2\cap \bar{1}}\right)} \tag{C.23}$$

In this equation, in the context of a significant load reduction, the contribution of the term which describes that all three defences fail can be approximated as being zero. Because of the perceived impact of a load reduction, given a failed defence 1 the probability of defence 2 and 3 failing will be much smaller. This is even more the case if both defence 1 and 2 have failed (resulting in an even greater load reduction). Therefore, the following approximation can be used:

$$\widehat{P}_1 \approx \frac{C_{v,1}\beta_1 r}{D_1 + D_2\left(\widehat{P}_{2|1} - \widehat{P}_{2|\bar{1}}\right) + D_3\left(-\widehat{P}_{\bar{2}|\bar{1}}\widehat{P}_{3|\bar{2}\cap \bar{1}} + \widehat{P}_{\bar{2}|1}\widehat{P}_{3|\bar{2}\cap 1} - \widehat{P}_{2|\bar{1}}\widehat{P}_{3|2\cap \bar{1}}\right)} \tag{C.24}$$

In this approximation, the probability that defence 2 fails given that defence 1 has failed ($\widehat{P}_{2|1}$) is assumed to be approximately zero; this also means that $\widehat{P}_{\overline{2}|1}$ is approximately one. Applying this to Eq. C.24 leads to the following approximation:

$$\widehat{P}_{2|1} \ll \widehat{P}_{2|\overline{1}} \quad \rightarrow \quad \widehat{P}_{2|1} - \widehat{P}_{2|\overline{1}} \approx -\widehat{P}_{2|\overline{1}} \tag{C.25}$$

$$\widehat{P}_1 \approx \frac{C_{v,1}\beta_1 r}{D_1 - D_2\widehat{P}_{2|\overline{1}} + D_3\left(-\widehat{P}_{\overline{2}|\overline{1}}\widehat{P}_{3|\overline{2}\cap\overline{1}} + \widehat{P}_{3|\overline{2}\cap 1} - \widehat{P}_{2|\overline{1}}\widehat{P}_{3|2\cap\overline{1}}\right)} \tag{C.26}$$

C

Furthermore, it can be safely assumed that the probability of defence 2 not failing is much larger than the probability that defence 2 does fail (i.e. $\widehat{P}_{2|\overline{1}} \ll \widehat{P}_{\overline{2}|\overline{1}}$). Finally, the probability that defence 3 fails given no load reduction can be assumed to be much larger than the probability that defence 3 fails given that defence 1 or defence 2 have failed (this is same underlying thought that was used already in Eq. C.25). This further simplifies the economically optimal exceedance probability of defence 1:

$$\widehat{P}_1 \approx \frac{C_{v,1}\beta_1 r}{D_1 - D_2\widehat{P}_{2|\overline{1}} - D_3\widehat{P}_{\overline{2}|\overline{1}}\widehat{P}_{3|\overline{2}\cap\overline{1}}} \tag{C.27}$$

ECONOMICALLY OPTIMAL DEFENCE 3

The economically optimal level for defence 3 can be found by taking the partial derivative of the total cost equation with respect to the height of flood defence 3 and equating it to zero:

$$\frac{\partial TC}{\partial h_3} = 0 \tag{C.28}$$

$$\frac{\partial TC}{\partial h_3} = C_{v,3} + \frac{D_3}{r}\left(P_{2\cap 1}\frac{\partial P_{3|2\cap 1}}{\partial h_3} + P_{\overline{2}\cap 1}\frac{\partial P_{3|\overline{2}\cap 1}}{\partial h_3} + P_{2\cap\overline{1}}\frac{\partial P_{3|2\cap\overline{1}}}{\partial h_3} + P_{\overline{2}\cap\overline{1}}\frac{\partial P_{3|\overline{2}\cap\overline{1}}}{\partial h_3}\right) \tag{C.29}$$

$$\frac{C_{v,3}r}{D_3} = \left(\widehat{P}_{2\cap 1}\frac{\widehat{P}_{3|2\cap 1}}{\beta_{3|2\cap 1}} + \widehat{P}_{\overline{2}\cap 1}\frac{\widehat{P}_{3|\overline{2}\cap 1}}{\beta_{3|\overline{2}\cap 1}} + \widehat{P}_{2\cap\overline{1}}\frac{\widehat{P}_{3|2\cap\overline{1}}}{\beta_{3|2\cap\overline{1}}} + \widehat{P}_{\overline{2}\cap\overline{1}}\frac{\widehat{P}_{3|\overline{2}\cap\overline{1}}}{\beta_{3|\overline{2}\cap\overline{1}}}\right) \tag{C.30}$$

The same assumption that was made for defence 1 can be made here as well: the contribution of the term which describes that all three defences fail can be approximated as being zero.

$$\frac{C_{v,3}r}{D_3} \approx \left(\widehat{P}_{\overline{2}\cap 1}\frac{\widehat{P}_{3|\overline{2}\cap 1}}{\beta_{3|\overline{2}\cap 1}} + \widehat{P}_{2\cap\overline{1}}\frac{\widehat{P}_{3|2\cap\overline{1}}}{\beta_{3|2\cap\overline{1}}} + \widehat{P}_{\overline{2}\cap\overline{1}}\frac{\widehat{P}_{3|\overline{2}\cap\overline{1}}}{\beta_{3|\overline{2}\cap\overline{1}}}\right) \tag{C.31}$$

The remaining three products within parenthesis are also worth looking at. The first two products will probably be in the same order of magnitude, as both describe the failure of a single defence. However, the third product describes the joint probability of defence 3 failing intersected with defences 1 and 2 not failing. Because there is no load reduction from defence 1 and 2, the conditional probability for defence 3 will be larger than if it would be conditional on defence 1 or 2 failing. Both these arguments suggest

that the third product within parenthesis will dominate, which means the other two can approximated as zero. Furthermore, the probability that defences 1 and 2 do not fail will be approximately one. The equation can now be rewritten in terms of the optimal exceedance probability for defence 3:

$$\widehat{P}_{\overline{2}\cap\overline{1}}\widehat{P}_{3|\overline{2}\cap\overline{1}} \approx \frac{C_{v,3}\, r\, \beta_{3|\overline{2}\cap\overline{1}}}{D_3} \tag{C.32}$$

These assumption can also be used on Eq. C.19, which results in $\widehat{P}_3 \approx \widehat{P}_{\overline{2}\cap\overline{1}}\widehat{P}_{3|\overline{2}\cap\overline{1}}$. Therefore, the economically optimal exceedance probability for defence 3 in case of a load reduction scenario can be described as:

$$\widehat{P}_3 \approx \frac{C_{v,3}\, r\, \beta_{3|\overline{2}\cap\overline{1}}}{D_3} \tag{C.33}$$

COMPARISON OF A SYSTEM OF TWO AND THREE DEFENCES

In the previous, simplified formulae were derived for the optimal failure probability of defence 1 (Eq. C.27) and 3 (Eq. C.33). Because these approximations are derived for a load reduction case, the effect of taking into account an additional defence (i.e. defence 3) can now be seen by comparing it to the results from Section C.1. For the optimal probability of defence 1, the denominator has an additional term with D_3. It is likely that if even more defences are added, these will be added in a similar manner. The impact of an additional defence is that sum of the contributions of these defences is subtracted from the flood damage D_1. However, as noted in Section C.1, these will typically be rather small subtractions, which will only start adding up to a significant factor if many flood defences are considered. This extrapolation is based on the assumptions that the flood damages for all three defences are in the same order of magnitude and that the optimal conditional failure probabilities of defence 2 and 3 are much smaller than one.

The economically optimal exceedance probability of defence 3 looks similar to the one derived in Eq C.15 for defence 2 in a system with two defences. The only real difference with the economically optimal probability of a single defence (Eq. C.5) is the beta parameter, which is now a beta parameter conditional on defence 1 and 2 not failing. In other words, for a load reduction scenario this would be either identical or very close to the beta parameter used in an evaluation of a single flood defence and the optimal exceedance probability for defence 3 will therefore not change significantly.

C.4. INFLUENCE OF CASCADING FAILURES

'Cascading failures' is defined here as a system of flood defences where in case of a breached upstream flood defence, all downstream defences will fail and breach as well. This is a real concern in for example the Netherlands, where a breach near the river Rhine in the eastern part of the country can lead to a shortcut towards the much smaller (in terms of discharge) river IJssel. A similar, simplified case is shown in Figure C.5a. An-

other case of cascading failures is shown in Figure C.5b, where cascading failures occur due to the breaching of (supposed) weak internal flood defences.

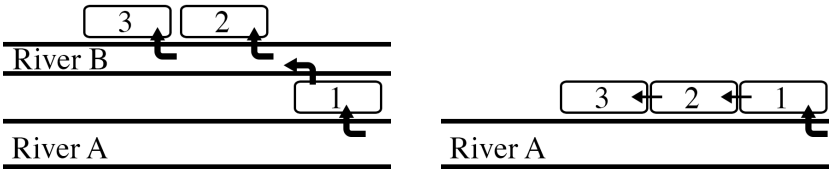

(a) The load on defence 2 and 3 will increase significantly if a breached defence 1 forms a shortcut from the large river A towards the smaller river B.

(b) Defences 2 and 3 breach internally due to a breach at flood defence 1 and (supposed) weak internal flood defences.

Figure C.5: Two possible types of cascading failures.

In this case, interest lies primarily what the optimal failure probability of the first defence should be. As this is a riverine flood defence system with three defences, the equations of Appendix C.2 can be re-used. Specifically, equation C.23 which describes the optimal exceedance probability of defence 1. This equation is shown here again in Eq. C.34. This equation can be simplified. First, the same approximation regarding a load increase that is described in Eq. C.8 can be re-used and is applied in Eq. C.35; this approximation describes that the probability of failure of defence 2 given a failed defence 1 is much larger than with a functioning defence 1.

$$\widehat{P}_1 = \frac{C_{v,1}\beta_1 r}{D_1 + D_2\left(\widehat{P}_{2|1} - \widehat{P}_{2|\overline{1}}\right) + D_3\left(\widehat{P}_{2|1}\widehat{P}_{3|2\cap 1} - \widehat{P}_{\overline{2}|\overline{1}}\widehat{P}_{3|\overline{2}\cap\overline{1}} + \widehat{P}_{\overline{2}|1}\widehat{P}_{3|\overline{2}\cap 1} - \widehat{P}_{2|\overline{1}}\widehat{P}_{3|2\cap\overline{1}}\right)} \tag{C.34}$$

$$\widehat{P}_1 \approx \frac{C_{v,1}\beta_1 r}{D_1 + D_2\widehat{P}_{2|1} + D_3\left(\widehat{P}_{2|1}\widehat{P}_{3|2\cap 1} - \widehat{P}_{\overline{2}|\overline{1}}\widehat{P}_{3|\overline{2}\cap\overline{1}} + \widehat{P}_{\overline{2}|1}\widehat{P}_{3|\overline{2}\cap 1}\right)} \tag{C.35}$$

Secondly, if the cascading effect is regarded as forceful, it can be assumed that all probabilities conditional on a failed defence 1 are approximately one. This also means that a probability describing a functioning downstream defence conditional on a failed defence 1 is approximately zero (i.e. $\widehat{P}_{\overline{2}|1} \approx 0$). This approximation is applied in Eq. C.36. Thirdly, because the term $\widehat{P}_{\overline{2}|\overline{1}}\widehat{P}_{3|\overline{2}\cap\overline{1}}$ describes a situation for flood defence 3 where none of the upstream defences have been breached, it can be approximated as $\widehat{P}_{3,single}$. This approximation will most likely result in the term having a small value ($\ll 10^{-1}$), and is applied in Eq. C.37. If the approximations used to derive Eq. C.37 are applicable for a case, Eq. C.37 shows that the optimal exceedance probability of defence 1 is significantly influenced by the potential flood damages of the downstream defences.

$$\widehat{P}_1 \approx \frac{C_{v,1}\beta_1 r}{D_1 + D_2 + D_3\left(1\cdot 1 - \widehat{P}_{\overline{2}|\overline{1}}\widehat{P}_{3|\overline{2}\cap\overline{1}} + 0\cdot 1\right)} \tag{C.36}$$

$$\widehat{P}_1 \approx \frac{C_{v,1}\beta_1 r}{D_1 + D_2 + D_3} \tag{C.37}$$

D

SUPPORTING INFORMATION REGARDING THE RIJN/IJSSEL RIVERINE CASE STUDY

D.1. FAILURE PROBABILITIES OF BREACH LOCATIONS

This appendix provides additional information pertaining the modelling of the probability of failure of breach locations for the case as described in Section 5.2. First, a (simplified) hydrodynamic model is described that describes the propagation of a (peak) discharge wave through the river branches. Then, once a breach occurs at a breach location, breach flows toward flood-prone areas are described as well as their interactions with the discharge flow through the river branches. Finally, it is described how this hydrodynamic model is used in conjunction with random variables in order to estimate failure probabilities of breach locations, and indicate how accurate these estimates are.

D.1.1. RIVER MODEL

The hydrodynamic model uses a discharge wave as input. This discharge wave is composed out of a normalized discharge wave as described in [15] and shown in Figure D.1. The discharge wave of Figure D.1 is scaled by multiplying the discharge wave with a sampled peak discharge (see D.1.3 for the sampling of peak discharges). These discharges are converted to water levels at each breach location using stage - discharge relations. The use of these stage - discharge relations is one of the key reasons why our model is computationally efficient; however, this computational efficiency comes at the cost of simplified river hydrodynamics.

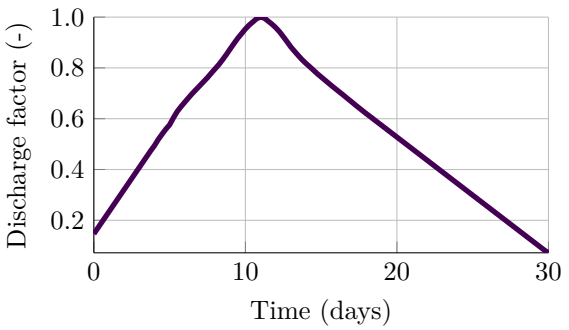

Figure D.1: Normalized discharge wave over time. The peak discharge, which coincides to a discharge factor of 1.0, occurs around day 11.

The stage - discharge relations are based on the Chézy formula using a single river profile as shown in Figure D.2. The Chézy formula is shown in Eq. D.1, which assumes equilibrium water levels:

$$Q_{riv} = 18\log\left(\frac{12 \cdot A/C_{wet}}{k}\right) A\sqrt{A/C_{wet} \cdot i} \tag{D.1}$$

where i is the slope, k is the Nikuradse coefficient, C_{wet} is the "wet" circumference of the river profile, A is the cross-sectional surface area and Q is the discharge. The river

profile of Figure D.2 is used for the river Rhine. stage - discharge relations for the Pannerden Canal and IJssel are derived from the stage - discharge relationship for the Rhine. This derivation is based on two assumptions. The first assumption is that a constant fraction (1/3) of the discharge from the Rhine flows into the Pannerden Canal, and that a constant fraction (again 1/3) of the discharge from the Pannerden Canal flows into the IJssel. The second assumption is that given a discharge Q in the Rhine and a discharge $1/3Q$ in the Pannerden Canal, the water depth in both river branches will be identical.

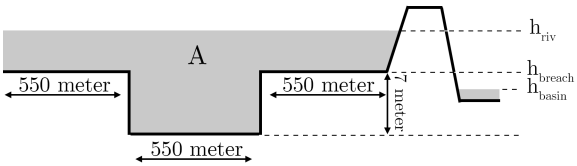

Figure D.2: Cross-sectional river profile as used for the river Rhine. The levels h_{riv}, h_{breach} and h_{basin} are relative to the bottom level of the river.

Based on the approach in [72], rather than iteratively solving Eq. D.1, a range of water levels and accompanying discharges is computed using Eq. D.1 and fitted (using a least squares method) to the following stage-discharge relation:

$$h_{riv} = a \cdot {Q_{riv}}^{b} \tag{D.2}$$

Where a and b are found as a result of the fitting process. The resulting stage - discharge relations are shown in Figure D.3. These relations are based on the the river Rhine profile of Figure D.2, along with a Nikuradse coefficient k of 0.05 meter and a slope i of 10^{-4}.

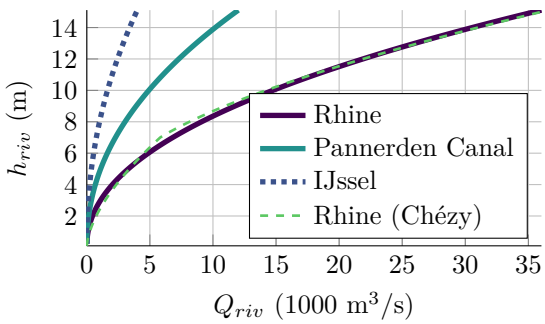

Figure D.3: Stage - discharge relationships for the three river branches using equation D.2. The Stage - discharge relationship for the river Rhine using the Chezy equation of Eq D.1 is shown as well.

D.1.2. BREACH AND FLOODING MODEL

The stage - discharge relations of the previous section are used to determine whether or not a breach occurs at a breach location. If the water depth at a breach location exceeds the 'critical height' of that breach location (see also D.1.3), the breaching process will start. The breach width B will then develop over time according to the Verheij - van der Knaap equation as shown in Eq D.3 [73], similar to (for example) [15, 16]. This equation is based on an analysis of a breached defence functioning as a (submerged) weir, connected to a basin where any inflow results in a constant increase of the water level over the basin surface (i.e. pumping mode assumption). A similar model is used for estimating the breach flow, and use an adjusted version of the Poleni weir equation (Eq. D.4) to estimate the breach flow Q_{breach}.

$$B = 1.3 \frac{g^{0.5} (h_{riv} - h_{basin})^{1.5}}{u_c} \log\left(1 + \frac{0.04g}{u_c} t\right) \tag{D.3}$$

$$Q_{breach} = \frac{2}{3} m \sqrt{g} B (h_{riv} - h_{breach}) \sqrt{h_{riv} - h_{basin}} \tag{D.4}$$

In Eq. D.3, g is the gravitational acceleration (set to 9.81 m/s^2), t is the elapsed time since the initial moment of breach and u_c is a critical flow velocity. The critical flow velocity has been set to 0.3 m/s for the application in this chapter, which is close the values used for sand in [73]. Furthermore, the breach width B is limited to a maximum of 200 meters in accordance with [16].

Eq. D.4 is an adjusted version of the Poleni weir equation in which the addition of $\sqrt{h_{riv} - h_{basin}}$ accounts for submerged flow. Furthermore, m is a flow factor for energy losses and is assumed to be equal to 1. In a more realistic application, this factor could be estimated more accurately, for example using an approach as shown in [74].

The height of the water level in flood prone areas is estimated using a simple 'bath tub' model as shown in Eq. D.5.

$$\frac{dh_{basin}}{dt} = \frac{Q_{net}}{A_{basin}} \tag{D.5}$$

In Eq. D.5, Q_{net} is the net flow towards or out of the basin due to breach flows, with A_{basin} as the surface area of the basin. The surface area for the basin 'D48' is set to 400 km^2, while the surface areas for 'D49', 'D50' and 'D51' are set to 100 km^2.

The internal breaching between two flood prone areas (i.e. 'B49i' and 'B50i') is treated slightly different from breaches from the river, as these internal dikes are lower and generally weaker. It is assumed that, in case of an internal breach, the water will distribute immediately over both areas, in accordance with the pumping mode assumption of Eq. D.5.

D.1.3. RANDOM VARIABLES

Random variables are introduced for both strength and load in the river model. The strength is represented by the critical heights of dikes at the breach locations, while the load is represented by the river discharge. Using the stage - discharge relations of D.1.1, the river discharge can be converted to a water level. If the local water level exceeds the critical height at a breach location, failure is induced and a breach will form.

The critical height (h_{crit}) or strength at a breach location is represented by a normal distribution. In the context of a reliability assessment, only the lower end of a strength distribution is of importance. This critical height represents the combined probability that the flood defence at a breach location fails due to various failure mechanisms (e.g. piping, overflow or macro-stability). The actual flood defence height (h_{def}) is assumed to be the mean of the normally distributed critical height, and will also be used as the input for determining the investment cost of a flood defence (see also Section 5.3.4).

The standard deviation of a critical height distribution is determined with a fixed coefficient of variation of 0.1. Furthermore, the internal breach locations are linked to their external counterparts by having a mean critical height at 90% of the external counterpart, similar to [15]. The mean of the critical height distribution of an external breach location for a desired failure probability is obtained by iteratively shifting the mean in Monte Carlo simulations (without hydrodynamic interactions) until it converges to the desired failure probability. This iterative shifting (regula falsi) of the mean is the same approach as described in [16].

The load is represented by a Gumbel distribution for the Rhine river discharge at Lobith (e.g. see [67]). The normalized discharge wave of Figure D.1 is multiplied with a peak discharge value. [67] investigated various importance sampling distributions. Based on that research, a uniform sampling distribution is used. The density functions of both the importance sampling and regular distribution are shown in Figure D.5.

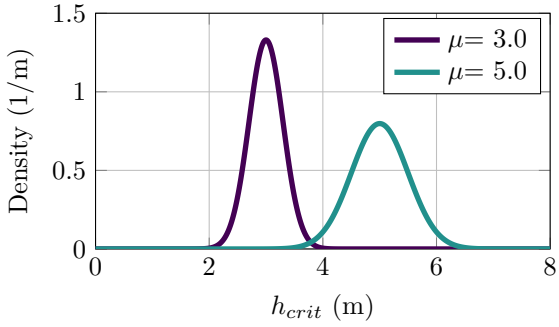

Figure D.4: Density functions of two normally distributed critical heights with a coefficient of variation of 0.1 and means of three and five meters, respectively.

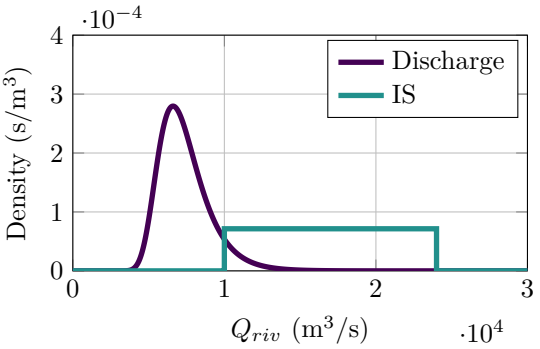

Figure D.5: Density functions of the Gumbel distributed discharge of the river Rhine, and the uniformly distributed importance sampling (IS) function.

D

D.1.4. VARIABILITY IN FAILURE PROBABILITY ESTIMATES

For reproducibility, the randomness of the failure probability estimation itself was removed by fixing the seed of the random number generation before each Monte Carlo simulation.

In order to obtain insight in the variability of failure probability estimates without resetting the seed, the failure probability was estimated for a range of sample sizes. The sample sizes tested range from 100 to 10,000 samples, which each were repeated 10,000 times to estimate the variability of each sample size. A sufficiently small variability is defined here as a maximum of around 10% over- or underestimation of the average estimate of the failure probability. It can be expected that as the number of samples goes up, the variability of the failure probability estimate goes down.

The failure probability results from evaluation of the simplified limit state function in Eq. D.6.

$$Z = h_{def} - h_{riv} \tag{D.6}$$

Where the load is a peak water level in a river (h_{riv}, in meters) and the strength is represented by critical height of the flood defence (h_{def}). h_{riv} is converted from a Gumbel distributed discharge (sampled using the Importance Sampling strategy described in D.1.3). The conversion from discharge to peak water level (h_{riv}) uses the conversion described in D.1.1. The strength is taken from a normal distribution with a CoV (coefficient of variation) of 0.1 and with a mean of three meters or five meters. The means of three and five meters represent the upper and lower bound of the range of expected strength in the economic optimisation; see also 5.3.5.

The results are shown in Figure D.6. The range which includes 95% of the failure estimates converges quicker for a mean of three meters than a mean of five meters in Figure D.6. Based on these figures, 5000 samples was seen as a sufficient number of samples, as the 95% variability range falls either within the ± 10% threshold, or closely approaches this threshold.

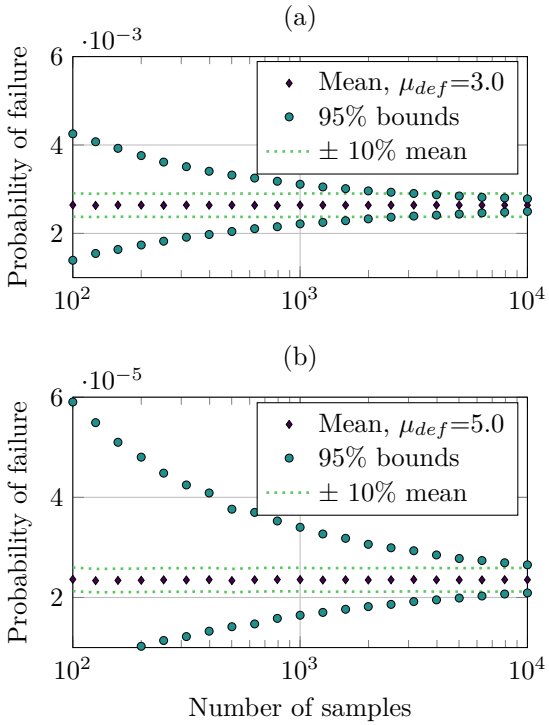

Figure D.6: Example of the variability of a failure probability estimate (using Eq. D.6) as a function of the number of samples. The load has a Gumbel distribution, while the strength has a Normal distribution with a mean (μ_{def}) of three meters (a) or five meters (b).

D.2. 'GOODNESS OF FIT' OF THE SURROGATE MODEL

A neural network was trained for each flood prone area in the case study area. For each neural network, the number of neurons on the input layer are the correlated breach locations as mentioned in Table 5.3. The output layer contains a single neuron which represents the EAD in that area. The neural network structures as described in Table D.1 were used.

Table D.1 shows the fit (R^2) and the number of neurons in each hidden layer. The number of layers and/or number of neurons needs to be increased for the downstream areas in order to attain a similar R^2, which indicates that the response of the flood risk cost is more complex for these areas: the further downstream a flood prone area is, the more flooding scenarios are possible.

With surrogate modelling, there is a possibility of overfitting. Overfitting is defined as having a very good fit on the training data, but as soon as new data is presented, poor fits are achieved instead. A few techniques were used to prevent this. First, the training was done using 70% of the data, with 15% used to test network generalization and another 15% as an independent measure of network performance. Secondly, Bayesian regularization was used to improve network generalization [75]. Nevertheless, even with the very high R^2 values, the neural nets do not always show accurate, expected behavior; compare for example the two lines in Figure D.7.

In order to test the accuracy of the neural networks, the correlation coefficients of Table 5.3 were re-calculated using the output of the fitted neural networks with 823,543 system configurations (7^7) of critical dike heights. The resulting correlation coefficients are shown in Table D.2. Comparing Table 5.3 & D.2 shows that there are only minor differences between the calculated correlation coefficients. The largest difference is found for the correlation coefficient between breach location B482 and flood prone area D49, which is 0.09 in Table 5.3 and -0.02 in Table D.2. Nevertheless, both are weak correlations.

Area	Neurons in HL1	Neurons in HL2	R^2
D48	30	0	0.99999
D49	40	0	0.99991
D50	30	3	0.99994
D51	30	4	0.99990

Table D.1: Amount of neurons in each hidden layer (called HL1 and HL2) in the neural nets used for approximating the modeled risk cost in D48, D49, D50 and D51. The R^2 is indicative of how well the neural net approximates the modeled data.

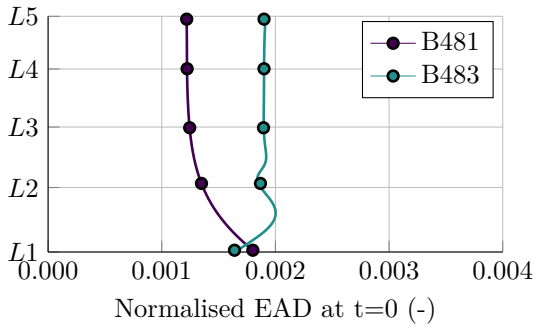

Figure D.7: Examples of expected and unexpected behavior of the neural network; the 'wobbling' between L1 and L3 for line B483 is unexpected. Shown is the normalised EAD of D48 versus the level of breach location B481. Also shown is the normalised EAD of D49 versus the level of breach location B483. Both lines assume that all other breach locations are kept at their L1 level and are, and are normalised on the maximum flood damage of the associated flood prone areas.

Breach location	D48	D49	D50	D51
GER	0.01	-0.54	-0.50	-0.37
B481	-0.67	0.06	0.05	0.05
B482	-0.48	-0.02	0.09	0.08
B483	-0.29	0.12	0.14	0.11
B49	0.00	-0.75	0.09	0.17
B50	0.00	0.00	-0.78	0.01
B51	0.00	0.00	0.00	-0.84

Table D.2: Spearman's correlation coefficients (calculated with the surrogate model) for the critical heights of breach locations (rows), versus the annual flood risk cost of the flood prone areas (columns).

E

EXTENSIONS TO OTHER AREAS OF INTEREST

Chapters 2-5 contain topics related to economic optimisation for riverine and coastal systems, focusing both on methods and case studies. However, aside from these topics there are other interesting flood defence-related topics where the same concepts can be applied. In this section, two such topics are discussed to stimulate further development of the presented approach based on first insights into the potential impact: retention areas and multi-functional flood defences.

E.1. INFLUENCE OF A RETENTION AREA

A retention area can be used in a riverine area to store some of the discharge of a river during an extreme discharge event. The general idea is that this retention area will 'shave off' the peak of a discharge wave (Figure E.1), which means that downstream flood defences experience a lower load. Ideally, this would then result in a milder extreme peak-discharge distribution (Figure E.2).[1]

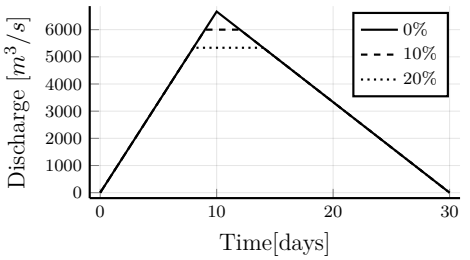

Figure E.1: An example of a simplified discharge wave (0%) and that same discharge wave with its peak reduced by ten and twenty percent.

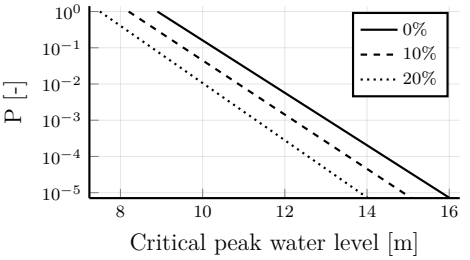

Figure E.2: Examples of (exponential) annual exceedance probabilities (P) as a function of critical peak water levels for peak discharges (0%) and reduced peak discharges downstream of the inlet of the retention area (10% and 20%).

Building such a retention area requires space and money. Sufficient space is needed to divert and store enough discharge to actually achieve the desired load reduction. While this space requirement is important, the purpose of this section is to explore the influence of including a retention area on the risk reduction and economically optimal safety targets. In order to explore the impact of a retention area on the period between and size of repeated investments, the method of Eijgenraam *et al.* [22] is used; see also Section 2.2.1.

However, this method is based on independent flood defences. This conflicts with the notion of a retention area that is interdependent with other flood defences (i.e. reduces loads for other flood defences). In order to still be able to apply this method, the properties of a retention area will be 'merged' with a regular flood defence. This single, merged flood defence will then be optimised with this method by doing the following:

- On the investment cost side, merging a retention area with a regular flood defence can be done by increasing the fixed costs of the flood defence by the same amount as the fixed cost of the retention area. This means that the fixed cost is higher each time a reinforcement is executed, because the method of Eijgenraam *et al.* as-

[1] A more realistic distribution for a retention area would be a peak-discharge distribution which is identical to the 0% line in Figure E.2 for lower discharges, but changes into the 10% or 20% line for higher, more extreme discharges. However, this can no longer be modelled with a simple exponential distribution and is beyond the scope of this section.

sumes equal constant costs.[2] This also means that the synchronisation is enforced between the timing of investments in the flood defence and retention area. Furthermore, this assumes that fixed costs are constant over the entire time period, even in the case of increased fixed costs. In practice, it is reasonable to assume that while building a retention area will be a significant investment, maintenance will be less frequent than that of a flood defence;

- The positive effect on the flood risk by the retention area is expressed by using exponential annual exceedance probabilities of critical water levels with reduced peak discharges (Figure E.2). This reduced load description will be used in the economic optimisation for the flood defence. This assumes that the retention area works perfectly, as in that it always reduces the peak of a discharge wave by the stated amount. Furthermore, in practice the mean effectiveness might be lower than the maximum reduction effect as shown by Kok *et al.* [76]. This means that the load reduction effect on the economic optimisation results will be over-estimated using the aforementioned approach.

By using the data for dike ring 48 (listed in [22]) as an example, it is possible to apply the method of Eijgenraam *et al.* for a range of conditions (i.e. reducing the peak discharge and increasing the fixed cost). The resulting periodic period between investments and the accompanying periodic dike height increase are compared in Figures E.3a & E.3b.

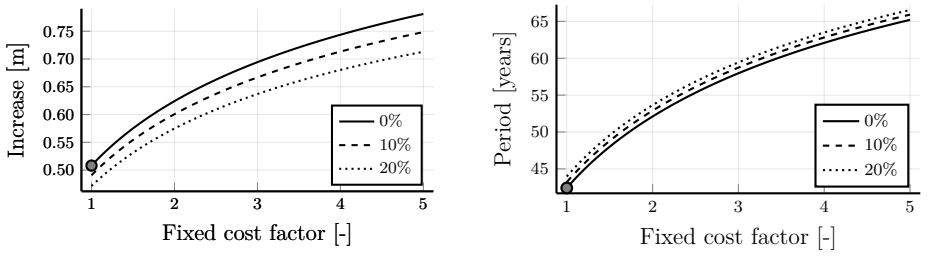

(a) Size of (optimal) *periodic dike height increase* as a function of an increasing fixed cost.

(b) Size of (optimal) *period of time between investments* as a function of an increasing fixed cost.

Figure E.3: periodic dike height increase and period of time between investments as a function of an increasing fixed cost. the fixed cost is multiplied with the 'fixed cost factor' on the x-axis. Peak discharge reductions of 0%, 10% and 20% are shown as separate lines. The dot indicates a flood defence *without* a retention area (0% reduction, fixed cost factor equals one).

The first thing that stands out from Figures E.3a & E.3b is that both the optimal investment size and optimal period between investments increases as the fixed cost increase. This can be explained by that it takes longer to 'overcome' the fixed cost. A longer

[2] An initial, single occurrence of higher fixed cost would be more realistic as a retention area is build only once. However, adapting the equations of Eijgenraam *et al.* to allow a single occurrence of higher fixed cost is beyond the scope of this section.

period also means that the accumulated expected annual damage increases, and therefore a higher increase is needed. For a given discharge reduction by a retention area, this means that the due to higher fixed costs of the retention area plus flood defence the (economically optimal) investment pattern changes to longer periods between investments and larger dike height increases when an investment occurs.

While an increased fixed cost inherently increases investment costs, a peak discharge reduction inherently reduces expected annual damages. In the shown solution, a larger peak discharge reduction leads to a lower investment size and a larger period between investments. This is because the solution has a relation between the optimal periodic dike heightening and the optimal periodic period between investments.[3] This relation essentially indicates that the accumulated damage between investments will be lower due to the peak discharge reduction, which leads to a lower investment size and/or a larger period between investments.

A different way of looking at the effect of a peak discharge reduction versus higher fixed costs is by plotting the development of the Expected Annual Damage (EAD) over time. In Figure E.4, the progression of the economically optimal Expected Annual Damage (EAD) over time is plotted for six combinations of load reductions and fixed costs. Figure E.4 has been set up in order to investigate what the net effect is (on the EAD) a fixed cost increase versus a load reduction due to those higher fixed costs.

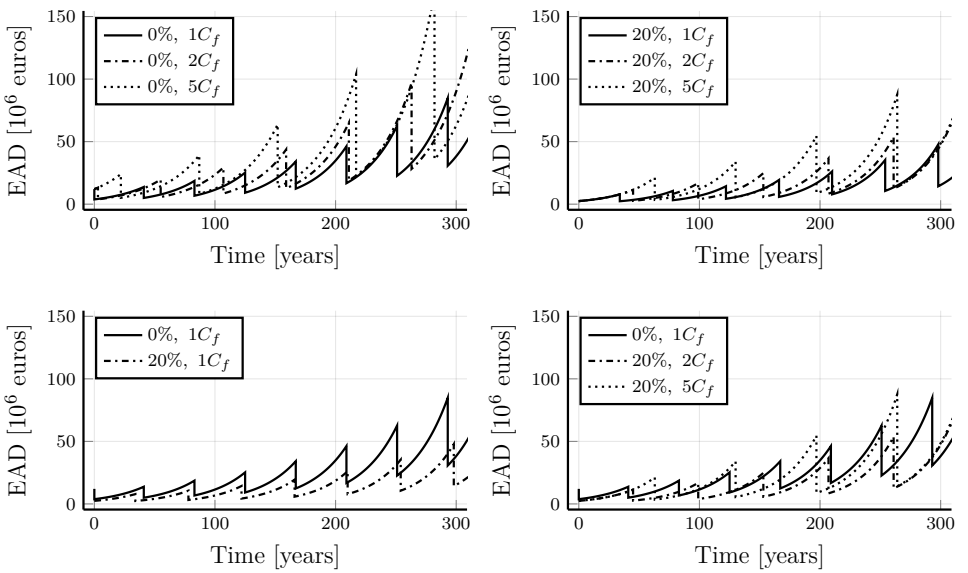

Figure E.4: Economically optimal Expected Annual Damage (EAD) over time for load reductions of 0% and 20%, combined with fixed costs (C_f) that are multiplied with a factor of 1, 2 and 5.

[3] This relation is also shown in Eq. 2.14.

Top left: Higher fixed costs for no load reduction leads to longer periods between investments. These longer periods affect the EAD as well, as the EAD over time is higher for higher fixed costs. Essentially, this is the effect as also discussed in Figure E.3.

Top right: Similar to the top left picture, higher fixed costs leads to longer periods between investments. However, the load reduction results in less risk over time. This can be seen by comparing the EAD development over time with the top left picture: the EAD is less 'peaky'.

Bottom left: A load reduction 'for free' (i.e. 20%, $1C_f$) leads to a lower EAD over time with slightly increased periods between investments.

Bottom right: Comparing a load reduction with higher fixed costs with the base case ('0%, $1C_f$') it becomes clear that the load reduction can offset the increase in EAD due to higher fixed costs (20%, $2C_f$), or at least partially (20%, $5C_f$).

In order to paint a complete picture of the costs, the size of investment costs over time are shown in Figure E.5 for the same combinations as shown in Figure E.4:

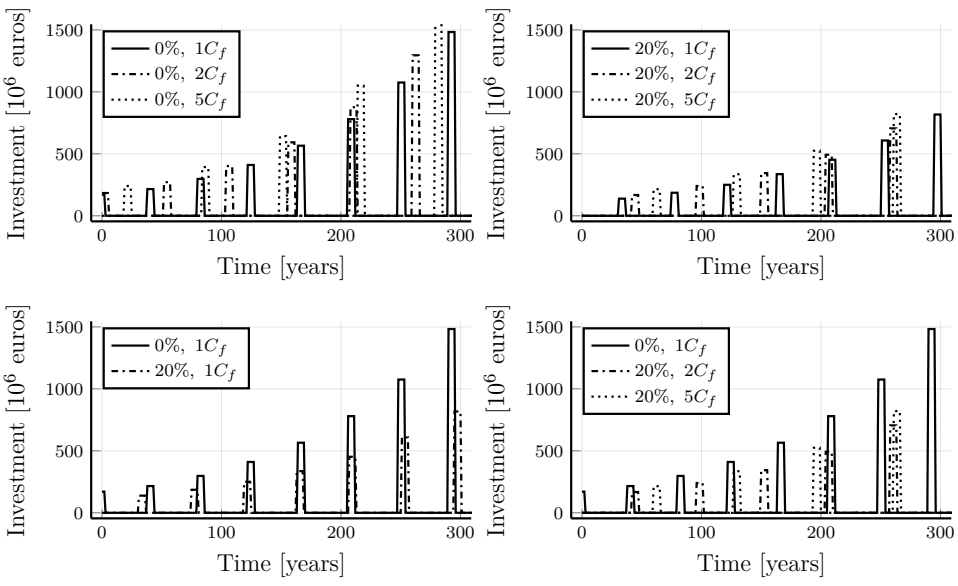

Figure E.5: Investments costs for dike heightening, combined with load reductions of 0% and 20% and fixed costs (C_f) that are multiplied with a factor of 1, 2 and 5.

Top left: Higher fixed costs for no load reduction leads to longer periods between investments. These longer periods affect the investment as well, as the investments are higher for higher fixed costs.

Top right: Similar to the top left picture, however the investments are slightly lower.

Bottom left: A load reduction 'for free' (i.e. 20%, $1C_f$) leads to a postponed initial investment and slightly increased periods between investments.

Bottom right: Comparing a load reduction with higher fixed costs with the base case ('0%, $1C_f$') it becomes clear that the investment costs are postponed due to a load reduction and higher fixed costs. Furthermore, the period between investments increases both due to a load reduction and due to higher fixed costs.

At the beginning of this section, a number of assumptions were made in order to be able to incorporate a retention area in the (unmodified) equations of Eijgenraam *et al.* [22]. The fixed cost were increased to account for the cost of a retention area, and exponential annual exceedance probabilities with reduced peak discharges were used to account for the load-reducing effect of a retention area. These assumptions impose limitations on the shown results:

- Assuming exponential annual exceedance probabilities of critical water levels with reduced peak discharges implies that that the reduction of the retention area can always be applied. This leads to a too optimistic result in the bottom right graph of Figure E.5: The first investment is not made in the first year, but the load reduction is applied anyway.

- The increase of fixed cost is applied each time an investment is made. This assumes that fixed costs are constant over the entire time period, also in the case of increased fixed costs. In practice, it is reasonable to assume that while building a retention area will be a significant investment, reinforcements will be less frequent than that of a flood defence. Therefore, subsequent fixed costs will most likely be lower than the initial fixed cost (i.e. building the retention area).

The second limitation leads to a conservative solution: if the results with this limitation in place indicate that building a retention area is a good idea, removing this limitation will put a retention area in an even more favourable spot. However, the first limitation does not lead to a conservative solution: the EAD is reduced when it shouldn't be, therefore leading to an overly positive solution with respect to a retention area.

In order to remedy the first limitation within the solution space of Figures E.4 & E.5, the total costs of the solutions in the bottom right graph of Figures E.4 & E.5 are compared. If the first investment is not made in the first year, then the size of the first investment is copied to the first year. The total cost (net present value) of the three strategies in the bottom right graph of Figures E.4 & E.5 then becomes: 405 million euros (0%, $1C_f$), 323 million euros (20%, $2C_f$) and 381 million euros (20%, $5C_f$). These numbers indicate that, in this simplified example, a retention area is a good idea from an economic optimisation point of view.

E.2. MULTI-FUNCTIONAL FLOOD DEFENCES

E.2.1. MULTIPLE FUNCTIONS WITH DISTINCT LIFE-CYCLES

If a flood defence has other functions besides providing protection against floods (i.e. a multi-functional flood defence), these functions have their own life-cycles. These life-cycles can be dictated by, for example, technical (e.g. technical reliability is too low) or economic reasons (e.g. economic lifespan). A simple example is a pipeline in a flood defence, or a road on top of a flood defence (e.g. see [77]). In the following, it is assumed that there will be a financial advantage by simultaneously executing maintenance on the flood protection function and on the secondary function (e.g. common mobilisation costs). Unless the economic optimisation also happens to result in an optimal period between investments which is identical to that of the secondary function, constraining the period between investments in flood safety will lead to 'less than optimal' results for the individual functions. The difference between the optimal and 'less than optimal' cost is the minimum which needs to be compensated by the benefits of synchronizing the investment-planning of the functions of a flood defence.

In order to get an impression of synchronizing the period between investment of a flood defence to a fixed life-cycle of 30 years, an example application is given for dike ring 48. The risk and investment equations, as well as the data regarding dike ring 48, have been re-used from the equations and data listed in [22]. The optimisation process is done numerically in order to properly deal with the fixed period between investments.[4] Figures E.6 & E.7 show such a comparison.

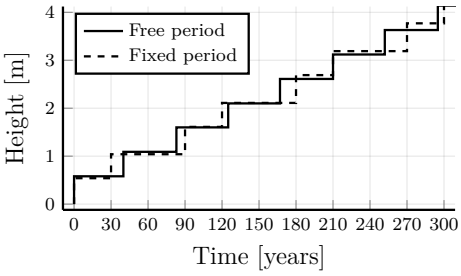

Figure E.6: The development over time of the height increase (relative to the height at time = 0 years) for an economic optimisation of dike ring 48 without constraints ('Free period') and with the period between investments constrained to 30 year intervals ('Fixed period').

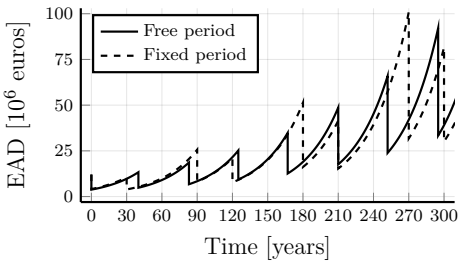

Figure E.7: The development over time of the expected annual damage (EAD) for an economic optimisation of dike ring 48 without constraints ('Free period') and with the period between investments constrained to 30 year intervals ('Fixed period').

Figures E.6 & E.7 compare the difference between the period between investments 'free' to be optimised and 'fixed' to a period of 30 years (without any benefit in cost). This comparison simulates in a simple way the effect of another function of the flood defence

[4] One such numerical method, and indeed the one used here, is the numerical method described in Chapter 4.

governing the periods between investments. The comparison shows that, without constraints on the period between investments, the solution is periodical (as described in [22]) after the first period of 41 years with a heightening of 51 centimetres each 42 years. However, the optimisation no longer produces periodical results (i.e. the same investment with the same period between investments) for the case where the period between investments is fixed to 30 years. In that case, it can be seen that the period between investments alternates between 30 and 60 years, with different accompanying investment sizes. Nevertheless, the development of the expected annual damage in Figure E.7 does not seem to be impacted too much by fixing the period between investments. In terms of the Net Present Value (NPV) over 600 years with a discount rate of 4%, the difference for dike ring 48 between a 'free' and 'fixed' period is approximately 0.7%, or 2.8 million euro. To put this further into perspective, the estimated fixed cost of any investment in flood protection for dike ring 48 is about 36 million euros in [22], indicating that indeed an increase of 2.8 million euros can be considered as small. Therefore, it seems feasible that a potential (monetized) benefit of synchronizing the investment schedules can outweigh the additional cost of synchronizing the investment schedules.

E.2.2. COSTS AND BENEFITS OF MULTIPLE FUNCTIONS

In the previous, the step size between investments in a flood defence was set to 30 years. This forced the optimal period between investments to be either a single time step of 30 years, or the sum of multiple time steps of 30 years (e.g. 60 or 90 years). This was done in order to simulate in a simple way the effect of another function of the flood defence governing the periods between investments. For the given example, the difference in total costs was found to be small, indicating that a potential (monetized) benefit of synchronizing the investment schedules can outweigh the additional cost of synchronizing the investment schedules.

In the following, the effect of another function of the flood defence governing the periods between investments will again be simulated. However, this time it will be done by a monetary incentive in terms of lower total fixed investment costs if an investment into flood safety and into the secondary function is done simultaneously.[5] This will be done by first setting the step size between possible decisions to a single year. This step size means that the economic optimisation can chose freely and is not forced to synchronize the investment schedules in flood safety and into the secondary function:

- It is assumed that the secondary function needs a recurring fixed investment every 30 years. This investment is carried out first in year 0 and afterwards every 30 years. This fixed investment is set at 20% of the fixed investment required for flood safety at that point in time.

- If an investment in flood safety is made simultaneously with an investment in the

[5] Note that the choice for higher fixed costs to incorporate the secondary function is similar to that of a retention area without any load reduction as discussed in Section E.1.

secondary function, the fixed cost of the flood safety investment will be reduced by 20%. This serves as an approximation of the idea that doing the two investments at the same time will lead to better cost-efficiency. This can incentivize the economic optimisation to chose a simultaneous investment over separate investments.

In order to test the synchronization benefits, two optimisations are shown. The first optimisation only adds the costs of the secondary function. The second optimisation adds the costs of the secondary function and offers reduced costs in case the investments are done simultaneously using the assumptions above. The comparison is made in order to investigate the effect of taking the benefit of synchronized maintenance into account: if the two solutions are identical, no synchronized investments have been made which means that synchronized investments did not have sufficient benefit.

The results for dike ring 48 using the data as listed in [22] are shown for the investment schedule over time (Figure E.8) and for the development of the Expected Annual Damage over time (Figure E.9).

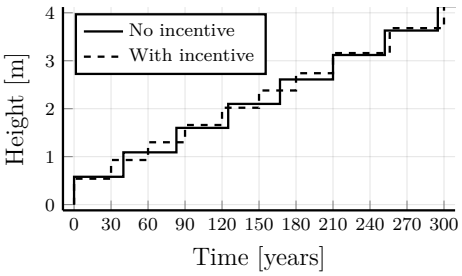

Figure E.8: The development over time of the height increase (relative to the height at time = 0 years) for an economic optimisation of dike ring 48 without reduced costs for synchronised investments ('No incentive') and with reduced costs for synchronised investments ('With incentive').

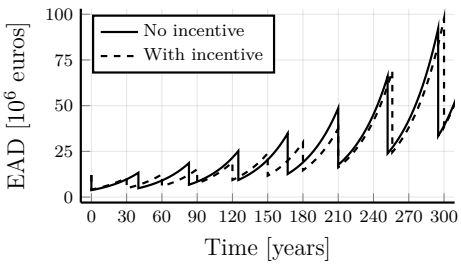

Figure E.9: The development over time of the expected annual damage (EAD) for an economic optimisation of dike ring 48 without reduced costs for synchronised investments ('No incentive') and with reduced costs for synchronised investments ('With incentive').

As the investment schedules differ in Figure E.8, the chosen set of assumptions for synchronized investments provided sufficient benefit to step away from the optimal path without the interaction between investments up to year year 210 (i.e. 'No incentive' in Figure E.8). In other words, the benefit of synchronised investments is high enough to compensate the incurred cost due to following a 'less than ideal' path ('less than ideal' as seen from only taking into account flood safety, i.e. 'No incentive'). The development of the EAD is shown in Figure E.9, and shows that the EAD is actually *reduced* in the first 210 years in case of the 'With incentive' approach; this is most likely due to the shorter periods between investments in flood safety.

Another way of looking at this problem is comparing the net present value of the two solutions in Figure E.8 & Figure E.9 with the solution that does not include the secondary function at all. By doing this, the monetary increase due to the secondary function can

be quantified and converted into the minimum yearly benefits that are needed to 'break even'.[6] For a sufficiently long period in time (i.e. 200-300 years), the net present value of a yearly revenue (B) using a discount rate r can be approximated as $B \big/ r$. In order to break even on the inclusion of (or synchronization with) the secondary function, the benefits need to outweigh the additional costs (C_a) of including the secondary function, or $B \geq r * C_a$.

To illustrate this notion of minimum yearly benefits, it is applied to the example of Figure E.8 & Figure E.9. It is assumed that the revenues start at year 0. The total costs (Net Present Value or NPV) for a period of 500 years without a secondary function are approximately 404.6 million euros. With the secondary function including the incentive to synchronize investments, the total costs increase to 409.2 million euros. Using a discount rate of 4%, the yearly revenue should then at least be $0.04 * (409.2 - 404.6) \approx 0.2$ million euros. To put this in perspective, if the incentive to synchronize investments would not have been included the total costs increase to 422 million euros (due to increased fixed cost), resulting in an increased required yearly benefit of $0.04 * (422.0 - 404.6) \approx 0.7$ million euros.

This simplified example may not be directly transferable to practice, as a waterboard might be obliged (e.g. by the national government) to run a pipeline through its flood defence, reaping no (direct) financial benefit. However, in a broader perspective this example does provide some beneficial information to support decision making. First of all, integrally considering multiple functions in, on, or alongside a flood defence in a cost-benefit analysis can lead to overall cost-savings (in this section seen from a NPV perspective). Secondly, if the total costs are not of a primary interest, the other mentioned factors such as the EAD, the height increase pattern, or the required benefits can be used as arguments for or against combining a flood defence with a secondary function.

[6] Adding such benefits to a cost-benefit analysis makes such a cost-benefit analysis more complete. However, from a flood safety perspective, constant yearly benefits (i.e. a lump sum added to the total costs) will not influence the optimal safety targets.

ACKNOWLEDGEMENTS

At the end of 2012, I was encouraged by Mark van Koningsveld, who supervised my master thesis, to undertake a doctoral research. It was his enthusiasm and sheer joy in regaling me with positive accounts of his own doctoral experiences, that convinced me 'working on a single subject alone for four years' might actually be fun. After initial talks with Bas Jonkman and Matthijs Kok, I was given the opportunity to start my PhD research in a full-time position at the university in 2013. This appointment ended in 2017, with only a minor part of the thesis to finish. Or so I thought. Turns out it takes quite some time and motivation to actually finish it next to a full-time job, and I do not know if I were able to without all the support I have gotten. This part of the thesis is a thank you to all who supported me.

This research was supervised by Matthijs Kok as my promotor and Timo Schweckendiek as my co-promotor. I am indebted to both of them for their guidance, insightfulness, support and fun discussions. They also gave me considerable freedom in shaping the contents of my research. Shaping my own research was exciting and probably one of the reasons I kept going, but it did give me a headache or two whenever I got stuck. Nonetheless, you were always there to support me and nudge me in the right direction again.

A special thanks to Bas Jonkman as well. Despite the fact that you were not officially involved during my PhD project, in many ways it felt you were. The many 'hallway discussions' combined with your sharp insight really helped me with various topics I was struggling with. Thank you as well for always finding 'small jobs' for me and other PhD students, which were a welcome distraction. Most of the time.

To all the people I shared an office with, either during my time at the university or now at HKV, thanks for listening to me sometimes ramble on about my PhD. Above all, I thoroughly enjoyed (and still do enjoy) the many discussions about our work, ethics, politics, parties, weather, and utter nonsense. Thanks as well for consistently asking the same question ('Is it done yet?'), which served as a pleasant reminder that I indeed eventually had to finish the dissertation. A big thanks to HKV as well, for understanding and giving me ample time and space to finish my PhD.

A special thanks to Vincent Vuik and Kasper Lendering, with whom I shared an office for the majority of my time at the university. I simply could not have wished for better roommates. Vincent, your can-do attitude during our discussions helped me see a simpler, better solution to problems I was struggling with. Kasper, in your own dissertation you mentioned that you regret our discussions never lead to a joint publication. As we are now both done with our dissertations, we should have ample time to write that

publication? Preferably in Curaçao...

And last but not least to all my friends, family and loved ones: thank you. Words cannot express how much I appreciate you. Even though I might not always have shown it, I greatly appreciate you all. And finally, to my parents Cas and Ine: Thank you. Thank you for your unconditional love and support, and for always being there when I most needed it. I am looking forward to making up for all the times I had to cancel friends and family in weekends and evenings.

Curriculum Vitæ

Egidius Johanna Cassianus Dupuits

24-12-1986	Born in Geleen, The Netherlands.
1999–2005	Pre-University Secondary Education (*cum laude*) VWO, Gymnasium, Science and Engineering Trevianum college, Sittard
2005–2012	MSc. Civil Engineering in Flood Risk Delft University of Technology, Delft
2013–2017	PhD Researcher Section of Hydraulic Structures and Flood Risk Faculty of Civil Engineering and Geosciences Delft University of Technology, Delft
2017–present	Consultant Risk and Disaster Management HKV Consultants, Lelystad and Delft

LIST OF PUBLICATIONS

PEER-REVIEWED JOURNAL PAPERS

4. **EJC Dupuits**, WJ Klerk, T Schweckendiek, KM de Bruijn, *Impact of including interdependencies between multiple riverine flood defences on the economically optimal flood safety levels*, Reliability Engineering & System Safety 191 (2019).

3. **EJC Dupuits**, FLM Diermanse, M Kok *Economically optimal safety targets for interdependent flood defences in a graph-based approach with an efficient evaluation of expected annual damage estimates*, Natural Hazards and Earth System Sciences 17 (2017).

2. A Sebastian, **EJC Dupuits**, O Morales-Nápoles, *Applying a Bayesian network based on Gaussian copulas to model the hydraulic boundary conditions for hurricane flood risk analysis in a coastal watershed*, Coastal Engineering 125 (2017).

1. **EJC Dupuits**, T Schweckendiek, M Kok, *Economic optimization of coastal flood defense systems*, Reliability Engineering & System Safety 159 (2017).

CONFERENCE PAPERS

3. **EJC Dupuits**, KM de Bruijn, FLM Diermanse, M Kok, *Economically optimal safety targets for riverine flood defence systems*, E3S Web of Conferences 7 (2016).

2. A Sebastian, **EJC Dupuits**, O Morales-Nápoles, *Assessing Flood Risk from Hurricane-induced Precipitation and Storm Surge: A Bayesian Network Approach*, AGU Fall Meeting Abstracts (2015).

1. **EJC Dupuits**, T Schweckendiek, *Flood risk and economically optimal safety targets for coastal flood defense systems*, ICASP12 (2015).

BOOK CHAPTERS

2. B Kothuis, M Kok, **EJC Dupuits**, *Economically efficient flood protection levels: Effects of system interdepencies*, Integral Design of Multifunctional Flood Defenses (2017).

1. B Kothuis, M Kok, **EJC Dupuits**, *Flood risk reduction systems optimization: Protecting Galveston Bay shores and the Barrier Islands*, Integral Design of Multifunctional Flood Defenses (2017).